OVEREXPRESSING FRAGMENTS OF CREB-BINDING PROTEIN (CBP) TO BLOCK TRANSCRIPTIONAL DYSREGULATION AND TOXICITY IN HUNTINGTON'S DISEASE

by

Gregory Hosier

Submitted in partial fulfilment of the requirements
for the degree of Master of Science

at

Dalhousie University
Halifax, Nova Scotia
July 2012

DALHOUSIE UNIVERSITY

DEPARTMENT OF PHARMACOLOGY

The undersigned hereby certify that they have read and recommend to the Faculty of Graduate Studies for acceptance a thesis entitled "OVEREXPRESSING FRAGMENTS OF CREB-BINDING PROTEIN (CBP) TO BLOCK TRANSCRIPTIONAL DYSREGULATION AND TOXICITY IN HUNTINGTON'S DISEASE" by Gregory Hosier in partial fulfilment of the requirements for the degree of Master of Science.

Dated: July 19, 2012

Supervisor: _____

Readers: _____

_____

_____

DALHOUSIE UNIVERSITY

DATE: July 19, 2012

AUTHOR: Gregory Hosier

TITLE: OVEREXPRESSING FRAGMENTS OF CREB-BINDING PROTEIN (CBP) TO BLOCK TRANSCRIPTIONAL DYSREGULATION AND TOXICITY IN HUNTINGTON'S DISEASE

DEPARTMENT OR SCHOOL: Department of Pharmacology

DEGREE: MSc CONVOCATION: October YEAR: 2012

_____

Signature of Author

TABLE OF CONTENTS

LIST OF TABLES

LIST OF FIGURES

ABSTRACT

Huntington's disease (HD) is caused by expression of the huntingtin gene containing an expanded CAG repeat. N-terminal mutant huntingtin protein (N-mHtt) accumulates in the nucleus and impairs transcription of a subset of genes through incorporation into transcriptional complexes or sequestration of proteins away from the promoter. CREB-binding protein (CBP) is a transcriptional co-activator and acetyltransferase (AT) that binds to N-mHtt. We hypothesized that overexpressing CBP fragments that lack a promoter association domain would block N-mHtt-mediated transcriptional dysregulation and toxicity. We found that overexpressing full-length CBP or CBP fragments did not reverse transcriptional dysregulation, but did decrease toxicity in a cell model of HD. Overexpressing fragments of CBP containing the AT domain increased toxicity in wild-type cells, while overexpressing a fragment lacking this domain had no effect. We conclude that excess AT activity was detrimental in wild-type cells, while overexpressing CBP or CBP fragments was protective in HD cells.

LIST OF ABBREVIATIONS USED

°C	degree Celsius
μg	microgram
μL	microlitre
μM	micromolar
AIMS	abnormal involuntary movement scale
AMPA	2-amino-3-(5-methyl-3-oxo-1,2- oxazol-4-yl) propanoic acid
Amp^r	ampicillin resistance
ANOVA	analysis of variance
AT	acetyltransferase
ATP	adenosine triphosphate
ATZnCBP	CBP fragment containing a portion of the AT domain and the adjacent third Zn finger region
BAC	bacterial artificial chromosome
BDNF	brain-derived neurotrophic factor
C	carboxy
CA1	*cornu ammonis* (Ammon's horn) 1
CA150	co-activator protein 150 kDa
Ca^{2+}	calcium
cAMP	cyclic adenosine monophosphate
caspase-$2^{-/-}$	homozygous deletion mutation of caspase-2
CB1	cannabinoid receptor 1
CBP	CREB-binding protein

C/EBP	CCAAT-enhancer-binding protein
CoA	coenzyme A
CoIP	co-immunoprecipitation
CO_2	carbon dioxide
CMV	cytomegalovirus
CMXrosamine	chloromethyl-X-rosamine
CRE	cAMP response element
CREB	cAMP response element binding protein
CtBP	C-terminal-binding protein
D_1	dopamine receptor D_1
D_2	dopamine receptor D_2
DARPP-32	dopamine and cAMP-regulated neuronal phosphoprotein 32 kDa
dATP	deoxyadenosine triphosphate
dCTP	deoxycytidine triphosphate
dGTP	deoxyguanosine triphosphate
dH_2O	distilled water
DMSO	dimethyl sulfoxide
DNA	deoxyribonucleic acid
dNTP	deoxyribonucleotide triphosphate
E3	ubiquitin-protein ligase
E. coli	*Escherichia coli*
EDTA	ethylenediaminetetraacetic acid
ERK	extracellular-signal-regulated kinase

EthD-1	Ethidium Homodimer-1
GABA	gamma-aminobutyric acid
GFP	green fluorescent protein
GAPDH	glyceraldehyde-3-phosphate dehydrogenase
GATA-1	GATA-binding protein 1
G_s	stimulatory G protein coupled-receptor
GST	glutathione S-transferase
h	hour
HAT	histone acetyltransferase
HD	Huntington's disease
Hdh	mouse huntingtin gene
HEK	human embryonic kidney
HEPES	4-(2-hydroxyethyl)-1-piperazineethanesulfonic acid
HMG-CoA reductase	3-hydroxy-3-methyl-glutaryl-Coenzyme A reductase
Htt	huntingtin gene
Htt	huntingtin protein
IgG	immunoglobulin G
kB	kilobase
LB	Luria-Bertani
M	molar
MAPK	mitogen-activated protein kinase
MDM2	murine double minute 2
mg	milligram

mHtt	mutant huntingtin gene
mHtt	mutant huntingtin protein
min	minute
miRNA	micro RNA
mL	milliliter
mm	millimeter
M_r	molecular weight
MRI	magnetic resonance imaging
mRNA	messenger RNA
mSin3A	mammalian SIN3 homolog A
N	amino
NCoR	nuclear receptor co-repressor protein
NF-E2	nuclear factor erythroid-derived 2
ng	nanogram
NII	neuronal intranuclear inclusion
nL	nanolitre
nm	nanometer
NMDA	N-methyl-D-aspartic acid
N-mHtt	N-terminal mutant huntingtin protein
PANSS	positive and negative syndrome scale for schizophrenia
PBS	phosphate buffered saline
PCR	polymerase chain reaction
PFA	paraformaldehyde

PGC-1α	peroxisome proliferator-activated receptor gamma co-activator 1-alpha
PIC	preinitiation complex
PKA	protein kinase A
PMSF	phenylmethaneslfonylfluoride
Pol II	RNA polymerase II
polyQ	polyglutamine
p53	protein 53 kDa
p300	protein 300 kDa
Q	glutamine
RAP30	RNA polymerase II associating protein 30
REST	repressor element silencing transcription factor
RFP	red fluorescent protein
RNA	ribonucleic acid
rpm	revolutions per minute
SEM	standard error of the mean
Siah1	E3 ubiquitin-protein ligase from seven in absentia homolog family
Sp1	specificity protein 1
SREBP	sterol regulatory element-binding protein
SSRI	selective serotonin reuptake inhibitor
ST14A	immortalized embryonic day 14 rat striatal cells
ST*Hdh*	immortalized cell line derived from striatal cells of *Hdh* knock-in mice
TBE	tris, boric acid, and EDTA solution

TBP	TATA-binding protein
TBS	tris buffered saline
TBS-T	tris buffered saline with tween 20
TE	tris EDTA
TF	transcription factor
TFIIB	general transcription factor II B
TFIIF	general transcription factor II F
Tpr	nuclear pore protein, translocated promoter region
Tris	tris(hydroxymethyl)aminomethane
TUNEL	terminal deoxynucleotidyl transferase dUTP nick end labeling
UV	ultraviolet
v/v	volume/volume
w/v	weight/volume
X-gal	5-Bromo-4-chloro-3-indolyl-β-D-galactoside
YAC	yeast artificial chromosome
YT	yeast tryptone
Zn	zinc
ZnCBP	CBP fragment containing the third Zn finger region

ACKNOWLEDGEMENTS

I would like to thank Dr. Eileen Denovan-Wright for being a wonderful mentor and always pushing me to do better work. I would like to thank my fellow lab members, Amina Bagher, Dr. Matthew Hogel, and Robert Laprairie, as well as technician Kay Murphy, for their help and support throughout my time at Dalhousie. Thanks to members of my supervisory committee, Dr. Johnathon Blay, Dr. Denis Dupre, and Dr. Barbara Karten for their guidance. I would like to thank my parents, Judy and Jerry, as well as my siblings, Laura, Eric, and Amy, for their support over the years. I am extremely grateful for the love and support of my girlfriend Ashley. Finally, I would like to acknowledge the financial support of Dalhousie University, the Canadian Institutes of Health Research (CIHR), Nova Scotia Health Research Foundation (NSHRF), and the Molly Appeal for Neuroscience Research.

CHAPTER 1 INTRODUCTION

1.1 GENERAL OVERVIEW

Huntington's disease (HD) is a progressive neurodegenerative disease caused by inheritance of a single copy of *huntingtin* (*Htt*) with an expanded CAG repeat (Huntington's Disease Collaborative Research Group, 1993). The pathogenic mechanism by which inheritance of *mutant Htt* (*mHtt*) leads to symptoms of HD is not known. Mutant Htt protein (mHtt) contains an expanded polyglutamine (polyQ) region in the N-terminal region and expression of mHtt leads to a number of cellular changes (reviewed in Zuccato *et al.,* 2010). N-terminal mHtt (N-mHtt), but not wild-type Htt, accumulates in the nucleus (Havel *et al.*, 2009) and impairs transcription of a subset of genes early in disease progression (Luthi-Carter *et al.,* 2000). This is believed to contribute to HD pathogenesis (Luthi-Carter *et al.,* 2000). The working model for how N-mHtt impairs transcription is that N-mHtt either sequesters certain necessary transcription factors away from the promoter (Perutz *et al.,* 1994; Steffan *et al.,* 2000) or incorporates into complexes at the promoter and inhibits binding of additional transcription factors (Cui *et al.,* 2006; Hogel *et al.,* 2012). We hypothesized that overexpressing protein fragments that bind N-mHtt and lack a promoter association domain would block abnormal interactions of N-mHtt at the promoter and slow progression of HD. CREB-binding protein (CBP) is a transcriptional co-activator with acetyltransferase (AT) activity. N-mHtt binds a fragment of CBP that lacks the promoter association domain (Steffan *et al.*, 2001). We tested whether overexpressing full-length CBP, or fragments of CBP lacking the promoter association domain, could block transcriptional dysregulation and toxicity in the ST*Hdh* cell line. The ST*Hdh* cell line is derived from the striatum of embryonic day

14 mice made to express human *Htt* exon 1 at physiological levels with 7 (non-pathogenic) or 111 (pathogenic) CAG repeats within the context of full-length mouse *Htt* (Trettel *et al.*, 2000).

1.2 CLINICAL OVERVIEW OF HUNTINGTON'S DISEASE

1.2.1 Incidence and symptoms

HD is a progressive neurodegenerative disease that occurs in approximately 1 in 10,000 people in the western world and is characterized by motor, cognitive, and psychiatric impairments (reviewed in Walker, 2007; reviewed in Ross and Tabrizi, 2011). The median age of symptom onset in patients with HD is typically between 35 and 55 years of age (Newcombe *et al.*, 1981; Adams *et al.*, 1988), however there have been juvenile cases reported (van Dijk *et al.*, 1986). Early motor changes typically involve excessive involuntary movements (chorea), while later motor changes typically involve impaired movement, including bradykinesia, incoordination, slowed saccadic eye movements, and rigidity (Thompson *et al.*, 1988; reviewed in Ross and Tabrizi, 2011). Involuntary movements are absent during deep sleep (Fish *et al.*, 1991).

Although formal diagnosis of HD is typically based on motor impairments and genetic testing, subtle cognitive and psychiatric changes often precede overt motor phenotypes in patients with HD (reviewed in Walker, 2007; reviewed in Ross and Tabrizi, 2011). Early cognitive impairments include problems in attention, working memory, verbal learning, and learning of random associations (Lemiere *et al.*, 2004). Common psychiatric impairments reported in patients with HD include: depression, irritability, apathy, anxiety, paranoia, and obsessive-compulsive disorder (Kirkwood *et*

al., 2001; Paulsen *et al.*, 2001; Anderson *et al.*, 2010). Depression in patients with HD has been reported at a lifetime incidence of approximately 41% (Folstein *et al.*, 1983), which is much higher than the 8-12% lifetime incidence reported in the general population (Andrade *et al.*, 2003). Higher incidence of depression is not solely due to natural concerns of being at risk for HD. Undiagnosed, at-risk patients who were retrospectively found to have the disease reported more feelings of depression compared to at-risk patients who were retrospectively found to not have HD (Julien *et al.*, 2007). The order and extent to which motor, cognitive, and psychiatric impairments occur is highly variable between patients with HD, as is the age of symptom onset.

Other symptoms that occur in patients with HD include weight loss and disruption in circadian rhythms. Significant weight loss and an inability to gain weight were reported in patients suffering from HD (Robbins *et al.*, 2006), despite the fact that patients had an increased appetite and increased caloric intake relative to unaffected individuals (Trejo *et al.*, 2004). Disruption in circadian rhythms has been demonstrated by frequent nocturnal awakening (Wiegand *et al.*, 1991), electroencephalographic abnormalities during sleep (Wiegand *et al.*, 1991), and increased sleeping during the day (Morton *et al.*, 2005).

HD is a progressive disease and over time motor, cognitive, and psychiatric impairments worsen. Death typically follows 15–20 years after initial symptom onset (reviewed in Walker, 2007; reviewed in Ross and Tabrizi, 2011). Analysis of mortality data in the United States has determined that the leading causes of death in patients with HD are pneumonia, nutritional deficiencies, choking, and suicide (Lanska *et al.*, 1988).

1.2.2 Pathology

Studies employing magnetic resonance imaging (MRI) suggest that some amount of atrophy occurs in almost all brain regions of HD patients, including total cerebrum, total white matter, cerebral cortex, caudae and putamen (collectively called the striatum), globus pallidus, amygdala, hippocampus, brainstem, and cerebellum (Rosas *et al.*, 2003; Fennema-Notestine *et al.*, 2004). Cell loss and atrophy is most prominent in the caudate and putamen as shown by post-mortem analysis of HD brains (Vonsattel *et al.*, 1985). Significant neurodegeneration also occurs in the frontal, parietal, and temporal cortex (Mann *et al.*, 1993). Other specific areas that show varying amounts of degeneration include the substantia nigra (Oyanagi *et al.*, 1989), CA1 region of the hippocampus (Spargo *et al.*, 1993), angular gyrus in the parietal lobe (Macdonald *et al.*, 1997), lateral tuberal nuclei of the hypothalamus (Kremer *et al.*, 1990), and centromedial parafascicular complex of the thalamus (Heinsen *et al.*, 1999). Importantly, decreases in striatal volume have been detected using MRI between 5 and 10 years before clinical diagnosis and show correlation with disease progression (Paulsen *et al.*, 2008; Aylward *et al.*, 2011). Neurodegeneration in the caudate and putamen is not homogeneous. GABAergic medium spiny neurons are susceptible to degeneration, while cholinergic aspiny interneurons are generally spared (reviewed in Mitchell *et al.*, 1999). Medium spiny neurons that express enkaphalin and dopamine D_2 receptors degenerate earlier than neurons that express substance P and dopamine D_1 receptors (Augood *et al.*, 1996). Consequently, although multiple brain regions undergo some amount of degeneration, certain tissues and cell types are more susceptible than others to degeneration during progression of HD. A key

question regarding HD pathophysiology is why some cell types are susceptible to degeneration while others are relatively resistant.

1.2.3 Treatments

Tetrabenazine is used to control chorea in HD and is the only therapeutic agent approved specifically for use in HD (reviewed in Paleacu, 2007). Tetrabenazine antagonizes dopamine D_2 receptors (Reches *et al.*, 1983; Paleacu, 2007) and inhibits vesicle monoamine transporter-2, which impairs synaptic packaging and release of dopamine, norepinephrine, and serotonin (Pettibone *et al.*, 1984; reviewed in Paleacu, 2007). Fifteen patients showed improved scores on the Abnormal Involuntary Movement Scale (AIMS) after 6 months of tetrabenazine treatment (Ondo *et al.*, 2002). In addition to tetrabenazine, neuroleptics such as, haloperidol, fluphenazine, perphenazine, pimozide, clozapine, olanzapine and thiopropazate have been used with limited success to control chorea in HD patients because of their ability to antagonize dopamine D_2 receptors (Bonelli and Wenning, 2006). Haloperidol was found to have no effect on chorea in a double-blind, randomized, cross-over study of six patients with HD (Leonard *et al.*, 1975), but was found to improve chorea in a single-blinded study of 13 HD patients (Koller and Trimble, 1985). Both tetrabenazine and neuroleptics can cause bradykinesia and rigidity, which can worsen motor impairment later in HD progression.

There is limited evidence indicating that anti-depressants and atypical anti-psychotics may improve some psychiatric symptoms of HD. One multi-subject study showed that four-week administration of the serotonin-norepinephrine reuptake inhibitor venlafaxine showed marked improvement in mood in 26 patients with HD as determined

by increased scores in two rating scales used to categorize depression (Holl *et al.*, 2010). Case studies report that agitation and irritability were ameliorated following administration of the selective serotonin reuptake inhibitor (SSRI) fluoxetine (De Marchi *et al.*, 2001) and obsessive compulsive behaviours dimished after treatment with the SSRI sertraline (Patzold and Brüne, 2002). Apiprazole treatment for 2 weeks reduced irritability and delusions in a 46 year-old HD patient in addition to improving chorea and gait (Lin and Chou, 2008). Quetiapine was effective in treating the positive (delusions, and paranoia), but not negative (apathy) symptoms of psychosis in an HD patient using the Positive and Negative Syndrome Scale (PANSS; Seitz and Millson, 2004).

Phase III clinical trials have been initiated for several potential therapies in HD. Tetrabenazine and the neuroleptic drugs olanzapine and tiapride (NCT00632645), the nutritional supplement creatine (NCT00712426), and the antioxidant coenzyme Q10 (NCT00608881) are all being independently administered in an attempt to improve the total functional capacity score of HD patients. The antihistamine latrepirdine (NCT01085266) is being tested for its ability to improve cognitive deficits in HD. Results from these studies are not yet available. Taken together, no treatments are currently available to stop or slow progression of HD. Some symptomatic treatments are available, but these are often of limited efficacy.

1.3 GENETICS OF HUNTINGTON'S DISEASE

1.3.1 Identification of the Huntington's disease gene

Restriction fragment length polymorphisms were mapped to chromosome 4 using genetic material from an American family with HD as well as an extended Venezuelan

family with HD (Gusella *et al.*, 1983). The culmination of a ten year collaborative project led to the identification of a gene, *Interesting Transcript 15* (subsequently renamed *Htt*), that contained a polymorphic CAG repeat in exon 1 (Huntington's Disease Collaborative Research Group, 1993). The length of the CAG repeat was substantially longer on HD-associated compared to non-HD-associated chromosomes (Huntington's Disease Collaborative Research Group, 1993).

To determine the relationship between CAG repeat length and progression of HD, a worldwide study examined approximately 1,000 patients with HD and approximately 1,600 control subjects (Kremer *et al.*, 1994). Patients with HD were found to possess between 36 and 121 CAG repeats with a median of 44 CAG repeats, while control subjects had between 10 and 29 CAG repeats, with a median of 18 CAG repeats in exon 1 of *Htt*. CAG repeat length is inversely correlated with age of symptom onset, meaning that patients with a greater CAG repeat length typically develop symptoms at an earlier age than patients with a smaller CAG repeat length (Duyao *et al.*, 1993). Patients that develop symptoms before the age of 20 (juvenile onset HD) typically have a CAG repeat length above 60 (Squitieri *et al.*, 2006). CAG repeat length also correlates with progression of HD, where patients with a greater CAG repeat length deteriorate faster after initial symptom onset than patients with a smaller CAG repeat length (Rosenblatt *et al.*, 2012). Individuals with a CAG repeat length 36-39 have a reduced penetrance form of HD. A recent study showed that individuals with reduced penetrance HD have a 40% and 30% chance of being free of HD symptoms at ages 65 and 75 respectively (Quarrell *et al.*, 2007). Although CAG repeat length is a strong determinant for age of symptom onset and progression of HD, individuals with the same CAG repeat length can display

different manifestations of HD. This indicates that genetic modifiers play a role in onset and progression of HD in addition to CAG repeat length (Gusella and MacDonald, 2009).

1.3.2 Impact of polyglutamine expansion on huntingtin function

Htt contains 67 exons and encodes Htt protein, which is 3,144 amino acids long and has a polyQ repeat region in the N-terminal region (Hoogeveen *et al.*, 1993; Huntington's Disease Collaborative Research Group, 1993). Htt is widely expressed throughout the body with the highest levels of Htt expression in the brain, lung, testes, and ovaries (Li *et al.*, 1993). Htt is required for normal development because mice homozygous for a *Htt* deletion die at embryonic day 8.5 (Duyao *et al.*, 1995). Within the cell, Htt is associated with a variety of organelles, including the nucleus, endoplasmic reticulum, Golgi complex, and mitochondrion (reviewed in Zuccato *et al.*, 2010). Htt is also found within neurites and at synapses, where it associates with various vesicular structures such as clathrin-coated vesicles, endosomal compartments or caveolae, as well as microtubules (reviewed in Zuccato *et al.*, 2010). Htt is known to have many interaction partners and is believed to act as a scaffold for other proteins during signaling and trafficking processes (Harjes and Wanker, 2003). Huntingtin is also believed to play a role in neuroprotection via inhibition of caspases and production of brain-derived neurotrophic factor (BDNF; reviewed in Zuccato *et al.*, 2010).

Shortly after the mutation in *Htt* was discovered, it was hypothesized that the disease phenotype could occur because of either haploinsufficiency of wild-type Htt or a toxic gain-of-function of mHtt. Heterozygous mice with a *Htt* deletion show no HD-like phenotype, suggesting that expression of one copy of *Htt* is sufficient to perform all of the

functions required of Htt (Duyao *et al.*, 1995). R6/2 mice overexpress exon 1 of the human *Htt* with 144 CAG repeats in addition to two copies of wild-type *Htt* (Mangiarini *et al.*, 1996). R6/2 mice recapitulate aspects of the HD pathology including development of neuronal intranuclear inclusions (NIIs) from birth, motor impairments starting at 35 days of age, failure to gain weight and brain atrophy observed at 90 and 60 days, respectively, and premature death at approximately 14 weeks (Stack *et al.*, 2005). In contrast, the YAC128 mouse model of HD express full-length human *Htt* with 128 CAG repeats within a yeast artificial chromosome (YAC; Slow *et al.*, 2003). YAC128 mice exhibit cognitive deficits starting at 2 months, hyper- followed by hypo-kinetic movement impairments observed 3 and 6 months of age, respectively, decreased striatal brain weight detected at 9 months, striatal and cortical volume loss observed at 9 and 12 months, respectively, and striatal neurodegeneration observed at 12 months (Slow *et al.*, 2003; van Raamsdonk *et al.*, 2005). Despite the fact that both the R6/2 and YAC128 models contain two copies of normal *Htt*, they develop a phenotype that resembles HD. Although loss-of-function may contribute to some aspects of HD, these data indicate that HD is predominantly a gain-of-function disorder. The fact that R6/2 mice display HD-like symptoms much earlier than YAC128 mice indicates that N-mHtt is more toxic than full-length protein, which is well supported in other animal (Schilling *et al.*, 1999; Menalled *et al.*, 2009), and cell (Hackam *et al.*, 1998; reviewed in Cattaneo and Sipione, 2001), models of HD.

1.4 CELLULAR EFFECTS OF MUTANT HUNTINGTIN

Decades of basic research have demonstrated that the pathogenesis of HD involves alterations to multiple biochemical pathways. Cellular effects of mHtt that have been identified include: 1) altered mRNA expression of a subset of genes, 2) impaired autophagy and proteosomal degradation, 3) excitotoxicty, 4) mitochondrial dysfunction, 5) decreased cholesterol biosynthesis, 6) decreased production of BDNF, and 7) increased p53-mediated apoptosis. Although mHtt is expressed from birth in HD patients, HD is a late-onset disorder. It is possible that some cellular changes are a direct effect of mHtt, while others may be compensatory changes that occur throughout the progression of HD. Given that changes that occur early in the disease are more likely to represent direct effects of mHtt, targeting early cellular effects of mHtt may represent the best method to stop or slow progression of HD.

1.4.1 Altered mRNA expression of a subset of genes

Altered mRNA expression of a subset of genes is one of the earliest detectable changes in patients with HD as well as animal models of HD. Altered mRNA expression was first observed in a study that demonstrated that dopamine receptor D_2 mRNA was decreased in the caudate and putamen of tissue from HD patients with absent to low grade degeneration compared to age-matched controls (Augood *et al.*, 1997). Importantly, this study showed that the number of copies of D_2 mRNA per cell was decreased, which eliminated the possibility that decreased overall D_2 mRNA expression was a consequence of cell death. Approximately 1.7% of genes were altered in 6 week-old, early symptomatic R6/2 mice relative to age-matched wild-type mice in a gene microarray

study that examined over 6000 genes (Luthi-Carter *et al.*, 2000). Similar gene expression changes were observed in mice expressing the N-terminal 171 amino acids of Htt with a polyQ repeat-length of 82 (Luthi-Carter *et al.*, 2000). Decreases in gene expression were more common than increases in gene expression by approximately 3:1 (Luthi-Carter *et al.*, 2000). Genes with decreased expression belonged primarily to signal transduction, ion channel, transcription, metabolism, and cell structure pathways, while genes with increased expression belonged primarily to the inflammatory response pathway (Luthi-Carter *et al.*, 2000). Decreases could be detected at earlier time points than increases in gene expression, which led authors to hypothesize that increased expression of certain genes may be a compensatory mechanism or part of neuroinflammation (Luthi-Carter *et al.*, 2000). Gene expression changes have been demonstrated at early time points in other animal models of HD, including R6/1 mice at 12 weeks of age concurrent with onset of motor changes and well before death which occurs at >1 year (Hodges *et al.*, 2008). Dopamine-and cAMP-regulated phosphoprotein 32 kDa (DARPP-32) and preproenkephalin mRNA was decreased in the striatum of 6 week old R6/2 mice, which was before the onset of motor symptoms at 8 weeks (Bibb *et al.*, 2000). Cannabinoid 1 (CB1) receptor mRNA was decreased in lateral striatum of R6/1 mice and R6/2 mice at 5 and 3 weeks of age respectively, which was before onset of motor symptoms at 12 and 8 weeks respectively (McCaw *et al.*, 2004). Phosphodiesterase 10A and 1B mRNA was decreased in R6/1 and R6/2 mice at 6 and 4 weeks of age respectively (Hebb *et al.*, 2004). Reduced expression of BDNF was observed in 6-month-old mice expressing Htt with a polyQ repeat-length of 97 in a bacterial artificial chromosome (BAC; Gray *et al.*, 2008). The reduction in BDNF was concurrent with the onset of motor symptoms and before

onset of striatal and cortical degeneration at 12 months of age (Gray *et al.*, 2008). Together, these data indicate that decreased mRNA expression of a subset of genes occurs early in HD pathogenesis and that increased expression of certain genes may be a compensatory mechanism or part of neuroinflammation.

Cell models of HD have shown that N-mHtt alters transcription of specific genes in a cell autonomous manner, and not as a consequence of altered cellular signaling. Decreases in mRNA of preproenkephalin, dopamine D_1 receptor, CB1 receptor, and DARPP-32 were detected in primary striatal neurons expressing N-mHtt (Runne *et al.*, 2008). Peroxisome proliferator-activated receptor gamma co-activator 1-alpha (PGC-1α) mRNA was decreased in immortalized striatal cells derived from knock-in mice made to express exon 1 of *Htt* containing 111 CAG repeats within the context of the full-length mouse *Hdh* gene (ST$Hdh^{Q111/Q111}$ cells) compared to cells derived from knock-in mice made to express *Htt* with 7 CAG repeats (ST$Hdh^{Q7Q/7}$ cells; Cui *et al.*, 2006). Microarray data from immortalized striatal cells expressing inducible N-mHtt showed changes in mRNAs involved in lipid metabolism, vesicle trafficking and transcription within 24 hours after induction of N-mHtt expression (Sipione *et al.*, 2002). These data support the hypothesis that transcriptional dysregulation is a direct effect of N-mHtt.

Altered mRNA expression leading to altered protein abundance may explain many of the cellular changes observed in HD patients and animal models. The transcriptional co-activator PGC-1α is expressed from nuclear DNA and regulates the expression of many mitochondrial genes (Lin *et al.*, 2005). PGC-1α mRNA expression is decreased in presymptomatic HD patients and cell models of HD (Cui *et al.,* 2006). Mitochondrial dysfunction including defective mitochondrial calcium handling, defective ATP

production, and impaired respiratory chain function has been reported in late stage post-mortem brain samples of HD patients and some cellular models of HD (reviewed in Oliveira, 2010). Overexpression of PGC-1α improved mitochondrial dysfunction in an HD cell model and was neuroprotective in R6/2 mice (Cui *et al.,* 2006). Reduction of PGC-1α levels has also been shown to increase extrasynaptic NMDA receptor activity and susceptibility to excitotoxic insults in rat cortical and striatal neurons expressing mHtt (Puddifoot *et al.*, 2012). Impaired cholesterol biosynthesis has also been hypothesized to play a role in progression of HD (Valenza *et al.,* 2005; reviewed in Valenza *et al.*, 2011). Microarray analysis of an inducible striatal cell model of HD revealed that 3-hydroxy-3-methyl-glutaryl-Coenzyme A reductase (HMG-CoA reductase) mRNA was decreased shortly after induction of mHtt expression (Sipione *et al.,* 2002), which was confirmed in 6 week-old R6/2 mice and striatal tissue from grades 1 and 2 HD patients (Valenza *et al.,* 2005). HMG-CoA reductase is the rate-limiting enzyme in the synthesis of cholesterol (DeBose-Boyd, 2008). Decreased expression of the rate-limiting enzyme in cholesterol synthesis early in disease progression would be expected to lead to decreased cholesterol levels, which could contribute to HD pathogenesis (Valenza *et al.,* 2005; Valenza *et al.,* 2007). Transcription of the neurotrophic factor, BDNF, is also impaired in the presence of mHtt in cortical cells (Zuccato *et al.,* 2001). Reduced mRNA expression of BDNF in cortical cells is believed to lead to reduced transport of BDNF to striatal cells, which is believed to contribute to dysfunction and death of striatal cells (Zuccato *et al.,* 2001). Together, these experiments show how altered mRNA expression of a subset of genes may explain changes seen in multiple cellular processes implicated in HD pathogenesis.

1.4.2 Pathogenic mutant huntingtin mRNA

Although aberrant cellular processes are linked to mHtt protein, mutant *Htt* mRNA may also contribute to HD pathophysiology. The *Htt* transcript forms stem-loop structures characteristic of microRNA (miRNA) secondary structure (De Mezer *et al.*, 2011). Evidence indicates that RNA is the pathogenic molecule in the nucleotide repeat disorders myotonic dystrophy 1 and 2, as well as Fragile-X associated tremor/ataxia (reviewed in Orr and Zoghbi, 2007). Expression of untranslatable *Htt* exon 1 with 80 CAG repeats increased cell death and levels of cleaved caspase-9 in differentiated human neuroblastoma SH-SY5Y cells compared to expression of untranslatable *Htt* exon 1 with a non-pathogenic 23 CAG repeat length (Bañez-Coronel *et al.*, 2012). Knockdown of Dicer or Argonaut 2, two proteins involved in the RNA interference pathway, decreased cell death and levels of cleaved caspase-9 in SH-SY5Y cells expressing untranslatable *Htt* exon 1 with 80 CAG repeats down to levels observed in cells expressing *Htt* exon 1 with a non-pathogenic CAG repeat length, thus implicating RNA interference in RNA-mediated HD pathogenesis.

1.5 Cleavage and Nuclear Accumulation of N-Terminal Mutant Huntingtin

1.5.1 Cleavage

Both Htt and mHtt have a number of caspase and calpain cleavage sites in the N-terminal region of the proteins. Cleavage of mHtt at these sites generates N-terminal fragments of mHtt, which were shown to be more toxic than full-length mHtt in cell models of HD (Hackam *et al.*, 1998). Htt and mHtt can be cleaved *in vitro* by calpains at amino acids 469 and 536 (Gafni and Ellerby, 2002; Gafni *et al.*, 2004), by caspase-2 at

amino acids 552, by caspase-3 at amino acids 513 and 552, and by caspase-6 at amino acids 586 (Goldberg *et al.*, 1996; Wellington *et al.*, 1998; Hermel *et al.*, 2004). Cleavage products corresponding to the 552 cleavage site have been detected in non-HD human brain lysates (Wellington *et al.*, 2002), indicating that cleavage of Htt is a natural process. However, *in vitro*, caspase-2, caspase-3, and calpain-mediated cleavage of Htt are all increased with increasing length of polyQ such that the relative proportion of N-terminal to full-length protein is greater for mHtt than Htt (Goldberg *et al.*, 1996; Gafni and Ellerby, 2002; Hermel *et al.*, 2004). Increased cleavage of mHtt compared to Htt has been demonstrated in humans, as calpain cleavage products were detected in the caudate of human HD tissue but not in age-matched controls (Gafni and Ellerby, 2002). Caspase-6 cleavage at amino acid 586 seems to be particularly important for development of the HD phenotype, as YAC128 mice that are resistant to cleavage at amino acid 586, but not 513 or 552, do not develop the HD phenotype (Graham *et al.*, 2006). Cleavage of mHtt by caspase-2 also contributes to some aspects of the HD phenotype as YAC128 mice lacking caspase-2 (caspase-$2^{-/-}$) show protection from motor and cognitive impairments, but not striatal volume loss (Carroll *et al.*, 2011). Together, increased cleavage of mHtt compared to Htt plays an important role in HD pathogenesis as blocking caspase cleavage of mHtt reduces or ameliorates the HD phenotype.

1.5.2 Nuclear accumulation

Following cleavage, both N-Htt and N-mHtt can translocate to the nucleus, but only N-mHtt accumulates in the nucleus (Wheeler *et al.*, 2000; Havel *et al.*, 2009). There are no known nuclear localization signals in the N-terminal region of Htt, so it was

hypothesized that N-Htt and N-mHtt fragments below 40 kDa entered the nucleus via passive diffusion (Hackam *et al.*, 1998). More recently, it has been shown that N-Htt and N-mHtt can enter the nucleus by forming a complex with glyceraldehyde-3-phosphate dehydrogenase (GAPDH) and Siah1, a ubiquitin-protein E3 ligase (Bae *et al.*, 2006). Siah1 contains a nuclear localization signal, which allows it to translocate to the nucleus after binding to GAPDH in complex with N-Htt or N-mHtt in the cytoplasm. The affinity of Siah1 was shown to be greater for GAPDH in complex with N-mHtt compared to GAPDH in complex with N-Htt (Bae *et al.*, 2006). The increased affinity of Siah1 for GAPDH in complex with N-mHtt is believed to lead to accumulation of N-mHtt in the nucleus (Bae *et al.*, 2006).

Reduced export of N-mHtt from the nucleus is also believed to contribute to nuclear accumulation of N-mHtt. Export of N-mHtt and N-Htt is mediated in part through interactions with the nuclear pore protein, Tpr [translocated promoter region, which received its name after being identified as part of a chromosomal translocation in an osteogenic sarcoma cell line (Cornett *et al.*, 2005)]. Expansion of the polyQ region in Htt leads to reduced interactions of N-mHtt with Tpr and accumulation of N-mHtt in the nucleus as shown using HeLa cells transfected with N-Htt containing varying polyQ lengths (Cornett *et al.*, 2005). Phosphorylation of N-mHtt at serine 16 has been shown to be important for regulation of N-mHtt nuclear export as phosphorylation at this site led to reduced interaction of N-mHtt with Tpr and reduced clearance of N-mHtt from the nucleus in cultured primary rat striatal neurons (Havel *et al.*, 2011). Together, these data indicate that N-mHtt, but not N-Htt, accumulates in the nucleus through increased import to and reduced export from the nucleus.

Studies using cell culture models of HD show that nuclear accumulation of N-mHtt directly correlates with toxicity of N-mHtt. The addition of a nuclear localization signal to N-mHtt and subsequent expression in mouse neuroblastoma N2a cells led to an increase in N-mHtt in the nucleus, and a 111% increase in cell death compared to N-mHtt without the nuclear localization signal (Peters *et al.*, 1999). When the nuclear localization signal was switched for a nuclear export signal, the amount of N-mHtt in the nucleus decreased and cell death was 57% lower compared to N-mHtt without the nuclear export signal (Peters *et al.*, 1999). Consequently, nuclear accumulation of N-mHtt contributes to HD pathology in neuronal cells, while blocking nuclear accumulation of N-mHtt plays a protective role.

1.5.3 Toxic role of soluble versus aggregated N-terminal mutant huntingtin

One of the pathological hallmarks of HD is formation of neuronal intranuclear inclusions (NIIs), which consist of aggregated N-mHtt, ubiquitin, and other proteins (Sieradzan *et al.*, 1999). NIIs have been identified in brains of human HD patients (DiFiglia *et al.*, 1997) and brains of rat and mouse models of HD (Davies *et al.*, 1997), although the role of NIIs (pathogenic, protective, or inert) is not known. After the discovery that multiple transcriptional proteins are found in NIIs, it was hypothesized that formation of NIIs contributes to HD pathology by reducing the number of available transcriptional proteins, thereby decreasing transcription of genes necessary for cell survival (Boutell *et al.*, 1999; Steffan *et al.*, 2000). However, more recent evidence suggests that NIIs may be protective and that soluble N-mHtt may be the more toxic form of the protein. Striatal cells expressing N-mHtt with 47 polyQ repeats that formed

aggregates were significantly less likely to die than cells that did not form aggregates (Arrasate *et al.*, 2004). Inactivation of the ubiquitin-conjugating enzyme led to a decrease in the formation of NIIs and an increase in the percentage of cells that succumbed to apoptosis, suggesting that the NIIs were inhibiting cell death (Saudou *et al.*, 1998). A point mutation within amino acids 1-18 of mHtt blocked the formation of NIIs, increased nuclear entry of N-mHtt, and led to a dramatic increase in cellular toxicity of N-mHtt (Atwal *et al.*, 2007). Together, these data indicate that interactions of soluble N-mHtt with transcriptional proteins is more toxic to cellular function than aggregation of transcriptional proteins into NIIs.

1.6 Abnormal Protein-Protein Interactions of Mutant Huntingtin

A growing body of evidence indicates that abnormal protein-protein interactions between mHtt and other cellular proteins may contribute to pathogenesis of HD. mHtt/Htt interaction partners have been identified using co-immunoprecipitation (CoIP), glutathione S-transferase (GST)-pull down assays, yeast-two hybrid assays, and database cross-referencing (reviewed in Li and Li, 2004; Goehler *et al.*, 2004). A recent high-throughput study using a combination of yeast-two hybrid and affinity purification/mass spectrometry identified 234 proteins that interact with mHtt/Htt (Kaltenbach *et al.*, 2007). Proteins that interact with Htt/mHtt are involved in transcription, trafficking and endocytosis, signaling, proteolysis, aggregation, apoptosis, metabolism, and other miscellaneous processes (reviewed in Li and Li, 2004). Binding between proteins and mHtt/Htt is often enhanced or weakened in a polyQ length-dependent manner (reviewed in Li and Li, 2004). It is more often the case that expansion of the polyQ increases the

binding affinity of mHtt compared to Htt (reviewed in Li and Li, 2004). The majority of studies looking at binding partners of mHtt/Htt used fragments consisting of amino acids 1-230 or 1-588 amino acids (reviewed in Li and Li, 2004). Consequently, abnormal interactions identified in these studies can be attributed more specifically to abnormal interactions between N-mHtt and other proteins, rather than full-length mHtt and other proteins.

Fifty-eight proteins known to interact with N-mHtt/N-Htt are involved in transcription (reviewed in Miller and Hughes, 2011). N-mHtt/N-Htt binds components of the preinitiation complex (PIC) including, TATA-binding protein (TBP; van Roon-Mom *et al.*, 2002) and the RAP30 subunit of transcription factor II F (TFIIF; Zhai *et al.*, 2005). N-mHtt/N-Htt binds gene-specific activators, such as specificity protein 1 (Sp1; Li *et al.*, 2002) and p53 (Steffan *et al.*, 2000), as well as co-activators, CREB-binding protein (CBP; Steffan *et al.*, 2000; Cong *et al.*, 2005) and CA150 (Holbert *et al.*, 2001). N-mHtt/N-Htt also binds gene-specific repressors such as RE1-silencing transcription factor (REST; Zuccato *et al.*, 2003) and co-repressors such as, nuclear receptor co-repressor (N-Cor; Boutell *et al.*, 1999), mammalian SIN3 homolog A (mSin3A; Boutell *et al.*, 1999), and C-terminal binding protein (CtBP; Kegel *et al.*, 2002). Before interactions of N-mHtt/N-Htt with transcriptional proteins were shown to occur, Max Perutz and colleagues showed that synthetic extended polyQ repeats formed polyQ monomers held together in a β-sheet conformation by hydrogen bonds, which they termed polar zippers (Perutz *et al.*, 1994). The group hypothesized that polar zippers may favour abnormal interactions with polyQ-containing transcription factors and lead to symptoms of HD through sequestration of transcriptional proteins away from their site of action (Perutz *et al.*, 1994). Although it

is now known that N-mHtt interacts with transcriptional proteins with and without polyQ regions, evidence supports the hypothesis that sequestration of transcriptional proteins away from their site of action either into NIIs or soluble complexes with N-mHtt contributes to HD pathology (Steffan *et al.,* 2000; Nucifora *et al.*, 2001). Figure 1.1 shows a hypothetical promoter in which the gene-specific transcription factors, A and B, bind to specific recogntion sites on the DNA and enhance assembly of the PIC. Figure 1.2 shows different models for N-mHtt-mediated transcriptional dysregulation. According to the hypothesis put forward by Perutz and colleagues, sequestration of B either into aggregates (Fig. 1.2A) or soluble complexes (Fig. 1.2B) containing N-mHtt would reduce the pool of transcription factor B available for formation of the PIC, thus inhibiting transcription initiation. This hypothesis fits with data that reducing cleavage and nuclear accumulation of N-mHtt blocks the HD phenotype in cell (Peters *et al.*, 1999) and animal (Graham *et al.*, 2006) models of HD, as interactions of N-mHtt with transcriptional proteins would occur almost exclusively in the nucleus.

It is possible that N-mHtt also impairs transcription by incorporating into transcriptional complexes at the promoter (Fig. 1.2C). mHtt, but not wild-type Htt, was associated at the PGC-1α promoter in brains of knock-in $Hdh^{Q111/Q111}$ mice and ST$Hdh^{Q111/Q111}$ cells compared to wild-type controls (Cui *et al.*, 2006). Furthermore, RNA polymerase II (Pol II) occupancy was decreased at the PGC-1α promoter and PGC-1α mRNA levels were decreased in brains of $Hdh^{Q111/Q111}$ knock-in mice and ST$Hdh^{Q111/Q111}$ cells compared to wild-type controls (Cui *et al.*, 2006). N-mHtt repressed transcription only when targeted to DNA by the Gal4 DNA binding domain, suggesting that N-mHtt can repress transcription by directly affecting components of the basal transcription

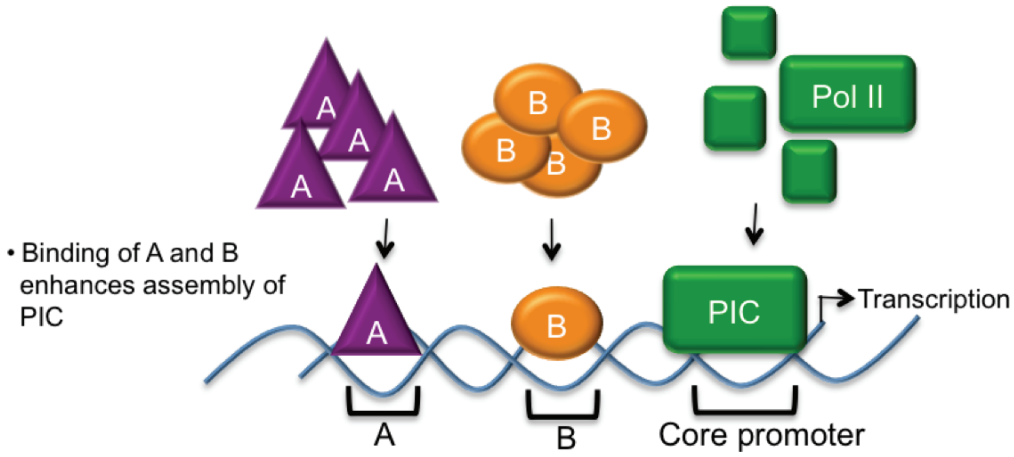

Figure 1.1. Hypothetical promoter. Gene-specific transcriptional proteins A and B bind recognition sites on the DNA and enhance binding of the preinitiation complex (PIC).

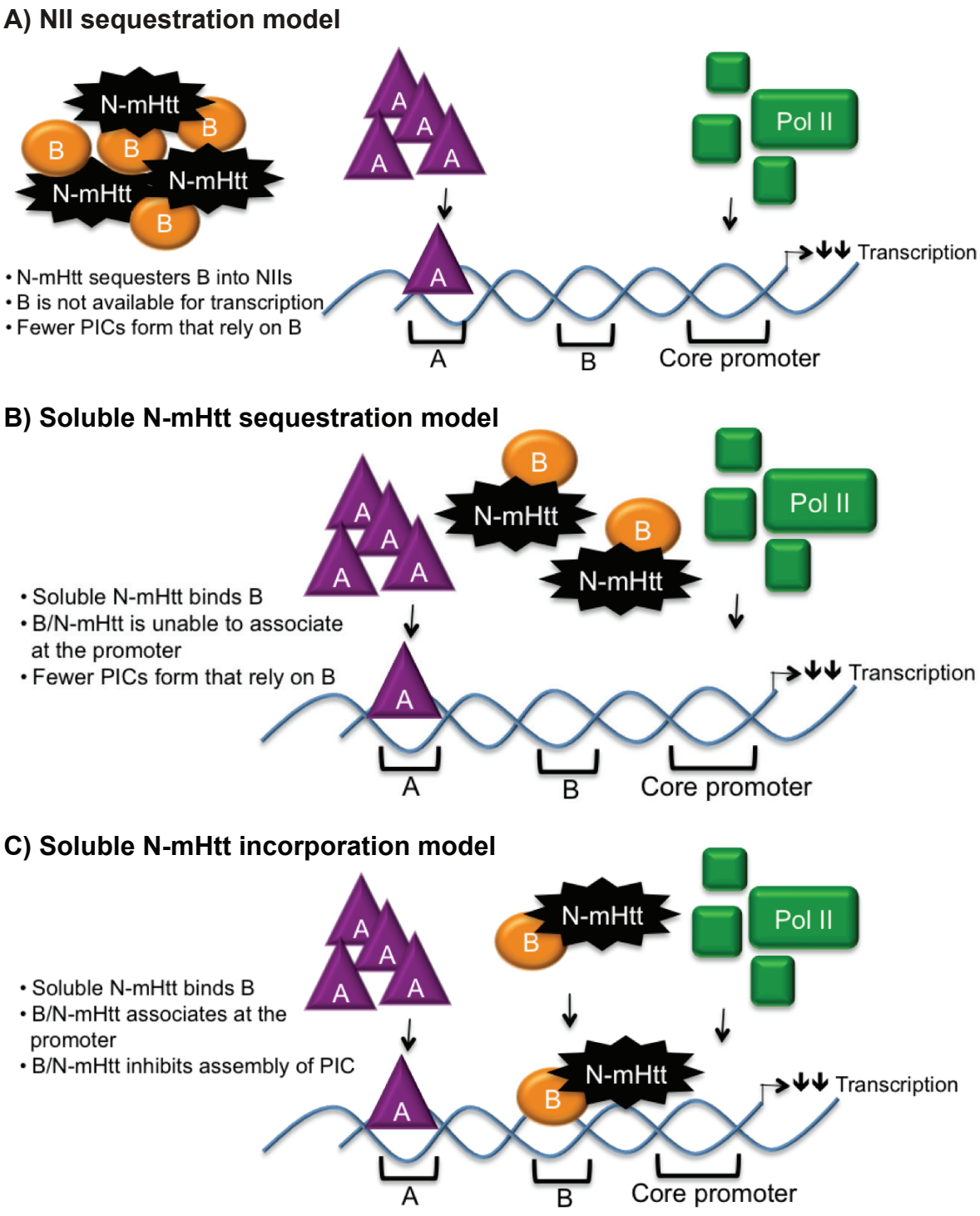

Figure 1.2. Models of N-mHtt-mediated transcriptional dysregulation. **A**) Neuronal intranuclear inclusions (NIIs) sequester transcriptional proteins and decrease soluble levels available for transcription. **B**) Soluble N-mHtt sequesters transcriptional proteins away from the promoter. **C)** Soluble N-mHtt incorporates into transcriptional complexes at the promoter, impairs binding of the preinitiation complex (PIC), and impairs transcription. A and B represent hypothetical gene-specific transcriptional proteins.

machinery rather than indirectly by sequestering essential transcription factors into aggregates (Kegel *et al.*, 2002). Htt with an expanded polyQ associated at the promoters of the N-mHtt affected genes, dopamine D_2 receptor and CB1 receptor, in brains of R6/2 mice (Benn *et al.*, 2008). Addition of Htt antibodies super-shifted several protein/probe chromatin complexes in an electromobility shift assay, indicating that Htt is associated with the PIC *in vitro* (Benn *et al.*, 2008). Recent evidence from our laboratory shows that N-mHtt associates at promoters of cytomegalovirus (CMV) and thymidine kinase, two viral promoters that are affected by N-mHtt (Hogel *et al.*, 2012). It is possible that N-mHtt is shuttled to the promoter through interactions with transcriptional proteins that contain promoter association domains. For example, for the hypothetical promoter described in figure 1.1, N-mHtt could bind to the transcription factor B, which contains a promoter association domain and, provided the interaction does not obstruct the promoter association domain, the entire B/N-mHtt complex could translocate to the promoter (Fig. 1.2C). At the promoter, N-mHtt could impair binding of components of the PIC and impair transcription initiation.

If abnormal interactions of N-mHtt with necessary transcription factors depletes the pool of functional transcription factors available for transcription, blocking abnormal interactions of N-mHtt in the nucleus may increase the pool of functional transcription factors and allow necessary transcription factors to perform their function. This may reverse symptoms and delay progression of HD. In theory, overexpressing proteins that bind specifically to N-mHtt, may be able to block abnormal interactions of N-mHtt. However, if N-mHtt impairs transcription by incorporating into transcriptional complexes at the promoter, overexpressing proteins that contain a promoter association domain

would not be expected to relieve transcriptional dysregulation, as the overexpressed protein would still be able to recruit N-mHtt to the promoter. For example at the hypothetical promoter described in figure 1.1, although overexpressing transcription factor B may increase the pool of B that is free to activate transcription, some amount of N-mHtt/B complexes would still be expected to associate at the promoter and impair transcription initiation (Fig. 1.3A). As an alternative, it may be possible to overexpress protein fragments that bind N-mHtt, but which lack a promoter association domain. As shown in figure 1.3B, overexpressing fragments of transcription factor B that are able to bind to N-mHtt, but lack a promoter association domain, may sequester N-mHtt away from the promoter, thereby allowing endogenous B to carry out its normal function of enhancing assembly of the PIC and initiating transcription. Thus, overexpressing protein fragments that bind N-mHtt but lack promoter association domains may block abnormal interactions of N-mHtt in the nucleus and normalize N-mHtt-mediated transcriptional dysregulation.

1.7 N-Terminal Mutant Huntingtin-Mediated Impairment of CREB-Binding Protein (CBP)

CBP is a gene-specific transcriptional co-activator with AT activity. CBP is localized exclusively to the nucleus where it can interact with the basal transcription factors TBP (Swope *et al.*, 1996; Dallas *et al.*, 1997), TFIIB (Kwok *et al.*, 1994), and RNA Pol II via an interaction with RNA helicase A (Nakajima *et al.*, 1997). In addition, CBP can bind to a variety of diverse nuclear proteins including, cAMP-response element binding protein (CREB; Kwok *et al.*, 1994), p53 (Lill *et al.*, 1997), c-Fos (Swope *et al.*, 1996), c-Jun (Bannister *et al.*, 1995), and c-Myb (Dai *et al.*, 1996). By interacting

A) Overexpressing N-mHtt interacting proteins with a promoter association domain

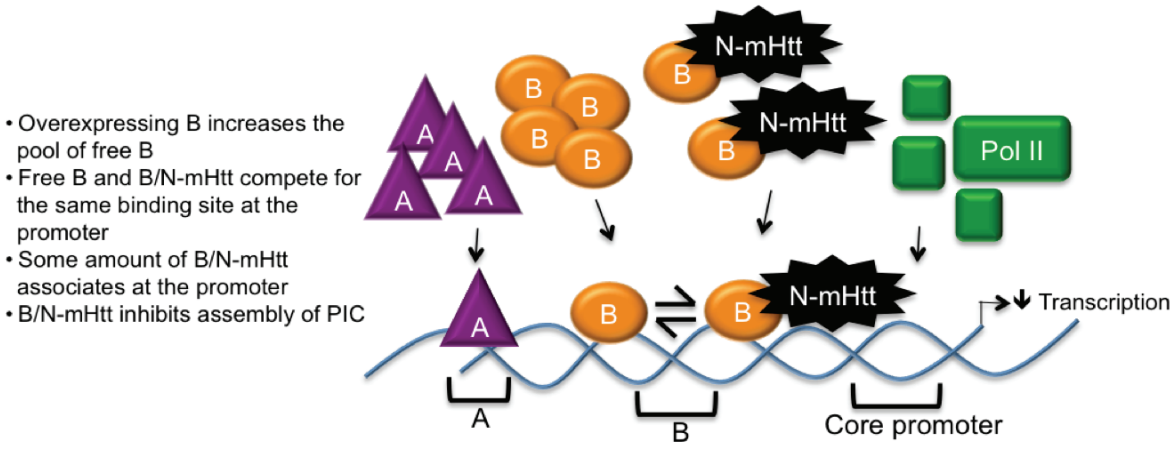

B) Overexpressing fragments of N-mHtt interacting proteins lacking a promoter association domain

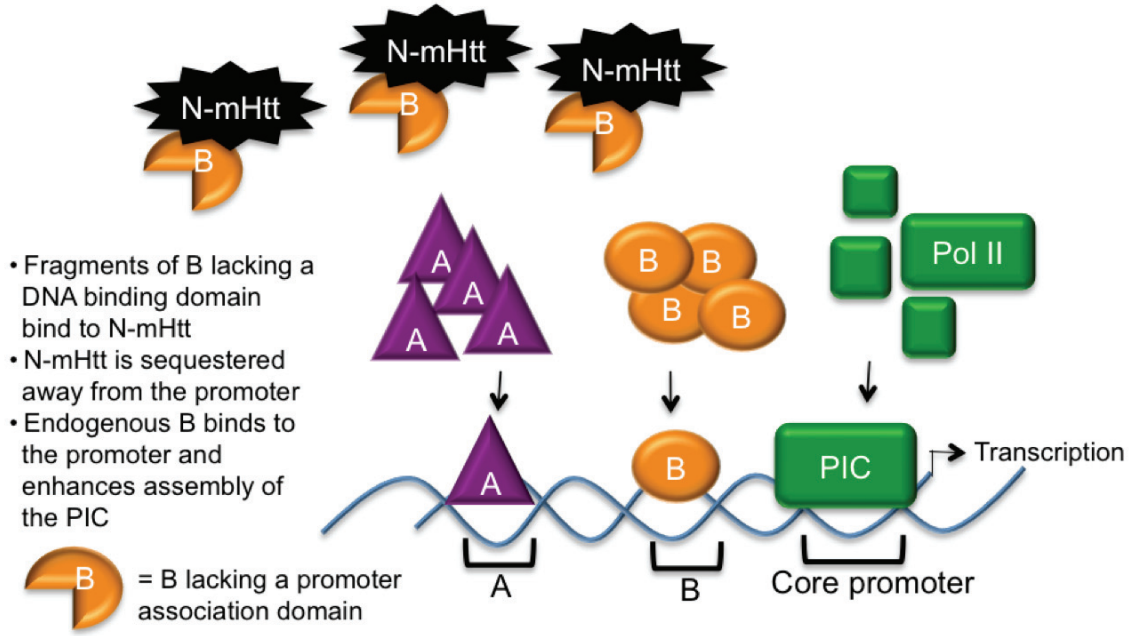

Figure 1.3. Overexpressing proteins to block abnormal interactions of N-mHtt in the nucleus. **A)** Overexpressing N-mHtt interacting proteins with a promoter association domain may allow N-mHtt to incorporate into transcriptional complexes at the promoter and inhibit transcription. **B)** Overexpressing fragments of N-mHtt interacting proteins that lack a promoter association domain may block abnormal interactions of N-mHtt at the promoter and reverse N-mHtt-mediated transcriptional dysregulation.

simultaneously with the basal transcription machinery and with one or more upstream transcription factors, CBP functions as a physical bridge or scaffold thereby enhancing assembly of the PIC and increasing efficiency of transcription initiation. The role of CBP in CREB signaling has been well studied (Goodman and Smolik, 2000; reviewed in Merz *et al.*, 2011). CREB binds to to cAMP-response element (CRE) at the promoter (reviewed in Merz *et al.*, 2011). CREB-mediated transcription is activated through a variety of pathways in response to different stimuli (reviewed in Merz *et al.*, 2011). Elevation of cAMP levels, through activation of stimulatory G ($G_{s)}$ protein coupled-receptors such as, dopamine D_1 and serotonin receptors, can activate protein kinase A (PKA), allow PKA to enter the nucleus, where it phosphorylates CREB at serine 133 (reviewed in Merz *et al.*, 2011). Phosphorylation of CREB at serine 133 allows CBP and the closely related transcriptional co-activator and AT, p300, to bind to CREB using a KIX domain (reviewed in Merz *et al.*, 2011). When bound to CREB, both CBP and p300 act as scaffolds for gene-specific transcription activators and components of the PIC (reviewed in Merz *et al.*, 2011). Phosphorylation of CREB at serine 133 can also occur through BDNF-mediated activation of mitogen-activated protein kinase (MAPK) and extracellular-signal-regulated kinase (ERK) pathways, as well as NMDA-, AMPA-, and kainate receptor-mediated activation of Ca^{2+} pathways (reviewed in Merz *et al.*, 2011).

A large number of the genes that are down-regulated in HD contain CRE in their promoters and are under the partial control of CBP, including preproenkephalin and preprosomatostatin (Luthi-Carter *et al.*, 2002) as well as PGC-1α (Cui *et al.*, 2006). After the finding that CBP was detected in NIIs in human HD brain tissue (Nucifora *et al.*, 2001) and striatal sections from R6/2 mice (Steffan *et al.*, 2000), it was hypothesized that

recruitment of CBP into aggregates leads to impaired CBP-dependent transcription via a reduction in the pool of functional CBP available for transcription (Steffan *et al.*, 2000; Nucifora *et al.*, 2001). CBP co-precipitated with N-mHtt containing 74 polyQ repeats, but not N-mHtt with 23 polyQ repeats (Cong et al, 2005). Binding of N-mHtt to p300, which is approximately 50% identical to CBP in amino acid sequence, was reduced compared to CBP, indicating that the interaction between CBP and N-mHtt is specific (Cong *et al.,* 2005). Depletion of nuclear CBP, but not p300, was associated with cellular toxicity in a single cell study of hippocampal HT22 cells transiently expressing the N-terminal 63 amino acids of mHtt with 148 polyQ repeats (Jiang *et al.*, 2006). Crossing of mice expressing N-mHtt with heterozygous knockout CBP mice led to progeny with decreased levels of CBP and decreased life expectancy compared to parental mice expressing N-mHtt (Klevytska *et al.*, 2010). Because CBP is a gene-specific co-activator, N-mHtt impairment of CBP could explain gene-specific alterations in mRNA levels observed in HD.

In addition to its co-activator function, CBP has AT activity, which allows CBP to enzymatically transfer a negatively charged acetyl group to lysine residues on the tail of core histones and other proteins (reviewed in Kalkhoven, 2004). Histone acetylation decreases the affinity of the positively charged histone tail for the negatively charged DNA, thereby relaxing chromatin structure, allowing transcriptional proteins to bind to the DNA, and thus facilitating gene transcription (reviewed in Kalkhoven, 2004). Acetylation of p53, GATA-binding protein 1 (GATA-1), and nuclear factor erythroid-derived 2 (NF-E2), by CBP can facilitate binding of these proteins to DNA and enhance gene transcription (reveiwed in Janknecht, 2002). Hypoacetylation of H3 has been

reported at the promoters of genes known to be down-regulated early in HD, including the dopamine D_2 receptor promoter, preproenkephalin, CB1 receptor, vitamin D receptor, and neural cell adhesion molecule, in R6/2 mice (Sadri-Vakili *et al.*, 2007). Steffan and colleagues (2001) demonstrated that N-mHtt with 51 polyQ repeats directly binds to fragments of CBP containing the AT domain using *in vitro* GST pull down assays. The group went on to show that the presence of N-mHtt *in vitro* leads to a loss of CBP histone acetyltransferase (HAT) activity (Steffan *et al.*, 2001). CBP HAT activity is critical for normal neurological function as point mutations that inactivate the AT domain of even one copy of CBP leads to Rubinstein-Taybi syndrome, a severe neurological disorder characterized by profound learning deficits and skeletal abnormalities (Kalkhoven *et al.*, 2003). Thus, evidence suggests that loss of CBP HAT activity contributes to HD pathology.

Based on the theory that loss of both HAT and transcriptional co-activator activity of CBP contributes to symptoms of HD, researchers have tested whether overexpressing CBP is beneficial in cell and animal models of HD. CBP overexpression resulted in decreased cell death in mouse neuroblastoma N2a cells and primary rat cortical neurons transiently expressing the 63 N-terminal amino acids of mHtt (Nucifora *et al.*, 2001). In addition, CBP overexpression restored H3 and H4 acetylation levels, normalized gene expression as shown using microarrays, and rescued retinal degeneration in *Drosophila* expressing a 127 polyQ fragment (Taylor *et al.*, 2003). Conversely, overexpressing CBP led to increased cell death in cerebellar granule neurons (Rouaux *et al.*, 2003). Cell death in the latter study was attributed to histone hyperacetylation, which led to non-specific gene expression (Rouaux *et al.*, 2003). These data indicate that fine-tuning of CBP HAT

activity is important for neuronal survival. Further studies aimed at compensating for CBP loss of function through overexpression of CBP have not been attempted.

In addition to compensating for CBP loss of function, it is possible that overexpressing CBP produced benefits in cells expressing N-mHtt, in part, by blocking abnormal interactions of N-mHtt with endogenous CBP and other nuclear proteins, thus increasing the pool of functional CBP and other nuclear proteins and overcoming N-mHtt-mediated transcriptional dysregulation. This is similar to the proposed effect of overexpressing the hypothetical transcription factor B described in figure 1.3A. However, if N-mHtt inhibits transcription by incorporating into transcriptional complexes at the promoter, overexpressing CBP would not be expected to reverse N-mHtt-mediated transcriptional dysregulation as the CBP/N-mHtt complex could associate at the promoter through the KIX domain. A region of CBP containing a portion of the AT domain and the entire third zinc (Zn) finger region was shown to bind N-mHtt *in vitro* (Steffan *et al.*, 2001). Importantly, ATZnCBP lacked the KIX domain. It is conceivable that overexpressing this fragment would be able to block abnormal interactions of N-mHtt without causing CBP-specific recruitment of N-mHtt to the promoter, similar to the proposed effect of overexpressing fragments of the hypothetical transcription factor B that lack a promoter association domain (Fig 1.3B).

1.8 HYPOTHESIS AND OBJECTIVES

The studies outlined above indicate that N-mHtt impairs transcription either through incorporation into transcriptional complexes at the promoter or by sequestration of necessary transcription factors away from the promoter. If N-mHtt impairs

transcription by sequestering transcription factors away from the promoter, overexpressing N-mHtt-interacting proteins would increase the pool of active transcription factors and relieve transcriptional repression. However, if N-mHtt acts at the promoter, overexpressing N-mHtt-interacting proteins would not alleviate repression because the overexpressed protein could still anchor N-mHtt at the promoter. We hypothesized that overexpressing protein fragments that bind N-mHtt, but lack a promoter association domain, would block abnormal interactions of N-mHtt at the promoter and overcome transcriptional repression. The objective of this study was to test whether overexpressing full-length CBP or ATZnCBP could block N-mHtt-mediated transcriptional dysregulation and toxicity in a cell model of HD. The ATZnCBP fragment was chosen because it was shown to bind N-mHtt *in vitro* (Steffan *et al.*, 2001). Fine-tuning of CBP AT activity is necessary for normal neuronal function (Rouaux *et al.*, 2004). Because it is possible that the ATZnCBP fragment may have AT activity, which could be detrimental to cell viability, we also tested the effect of overexpressing a fragment of CBP containing only the third Zn finger region (ZnCBP). The cell model we used was the ST*Hdh* cell line. ST$Hdh^{Q7/Q7}$ cells were derived from mice with two copies of *Htt* containing 7 CAG repeats, ST$Hdh^{Q7/Q111}$ were derived from mice with one copy of *Htt* containing 7 CAG repeats and one copy of *mHtt* containing 111 CAG repeats, and ST$Hdh^{Q111/Q111}$ cells were derived from mice with two copies of *mHtt* containing 111 CAG repeats (Trettel *et al.*, 2000). ST*Hdh* cells were immortalized by infection with a defective retrovirus transducing the temperature-sensitive alleles (*A58/U19*) of the simian virus 40 large tumor antigen and geneticin-resistance genes (Trettel *et al.*, 2000). To determine the effect of overexpressing full-length CBP or CBP fragments on N-mHtt-

mediated transcriptional dysregulation, we used luciferase promoter activity assays. The effect of overexpressing full-length CBP or CBP fragments on toxicity was determined using Ethidium Homodimer-1 (EthD-1) and Fluoro-Jade C stains. EthD-1 emits red fluorescence upon intercalation with nucleic acids in membrane permeable cells. The loss of structural integrity of the plasma membrane is detrimental to cell viability and occurs during both apoptosis and oncosis (non-programmed, accidental cell death characterized by cell swelling; Fink and Cookson, 2005). Fluoro-Jade C staining correlates with TUNEL staining and is used to identify degenerating neurons (Wang *et al.*, 2011). The precise molecular target of Fluoro-Jade C staining in degenerating neurons is not known (Schmued *et al.*, 2005). By contrasting the effects of overexpressing full-length CBP and CBP fragments that lack the KIX-promoter association domain, we aimed to provide evidence for or against the incorporation model of N-mHtt-mediated transcriptional dysregulation.

CHAPTER 2 MATERIALS AND METHODS

2.1 CLONING

2.1.1 Preparation of electrocompetent InvF' *E. coli*

InvF' *E. coli* were grown overnight on Luria-Bertani (LB) agar plates at 37°C. The following day, a colony was selected and grown in 25 mL of 2x yeast tryptone (YT) broth [31 g/L 2x YT Microbial Medium (Sigma-Aldrich; Oakville, ON) in distilled water (dH_2O)] and grown overnight at 37°C with shaking at 250 rpm. The following morning, 5 mL of the overnight culture was subcultured in 500 mL of 2x YT broth and grown at 37°C with shaking at 250 rpm until an absorbance of 0.6-1.0 was reached at a wavelength of 600 nm. Cells were kept on ice for 30 min then centrifuged at 2,500 x *g* and 4ºC for 20 min. The cell pellet was washed 3 times with ice cold dH_2O followed by 1 final wash with 1% glycerol (in dH_2O). Cells were resuspended in 3 mL of 1% glycerol, divided into 40 µL aliquots, and stored at -80°C.

2.1.2 PCR amplification and gel extraction

DNA regions corresponding to amino acids 1405-1846 (ATZnCBP) and 1709-1846 (ZnCBP) of CBP were amplified from full-length CBP (GenBank: AB210043.1) cloned into pBluescript II SK+ (Product ID: ORK07683; Kazusa; Japan) using primers described in table 1. Sense primers contained a 5' *Bam*H1 restriction site, while antisense primers contained a 5' *Not*1 restriction site. Sense and antisense primers (500 nM) were combined with 100 ng DNA template, 500 µM dNTP mix (dATP, dGTP, dTTP, dCTP nucleotide mixes from Fermentas; Burlington, ON), 1x PCR Buffer, and 2 U Hot Start Taq Polymerase Enzyme [Buffers and Taq contained in Qiagen (Toronto, ON) Hot Start

Table 2.1. Primers used for PCR.

Primer Name	Orientation	Sequence	Annealing Temp
ATZnCBP	Sense	GGATCCCGTTGCCCTCCGCACAGCC	60°
ATZnCBP	Antisense	GCGGCCGCAGAAGGCAGACTCTGC	60°
ZnCBP	Sense	GGATCCCTGGGCCTGGATGACGAG	60°
ZnCBP	Antisense	GGATCCGGCTTAGATGATGAGAGCAAC	60°

Taq PCR Kit]. The PCR reaction was 10 min at 95°C followed by 40 cycles of 95°C for 30 s, 60°C for 30 s, and 72°C for 1 min, followed by a final 10 min extension at 72°C. PCR reaction products were resolved on 1% agarose gels in 0.5x TBE [44.5 mM Tris, 44.5 mM Boric acid, 1 mM EDTA and 0.25 μg/ml ethidium bromide] and visualized under ultraviolet (UV) illumination alongside a 1 kB DNA ladder. The desired PCR products were identified based on size, extracted using GenElute™ Gel Extraction Kit (Sigma-Aldrich), and eluted in 50 μL Tris-EDTA elution buffer (Sigma-Aldrich). DNA was purified using GenElute™ PCR clean-up kit (Sigma-Aldrich) according to manufacturer's instructions and eluted in 50 μL Tris-EDTA elution buffer (Sigma-Aldrich).

2.1.3 DNA precipitation

DNA solution was combined with 1/10 volume sodium acetate (3 M) and 2x volume 100% ice cold ethanol, mixed, and incubated at -20ºC for 1 h. DNA solution was centrifuged (20 min; 12,000 x *g*; 4ºC), supernatant was removed, and the DNA pellet was washed with 400 μL of 70% ethanol. DNA solution was centrifuged for 10 min at 12,000 x *g* and 4ºC and the supernatant was removed. An additional 2 min spin at 12,000 x *g* and 4ºC was performed to further separate DNA and ethanol. A 1 mL syringe and needle was used remove the remaining ethanol. The tube containing DNA was left open on ice for 10 min to allow residual ethanol to evaporate. DNA was resuspended in 10 μL dH_2O and the DNA concentration was measured using a spectrophotometer (Genequant III pro, Biochrom; Holliston, MA).

2.1.4 Cloning into pGEM-T vector

Resuspended PCR product was combined with 50 ng pGEM-T Vector, 1x T4 Ligation Buffer and 3 U T4 Ligase (all from Promega; Madison, WI) and incubated overnight at 4°C. The ligation reaction was precipitated with ethanol as described in section 2.1.3 and resuspended in 10 µL dH_2O. Ligation product was electroporated into InvF' electrocompetent *E. coli* cells. Electroporated cells were grown in LB broth at 37°C with shaking at 250 rpm for 1 h. After 1 h, 100 µL of bacterial culture was grown on LB plates containing 50 µg/mL carbenicillin (Sigma-Aldrich) and 25 mg/mL X-gal (Promega). Plates were incubated overnight at 37°C. pGEM-T colonies positive for insert presence were selected based on X-gal blue/white screening. White colonies were picked and inoculated into 1.5 mL of 2x YT broth containing 50 µg/mL carbenicillin. Cultures were grown overnight at 37°C with shaking at 250 rpm. Plasmids were isolated using GenElute^{TM} Plasmid Miniprep Kit (Sigma-Aldrich) according to the manufacturer's protocol. To confirm if ATZnCBP-pGEM and ZnCBP-pGEM had been obtained, isolated plasmid DNA was sequenced (GeneWiz; South Plainfield, NJ).

2.1.5 Subcloning into mammalian expression vectors

ATZnCBP and ZnCBP were digested out of pGEM-T vector using *Bam*H1 and *Not*1 restriction enzymes (Fermentas). According to manufacturer instructions, 50 ng DNA was combined with 1 U of *Bam*H1 and *Not*1, 10x buffer plus loading dye, and dH_2O up to 20 µL. Solutions were mixed then incubated at 37ºC for 30 min. Heating at 80ºC for 5 min inactivated restriction enzymes. Digestion products were fractionated on 1% agarose gel (80 V for 90 min) alongside a 1kB DNA ladder and visualized under UV

light. ATZnCBP and ZnCBP fragments were identified based on size, extracted using GenElute™ Gel Extraction Kit (Sigma-Aldrich), eluted in 50 µL Tris-EDTA elution buffer (Sigma-Aldrich), and purified by DNA precipitation as described in section 2.1.3. A 10 µg batch of pcDNA4HisC (Invitrogen; Burlington, ON) was digested with *Bam*H1 and *Not*1 restriction enzymes as described in section 2.1.4. DNA precipitation was performed as described in section 2.1.3. Following this, digested pcDNA4HisC was dephosphorylated to prevent re-circularization of cut vector during ligation. pcDNA4HisC (5 µg) was combined with 5 U alkaline phosphatase (Fermentas), 10 µL 10X buffer (Fermentas) and dH_2O up to 100 µL. The solution was mixed thoroughly, heated at 37ºC for 15 min, and heated at 75ºC for 5 min to inactivate the phosphatase enzyme. Following dephosphorylation, DNA precipitation was performed as described in section 2.1.3. DNA concentration was measured using a spectrophotometer (Genequant III pro). ATZnCBP and ZnCBP, previously digested with *Bam*H1 and *Not*1, were ligated into pcDNA4HisC (cut with *Bam*H1 and *Not*1) using T4 DNA ligase (Fermentas). Insert (75 ng) was combined with vector (25 ng), T4 DNA ligase (1 U; Fermentas), 5x T4 DNA ligase buffer (Fermentas), and dH_2O up to 20 µL. Solution was mixed and incubated at 4ºC overnight. Ligation product was precipitated using ethanol as described in section 2.1.3 and transformed into electrocompetent *E. coli*. *E. coli* were grown overnight on LB agar plates containing carbenicillin as described in section 2.1.4. Colonies were selected, inoculated in LB broth containing carbenicillin, and grown overnight as described in section 2.1.4. Plasmids were isolated using GenElute™ Plasmid Miniprep Kit (Sigma-Aldrich) according to the manufacturer's protocol. Identification of ATZnCBP-pcDNA4HisC was carried out using *Bam*H1 and *Not*1 restriction digest and DNA

sequencing (GeneWiz). Subcloning of ZnCBP from pGEM-T into pcDNA4HisC was carried out by Lake Pharma (Belmont, CA) and confirmed by DNA sequencing (Gene Wiz). Subcloning of full-length CBP from pBluescript II SK+ into pcDNA3.1+ was carried out by Lake Pharma and confirmed by DNA sequencing (Gene Wiz).

2.2 CELL CULTURE

2.2.1 Cells and media

Conditionally immortalized striatal progenitor cells derived from embryonic day 14 mice made to express human *Htt* exon 1 with 7 or 111 CAG repeats (within the context of full-length mouse *Htt*) were obtained from Coriell Institute for Medical Research (Camden, NJ). ST*Hdh*$^{Q7/Q7}$, ST*Hdh*$^{Q7/Q111}$, and ST*Hdh*$^{Q111/Q111}$ cells were grown at the permissive temperature of 33ºC with 95% air and 5% CO_2 in growth media: Dulbecco's Modified Eagle Medium supplemented with glutamine (0.29 g/L), Penicillin-Streptomycin (10,000 U) and 10% (v/v) Fetal Bovine Serum (all from Invitrogen) in 25 or 75 cm^2 flasks (Nunc; Rochester, NY). Twenty-four hours after reviving frozen cells, media was replaced with growth media (described above) supplemented with 400 μg/mL geniticin (Invitrogen). Cells were subcultured before reaching 100% confluence by washing cells twice with 1x Phosphate Buffered Saline (PBS) Solution (Sigma-Aldrich), harvesting with TrypLE (Invitrogen), and plating a known number of cells in a new flask containing fresh media. To induce differentiation of ST*Hdh* cells into a more neuronal-like phenotype, cells were subjected to serum-deprivation by washing cells twice with 1x PBS and incubating cells in ST*Hdh* media lacking Fetal Bovine Serum, a procedure that has been used elsewhere (Trettel *et al.*, 2000; Blázquez *et al.*, 2011). ST*Hdh* cells were

serum-deprived for 6 h prior to transfection, at which time development of projections, characteristic of post-mitotic ST*Hdh* cells, could be observed.

2.2.3 Preparation of cell culture plates

For all experiments, cells were grown on 24-, or 96-well cell culture plates (Corning costar, Sigma-Aldrich). Cell culture plates were incubated in 0.01% (w/v in cell culture grade dH_2O) poly-D-lysine (Sigma-Aldrich) for 1 h at 37°C. Each well was washed twice with dH_2O and dried overnight. Plates were stored at 4°C prior to use.

2.3 TRANSFECTIONS

2.3.1 Lipofectamine 2000 procedure

Cells were transfected using Lipofectamine 2000 (Invitrogen) according to the manufacturer's recommendations. Lipofectamine 2000 (1 mg/mL) was combined with Opti-MEM reduced serum media (Invitrogen), mixed, and incubated for 20 min at room temperature. DNA was combined with Opti-MEM, mixed, and incubated for 5 min at room temperature. Lipofectamine-DNA solutions [3:1 (uL:µg) respectively] were mixed and incubated at room temperature for 30 min to allow Lipofectamine-DNA complexes to form. Lipofectamine-DNA complexes were added to each well. Cells were incubated at 33ºC with 95% air and 5% CO_2 for 18-24 hours before further experimentation.

2.3.2 Quantification of transfection efficiency

Cells were grown in 96-well plates, serum-deprived for 6 h, and transfected with 50 ng GFP expressing vector (pEGFP-N1; BD Biosciences, Mississauga, Ontario) as

described in section 2.3.1. Eighteen hours later, cells were excited with UV light from an X-cite series 120 box (Lumen Dynamics; Missausaga, ON) and the green fluorescence emission was viewed using an inverted Zeiss Axiovert 100 microscope (Carl Zeiss Canada; Toronto, Ontario). Images were captured from 3 randomly selected areas of the well using an Infinity 3 camera and recorded using the Infinity Capture program (both from Carl Zeiss Canada). Bright field images were taken in the same field as fluorescence images to allow for quantification of the total number of cells present in each field of view. Image J was used to quantify the number of GFP positive cells and total cells. Transfection efficiency was calculated as the number of GFP positive cells divided by the total number of cells for each well. Three independent experiments were performed with 3 wells per cell type/treatment for each experiment, giving a total replicate number of 9 for each cell type/treatment.

2.4 PROMOTER ACTIVITY ASSAYS

2.4.1 Luciferase assay

ST*Hdh*$^{Q7/Q7}$, ST*Hdh*$^{Q7/Q111}$, and ST*Hdh*$^{Q111/Q111}$ cells were grown in 24-well plates, serum-deprived for 6 h, and transfected as described in section 2.4.1. Eighteen hours after transfection, cells were incubated with 10 μM forskolin (in DMSO) or an equal volume of DMSO for 2 h at 33°C with 95% air and 5% CO_2. Promoter activity was measured using the Dual-Luciferase® Reporter Assay System (Promega). Cells were washed twice with 200 μL of 1x PBS and incubated in 100 μL of 1x Passive Lysis Buffer for 30 min at room temperature with gentle shaking. Cells were scraped and collected into 0.5 mL eppendorf tubes. Luciferase activity was measured by adding 10 μL of

soluble sample to 50 µL of Luciferase Assay Substrate and quantifying the amount of light produced in the enzymatic reaction using a 20/20^{n} luminometer (Turner Biosystems by Promega). To account for any differences in cell number, firefly luciferase activity was normalized to total protein.

2.4.2 Protein quantification

Protein quantification was performed using Protein Assay Dye-Reagent (Bio-Rad; Mississauga, ON) according to the microassay procedure in 24-well plates. Protein assay dye-reagent consists of acidic Coomassie Brilliant Blue G-250 dye, which upon binding to protein, shifts the absorption maximum of the dye from 465 to 595 nm. A standard curve was created using known concentrations of bovine serum albumin (0, 1.2, 2.5, 5, 7, and 10 µg) in 800 µL dH_2O. Sample (4µL) was combined with 796 µL dH_2O. Bio-Rad dye reagent (200 µL/well) was added and the entire solution was mixed thoroughly by pipetting the solution up and down. Solutions were incubated at room temperature for 5 min. Standards and samples were analyzed in duplicate and averaged. Readings were taken using an EL_X-800 Universal Microplate Reader (Bio-Tek; Winooski, VT) at the 595 nm wavelength. The mass of protein in the unknown sample was determined by extrapolating from the standard curve using the light emission detected at 595 nm.

2.5 CMXROSAMINE STAIN

Chloromethyl-X-rosamine (CMXrosamine) is a lipophilic cationic dye that is concentrated inside functioning mitochondria through activity of the oxidative respiratory chain, which generates a negative mitochondrial membrane potential. ST*Hdh*$^{Q7/Q7}$and

ST*Hdh*$^{Q111/Q111}$ cells were grown in 96-well plates, serum-deprived for 24 or 72 h, and stained with 20 nM CMXrosamine in 1x PBS for 25 min at 33° C with 95% air/5% CO_2. Cells were washed 3 times for 5 min with 1x PBS with gentle shaking, protected from light. Cells were excited at 546 nm and the fluorescence emitted at 590 nm was detected using an inverted Zeiss Axiovert 100 microscope at 400x magnification. For each replicate, the gain was set to a level that allowed minimal detection of fluorescence in ST*Hdh*$^{Q111/Q111}$ cells and this was maintained for ST*Hdh*$^{Q7/Q7}$ cells of the same replicate. Images were captured using an Infinity 3 camera and recorded using the Infinity Capture program. Three images were acquired at random per well. Bright field images were taken in the same field of view as fluorescent images. Fluorescence levels were quantified using Image J and normalized to the total number of cells, as determined from bright field images.

2.6 Cytotoxicity Assays

2.6.1 Ethidium Homodimer-1 stain

ST*Hdh*$^{Q7/Q7}$, ST*Hdh*$^{Q7/Q111}$, and ST*Hdh*$^{Q111/Q111}$ cells were grown in 96-well plates, serum-deprived for 24 h, washed twice with 1x PBS, and incubated with 50 µL of 4 µM Ethidium Homodimer-1 (EthD-1; Invitrogen) in 1x PBS for 40 min at room temperature with gentle shaking, protected from light. Cells were washed once with 1x PBS then maintained in 1x PBS. Cells were excited at 509 nm and emission at 617 nm was viewed using an inverted Zeiss Axiovert 100 microscope. Images were captured using an Infinity 3 camera and recorded using the Infinity Capture program. Fields in the top, bottom, and middle area of the well were captured at random for each replicate. Bright field images

were taken in the same field of view as fluorescent images. The percentage of EthD-1 positive cells per total cells (as determined from bright field images) was determined for each replicate.

To determine if overexpressing CBP, ATZnCBP, or ZnCBP had an effect on EthD-1 staining, ST*Hdh*$^{Q7/Q7}$, ST*Hdh*$^{Q7/Q111}$, and ST*Hdh*$^{Q111/Q111}$ cells were grown in 96-well plates, transfected with 200 ng of either pcDNA3+, pcDNA4HisC, CBP-pcDNA3+, ATZnCBP-pcDNA4HisC, or ZnCBP-pcDNA4HisC, and stained with EthD-1. To identify transfected cells, cells were co-transfected with 50 ng GFP expressing vector (pEGFP-N1). Eighteen hours post-transfection, cells were stained with EthD-1 as described above. Cells were excited at 488 nm and 528 nm and emission at 509 nm and 617 nm was viewed. Fields in the top, bottom, and middle area of the well were captured at random for each replicate from which the percentage of EthD-1 and GFP positive cells per GFP positive cells was determined.

2.6.2 Fluoro-Jade C stain

ST*Hdh*$^{Q7/Q7}$, ST*Hdh*$^{Q7/Q111}$, and ST*Hdh*$^{Q111/Q111}$ cells were grown in 96-well plates, serum-deprived for 24 h, washed twice with 1x PBS, and fixed with 2% PFA for 1 h at room temperature. Cells were washed twice with dH_2O and incubated with 0.0001% Fluoro-Jade C for 10 min, protected from light, with gentle shaking. Cells were washed twice with dH_2O. Cells were excited at 488 nm and emission at 509 nm was viewed. Fields in the top, bottom, and middle area of the well were captured at random for each replicate. Bright field images were taken in the same field of view as fluorescent images.

The percentage of Fluoro-Jade C positive cells per total cells (as determined from bright field images) was determined for each cell type/treatment.

To determine whether overexpressing CBP, ATZnCBP, or ZnCBP had an effect on Fluoro-Jade C staining, ST*Hdh*$^{Q7/Q7}$, ST*Hdh*$^{Q7/Q111}$, and ST*Hdh*$^{Q111/Q111}$ cells were grown in 96-well plates, serum-deprived for 6 h, transfected with 200 ng of pcDNA3+, pcDNA4HisC, CBP-pcDNA3+, ATZnCBP-pcDNA4HisC, or ZnCBP-pcDNA4HisC, and stained with Fluoro-Jade C. To identify transfected cells, cells were co-transfected with 50 ng RFP expressing vector (mCherry-3L). Eighteen hours post-transfection, cells were stained with Fluoro-Jade C as described above. Cells were excited at 488 nm and 528 nm and emission at 509 nm and 617 nm was viewed. The percentage of Fluoro-Jade C and RFP positive cells per RFP positive cells was determined.

CHAPTER 3 RESULTS

PGC-1α mRNA is decreased in cell and animal models of HD as well as HD patients (Cui *et al.*, 2006). To test whether PGC-1α promoter activity was different in ST*Hdh*$^{Q7/Q7}$, ST*Hdh*$^{Q7/Q111}$, and ST*Hdh*$^{Q111/Q111}$ cells, we transfected cells with vector containing the -2533 to +78 region of the mouse PGC-1α gene driving expression of *luciferase* (PGC-1α-pGL3). To ensure that mHtt did not affect the ability of cells to take up DNA, we measured transfection efficiency in each ST*Hdh* cell type. Cells were transfected with equal amounts of vector expressing GFP (pEGFP-N1) and the percentage of GFP positive cells per total cells was determined 18 h later. There was no difference in the number of GFP positive cells per total cells between ST*Hdh*$^{Q7/Q7}$, ST*Hdh*$^{Q7/Q111}$, and ST*Hdh*$^{Q111/Q111}$ cells (Fig. 3.1), indicating that the presence of mHtt did not affect the ability of ST*Hdh* cells to take up DNA. For all promoter assays, luciferase activity was normalized to total protein concentration in each cell lysate. PGC-1α-driven-luciferase activity was low in all cell types tested. We hypothesized that treatment with the cAMP-elevating agent forskolin would increase PGC-1α promoter activity in ST*Hdh*$^{Q7/Q7}$, ST*Hdh*$^{Q7/Q111}$, and ST*Hdh*$^{Q111/Q111}$ as a previous study showed that PGC-1α expression in neurons is driven largely by a cAMP-response element (CRE) in the proximal region of the promoter (Cui *et al.*, 2006). We found that PGC-1α-driven luciferase activity was increased in ST*Hdh*$^{Q7/Q7}$, ST*Hdh*$^{Q7/Q111}$, or ST*Hdh*$^{Q111/Q111}$ cells incubated with 10 μM forskolin for 2 h compared to the same respective cell type incubated with and equal volume of DMSO (Fig. 3.2). PGC-1α-driven luciferase activity was lower in ST*Hdh*$^{Q111/Q111}$ cells compared to both ST*Hdh*$^{Q7/Q7}$ and ST*Hdh*$^{Q7/Q111}$ cells treated with

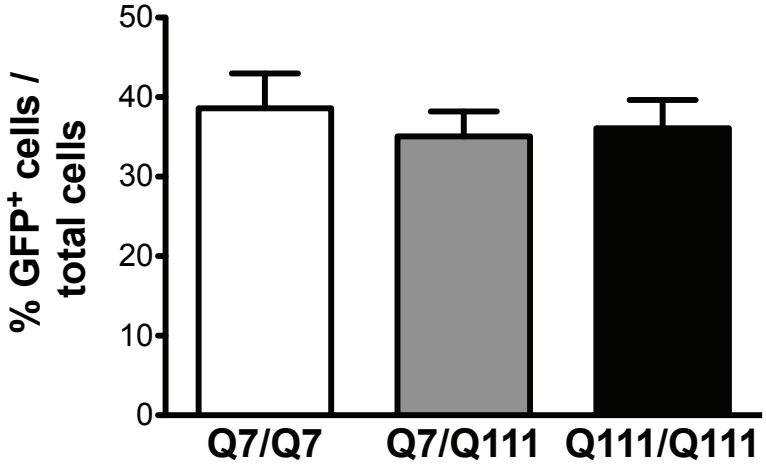

Figure 3.1. Transfection efficiency was not different between ST*Hdh*$^{Q7/Q7}$, ST*Hdh*$^{Q7/Q111}$, and ST*Hdh*$^{Q111/Q111}$ cells. Cells were grown to 60% confluence, serum-deprived, and transfected with vector expressing green fluorescent protein (GFP). Transfection efficiency was calculated as the percentage of GFP positive cells per total cells. Mean ± SEM (n = 9) is shown. $P > 0.05$ as determined by one-way ANOVA and Tukey *post-hoc* test.

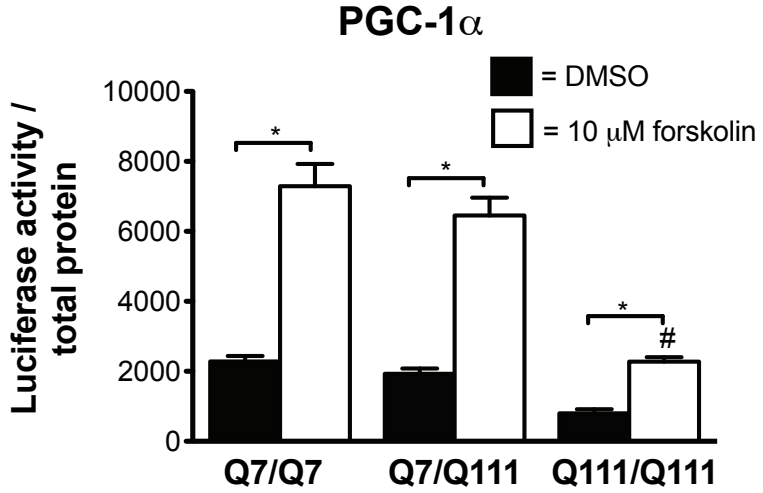

Figure 3.2. Forskolin treatment increased PGC-1α promoter activity in ST*Hdh*$^{Q7/Q7}$, ST*Hdh*$^{Q7/Q111}$, and ST*Hdh*$^{Q111/Q111}$ cells. PGC1-α promoter activity was decreased in ST*Hdh*$^{Q111/Q111}$ cells compared to ST*Hdh*$^{Q7/Q7}$and ST*Hdh*$^{Q7/Q111}$ cells treated with forskolin. Cells were transfected with 200 ng of vector containing PGC-1α promoter driving expression of firefly *luciferase* (PGC-1α-pGL3). Eighteen hours later, cells were incubated with 10 μM forskolin or an equal volume of DMSO (vehicle) for 2 h. Cells were lysed, luciferase activity was measured, and luciferase activity was normalized to total protein. Mean ± SEM (n = 6) is shown. * $P < 0.05$, and # $P < 0.05$ compared to ST*Hdh*$^{Q7/Q7}$and ST*Hdh*$^{Q7/Q111}$ cells treated with forskolin, as determined by one-way ANOVA and Tukey *post-hoc* test.

forskolin (Fig. 3.2). Luciferase activity was negligible in ST*Hdh*$^{Q7/Q7}$, ST*Hdh*$^{Q7/Q111}$, and ST*Hdh*$^{Q111/Q111}$ cells transfected with control pGL3 vector that lacked the PGC-1α promoter (data not shown). Thus, PGC-1α promoter activity was decreased in cells expressing 2 copies of mHtt (ST*Hdh*$^{Q111/Q111}$ cells) compared to cells expressing 1 copy of mHtt and 1 copy of wild-type Htt (ST*Hdh*$^{Q7/Q111}$ cells), and cells expressing 0 copies of mHtt and 2 copies of wild-type Htt (ST*Hdh*$^{Q7/Q7}$ cells).

Previous work in our laboratory has shown that cytomegalovirus (CMV) promoter activity is decreased in ST14A cells expressing the N-terminal 548 amino acids of Htt with an expanded polyQ and in ST*Hdh* cells expressing full-length mHtt compared to wild-type controls. Although CMV is not an endogenous promoter, we used it as a model for studying N-mHtt-mediated transcriptional dysregulation. To test whether forskolin treatment affected CMV promoter activity in ST*Hdh*$^{Q7/Q7}$, ST*Hdh*$^{Q7/Q111}$, and ST*Hdh*$^{Q111/Q111}$ cells, we transfected cells with vector containing the -757 base pair promoter region of CMV driving expression of *luciferase* (CMV-pGL3) and incubated cells with 10 μM forskolin or an equal volume of DMSO for 2 h prior to measuring luciferase activity. CMV-driven luciferase activity was not different between ST*Hdh*$^{Q7/Q7}$, ST*Hdh*$^{Q7/Q111}$, and ST*Hdh*$^{Q111/Q111}$ cells treated with forskolin and the same respective cell type treated with DMSO (Fig. 3.3). CMV-driven luciferase activity was decreased in ST*Hdh*$^{Q7/Q111}$ cells compared to ST*Hdh*$^{Q7/Q7}$ cells treated with DMSO or forskolin (Fig. 3.3). CMV-driven luciferase activity was decreased in ST*Hdh*$^{Q111/Q111}$ cells compared to both ST*Hdh*$^{Q7/Q7}$and ST*Hdh*$^{Q7/Q111}$ cells treated with DMSO or forskolin (Fig. 3.3). Luciferase activity was negligible in ST*Hdh*$^{Q7/Q7}$, ST*Hdh*$^{Q7/Q111}$, and ST*Hdh*$^{Q111/Q111}$ cells transfected with control pGL3 vector that lacked the CMV promoter (data not shown).

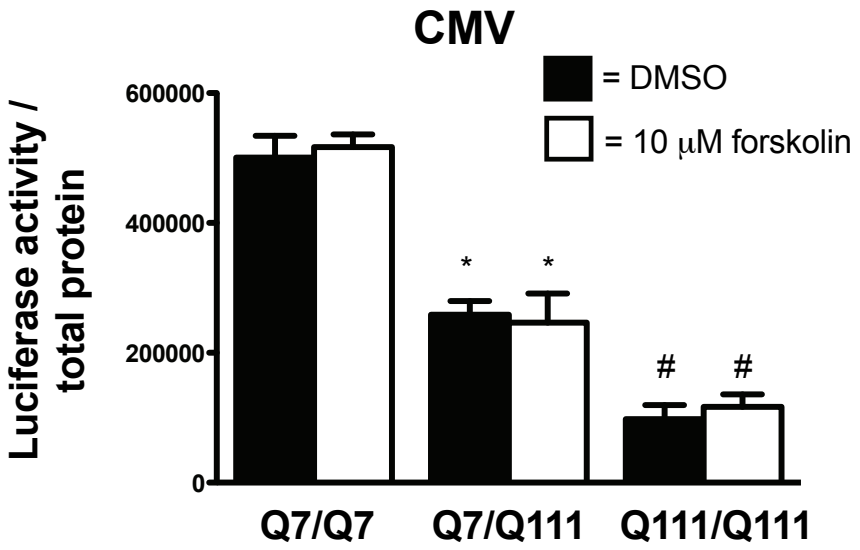

Figure 3.3. CMV promoter activity was decreased in ST*Hdh*$^{Q7/Q111}$ and ST*Hdh*$^{Q111/Q111}$ cells compared to ST*Hdh*$^{Q7/Q7}$ cells and CMV promoter activity was not affected by forskolin treatment. Cells were transfected with 50 ng of vector containing CMV promoter driving expression of firefly *luciferase* (CMV-pGL3). Eighteen hours later, cells were incubated with 10 μM forskolin or an equal volume of DMSO for 2 h. Cells were lysed, luciferase activity was measured, and luciferase activity was normalized to total protein. Mean ± SEM (n = 6) is shown. * $P < 0.05$ compared to ST*Hdh*$^{Q7/Q7}$ cells, # $P < 0.05$ compared to ST*Hdh*$^{Q7/Q7}$ and ST*Hdh*$^{Q7/Q111}$ cells as determined by one-way ANOVA and Tukey *post-hoc* test.

Consequently, CMV promoter activity was not affected by forskolin treatment. CMV promoter activity was decreased in a dose-dependent manner by mHtt.

It has been hypothesized that sequestration of CBP contributes to N-mHtt-mediated transcriptional dysregulation (Steffan *et al.*, 2000; Nucifora *et al.*, 2001). To determine whether overexpressing full-length CBP could overcome N-mHtt-mediated transcriptional dysregulation at the PGC-1α and CMV promoters, we measured promoter-driven luciferase activity in ST*Hdh*$^{Q7/Q7}$, ST*Hdh*$^{Q7/Q111}$, and ST*Hdh*$^{Q111/Q111}$ cells co-transfected with PGC-1α-pGL3 or CMV-pGL3 and either pcDNA3+ (empty vector) or CBP-pcDNA3+. PGC-1α-driven luciferase activity was decreased in ST*Hdh*$^{Q111/Q111}$ cells compared to both ST*Hdh*$^{Q7/Q7}$and ST*Hdh*$^{Q7/Q111}$ cells transfected with empty vector (Fig. 3.4). PGC-1α-driven luciferase activity was increased in ST*Hdh*$^{Q7/Q7}$ and ST*Hdh*$^{Q7/Q111}$ cells transfected with CBP vector compared to ST*Hdh*$^{Q7/Q7}$and ST*Hdh*$^{Q7/Q111}$ cells, respectively, transfected with empty vector, but was not different between ST*Hdh*$^{Q111/Q111}$ cells transfected with CBP vector and ST*Hdh*$^{Q111/Q111}$ cells transfected with empty vector (Fig. 3.4). Therefore, overexpressing full-length CBP increased PGC-1α promoter activity in cells expressing 0 or 1 copies of mHtt, but not in cells expressing 2 copies of mHtt, in which PGC-1α promoter activity was decreased compared to wild-type or heterozygous cells. CMV-driven luciferase activity was decreased in ST*Hdh*$^{Q7/Q111}$ cells compared to ST*Hdh*$^{Q7/Q7}$ cells transfected with empty vector (Fig. 3.5). CMV-driven luciferase activity was decreased in ST*Hdh*$^{Q111/Q111}$ cells compared to both ST*Hdh*$^{Q7/Q7}$and ST*Hdh*$^{Q7/Q111}$ cells transfected with empty vector (Fig. 3.5). CMV-driven luciferase activity was increased in ST*Hdh*$^{Q7/Q7}$cells transfected with CBP vector compared to ST*Hdh*$^{Q7/Q7}$cells transfected with empty vector, but was not

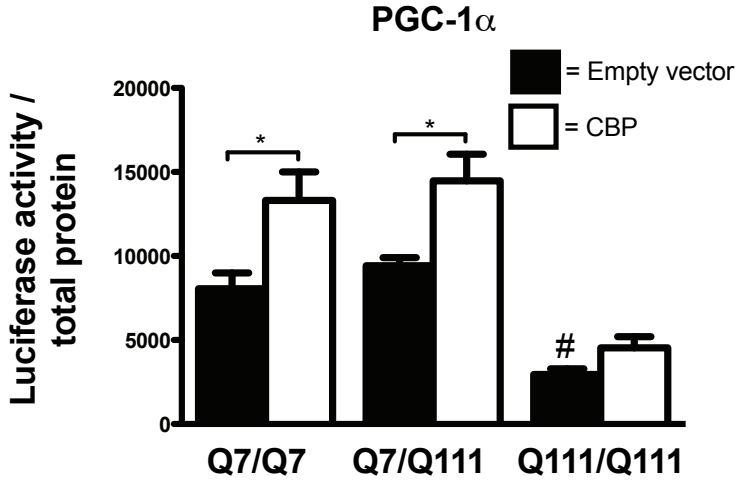

Figure 3.4. Overexpressing full-length CBP increased PGC-1α promoter activity in ST*Hdh*$^{Q7/Q7}$ and ST*Hdh*$^{Q7/Q111}$ cells, but not in ST*Hdh*$^{Q111/Q111}$ cells. Cells were transfected with 200 ng of vector containing PGC-1α promoter driving expression of firefly *luciferase* (PGC-1α-pGL3) along with 800 ng of empty vector (pcDNA3+) or 800 ng of CBP-pcDNA3+. Eighteen later, cells were incubated with 10 μM forskolin for 2 h. Cells were lysed, luciferase activity was measured, and luciferase activity was normalized to total protein. Mean ± SEM (n = 8) is shown. * $P < 0.05$, and # $P < 0.05$ compared to ST*Hdh*$^{Q7/Q7}$ and ST*Hdh*$^{Q7/Q111}$ cells transfected with empty vector, as determined by one-way ANOVA and Tukey *post-hoc* test.

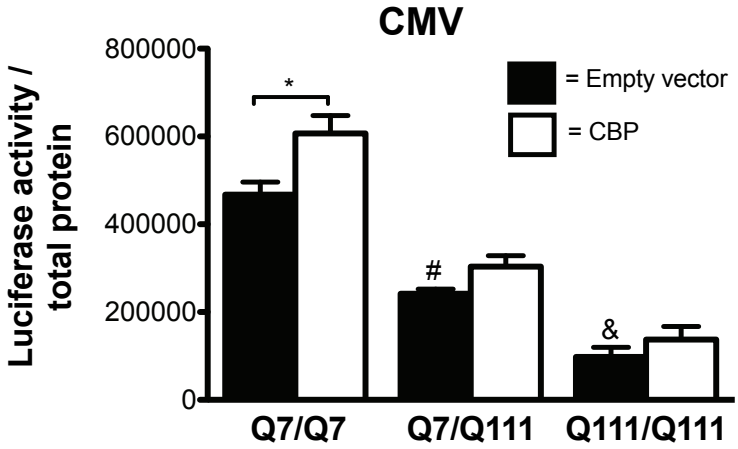

Figure 3.5. Overexpressing full-length CBP increased CMV promoter activity in ST*Hdh*$^{Q7/Q7}$cells, but not in ST*Hdh*$^{Q7/Q111}$ and ST*Hdh*$^{Q111/Q111}$ cells. Cells were transfected with 200 ng of vector containing CMV promoter driving expression of firefly *luciferase* (CMV-pGL3) along with 800 ng of empty vector (pcDNA3+) or 800 ng of CBP-pcDNA3+. Eighteen hours later, cells were incubated with 10 μM forskolin for 2 h. Cells were lysed, luciferase activity was measured, and luciferase activity was normalized to total protein. Mean ± SEM (n = 6) is shown. * $P < 0.05$, # $P < 0.05$ compared to ST*Hdh*$^{Q7/Q7}$ cells transfected with empty vector, and & $P < 0.05$ compared to ST*Hdh*$^{Q7/Q7}$ and ST*Hdh*$^{Q7/Q111}$ cells transfected with empty vector, as determined by one-way ANOVA and Tukey *post-hoc* test.

different between ST*Hdh*$^{Q7/Q111}$and ST*Hdh*$^{Q111/Q111}$ cells transfected with CBP vector compared to ST*Hdh*$^{Q7/Q111}$and ST*Hdh*$^{Q111/Q111}$ cells transfected with empty vector, respectively (Fig. 3.5). Thus, overexpressing full-length CBP increased CMV promoter activity in the absence of mHtt, but failed to overcome transcriptional repression in cells expressing 1 or 2 copies of mHtt. Because overexpressing full-length CBP increased PGC-1α and CMV promoter activity only in cells in which promoter activity was not different than wild-type cells, overexpressing full-length CBP did not reverse N-mHtt-mediated transcriptional dysregulation, but rather increased PGC-1α and CMV promoter activity in a general manner.

Mitochondrial dysfunction including, defective mitochondrial calcium handling, defective ATP production, and impaired respiratory chain function, has been reported in late-stage post-mortem brain samples of patients with HD and some cellular models of HD (reviewed in Oliveira, 2010). To test whether mitochondrial function was impaired in ST*Hdh*$^{Q111/Q111}$ cells compared to ST*Hdh*$^{Q7/Q7}$, we incubated each cell type with CMXrosamine after 24 h serum-deprivation and quantified relative fluorescence levels normalized to total cell number. CMXrosamine is a lipophilic cationic dye that is concentrated inside functioning mitochondria through activity of the oxidative respiratory chain, which generates a negative mitochondrial membrane potential (Pendergrass *et al.*, 2004). CMXrosamine fluorescence was not different between ST*Hdh*$^{Q7/Q7}$ and ST*Hdh*$^{Q111/Q111}$cells after 24 h serum-deprivation (Fig. 3.6). To determine whether a longer period of serum-deprivation would result in impaired mitochondrial function in ST*Hdh*$^{Q111/Q111}$ cells compared to ST*Hdh*$^{Q7/Q7}$ cells, we serum-deprived cells for 72 h and stained cells with CMXrosamine. CMXrosamine fluorescence was not different between

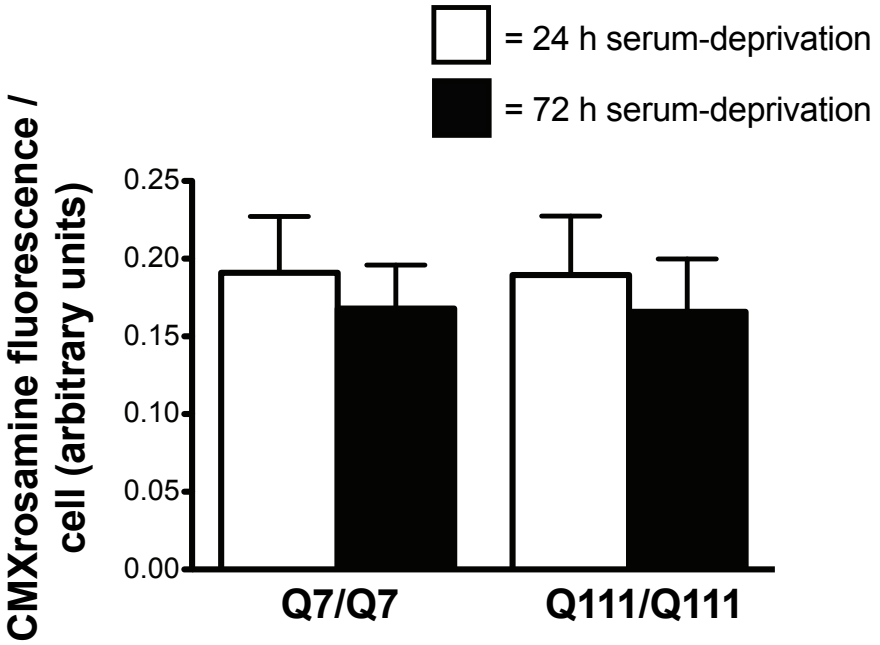

Figure 3.6. CMXrosamine fluorescence was not different between ST*Hdh*$^{Q7/Q7}$and ST*Hdh*$^{Q111/Q111}$ cells after 24 or 72 h serum-deprivation. Cells were grown in 96-well plates, serum-deprived for 24 or 72 h, and stained with 20 μM CMXrosamine, which labels metabolically active mitochondria. Mean ± SEM (n = 6) is shown. $P > 0.05$ as determined by one-way ANOVA and Tukey *post-hoc* test.

ST*Hdh*$^{Q7/Q7}$and ST*Hdh*$^{Q111/Q111}$ cells serum-deprived for 72 h (Fig. 3.6), indicating that mitochondrial membrane potential was not different between ST*Hdh*$^{Q7/Q7}$and ST*Hdh*$^{Q111/Q111}$ even after 72 h serum-deprivation. Because no difference in mitochondrial membrane potential was observed between ST*Hdh*$^{Q7/Q7}$and ST*Hdh*$^{Q111/Q111}$ cells after 24 or 72 h serum-deprivation, the effect of overexpressing CBP on CMXrosamine fluorescence was not examined.

Cells expressing mHtt are more sensitive to environmental insults and undergo increased degeneration compared to cells expressing wild-type Htt (Clarke *et al.*, 2000). To determine whether ST*Hdh* cells expressing mHtt undergo increased degeneration compared to cells expressing wild-type Htt in response to serum-deprivation, we stained ST*Hdh*$^{Q7/Q7}$, ST*Hdh*$^{Q7/Q111}$, and ST*Hdh*$^{Q111/Q111}$ cells with Ethidium Homodimer-1 (EthD-1) or Fluoro-Jade C following 24 h serum-deprivation. EthD-1 stains nucleic acids in membrane permeable cells. The loss of plasma membrane integrity is a late stage event during both apoptosis and non-programmed cell death (Fink and Cookson, 2005). Fluoro-Jade C staining correlates with TUNEL staining and is used to identify degenerating neurons (Wang *et al.*, 2011), although the mechanism of how Fluoro-Jade C specifically stains degenerating neurons is not known (Schmued *et al.*, 2005). The percentage of cells stained with EthD-1 (Fig. 3.7) or Fluoro-Jade C (Fig. 3.8) per total cells was increased in ST*Hdh*$^{Q7/Q111}$ cells compared ST*Hdh*$^{Q7/Q7}$cells, and ST*Hdh*$^{Q111/Q111}$cells compared to both ST*Hdh*$^{Q7/Q111}$cells and ST*Hdh*$^{Q7/Q7}$cells, after 24 h serum-deprivation. Thus, expression of mHtt increased toxicity in a dose-dependent manner following serum-deprivation.

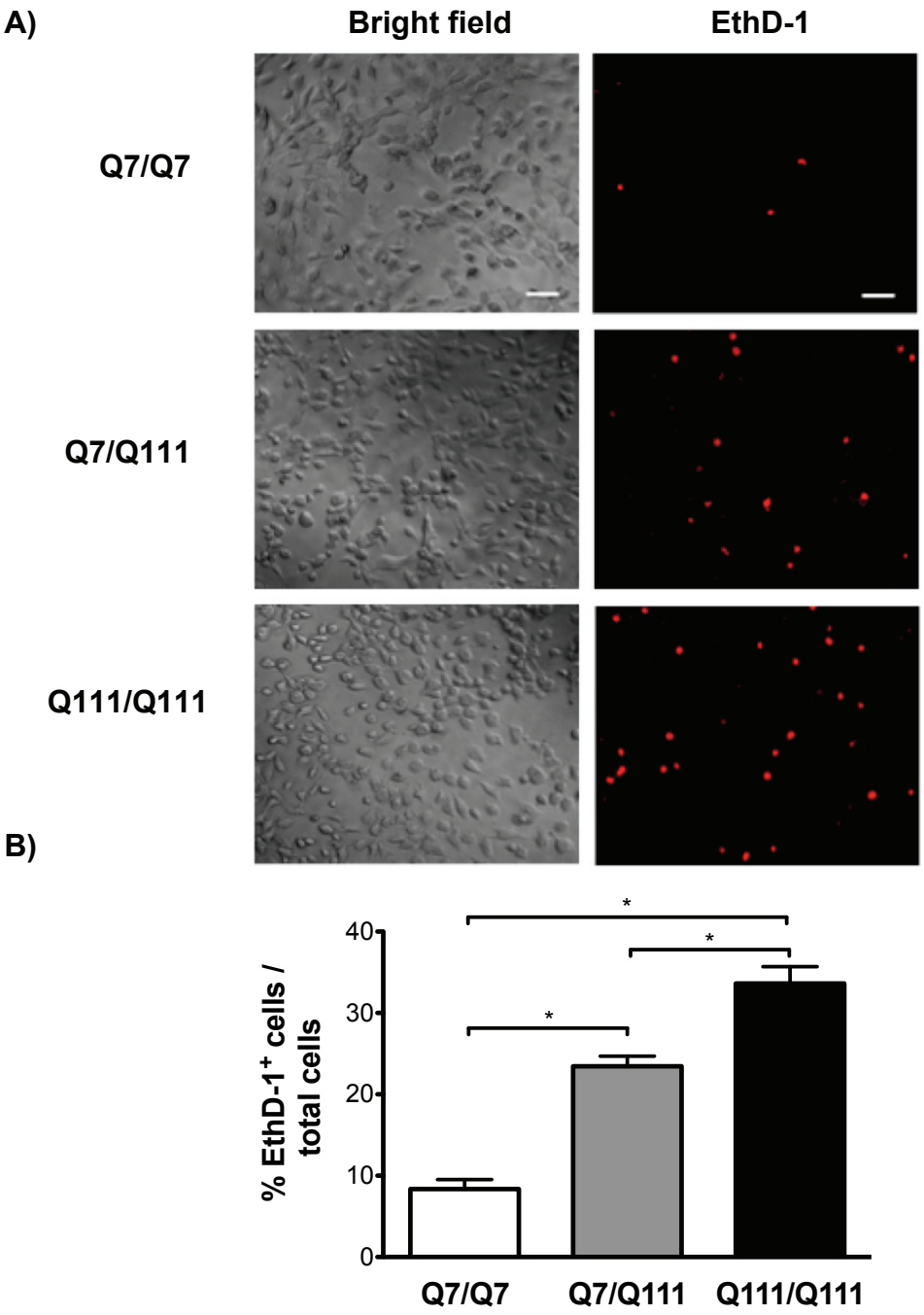

Figure 3.7. Ethidium Homodimer-1 (EthD-1) staining was higher in ST*Hdh*$^{Q7/Q111}$and ST*Hdh*$^{Q111/Q111}$ cells compared to ST*Hdh*$^{Q7/Q7}$cells after 24 h serum-deprivation. Cells were grown in 96-well plates, serum-deprived, and stained with 4 μM EthD-1, which stains nucleic acids in membrane permeable cells. **A)** Representative bright field or fluorescent images of ST*Hdh*$^{Q7/Q7}$, ST*Hdh*$^{Q7/Q111}$, and ST*Hdh*$^{Q111/Q111}$ cells stained with EthD-1 (red). **B)** Mean ± SEM (n = 6) percentage of EthD-1 positive cells per total cells. * $P < 0.05$ as determined by one-way ANOVA and Tukey *post-hoc* test. Scale bars equal 100 μm.

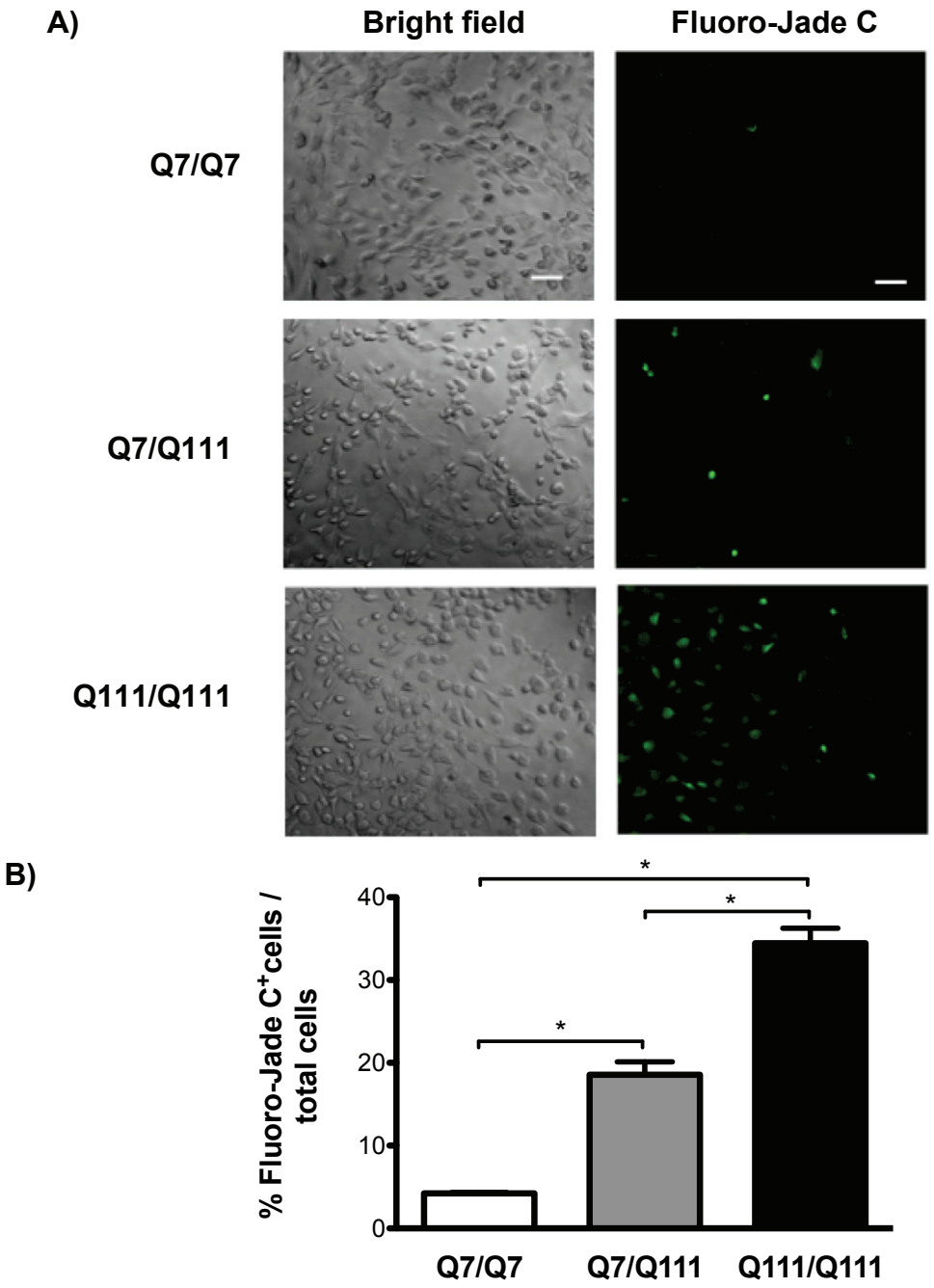

Figure 3.8. Fluoro-Jade C staining was higher in ST*Hdh*$^{Q7/Q111}$and ST*Hdh*$^{Q111/Q111}$ cells compared to ST*Hdh*$^{Q7/Q7}$cells after 24 h serum-deprivation. Cells were grown in 96-well plates, serum-deprived, and stained with 0.0001% Fluoro-Jade C, which labels degenerating neurons. **A)** Representative bright field and fluorescence images of ST*Hdh*$^{Q7/Q7}$, ST*Hdh*$^{Q7/Q111}$, and ST*Hdh*$^{Q111/Q111}$ cells stained with Fluoro-Jade C (green). **B)** Mean ± SEM (n = 6) percentage of Fluoro-Jade C positive cells per total cells. * $P <$ 0.05 as determined by one-way ANOVA and Tukey *post-hoc* test. Scale bars equal 100 μm.

Overexpressing full-length CBP was previously shown to increase toxicity in cerebellar granule neurons expressing wild-type Htt (Rouaux *et al.*, 2003), but decrease toxicity in neuroblastoma cells expressing mHtt (Nucifora *et al.*, 2001). To determine whether overexpressing CBP had an effect on toxicity in ST*Hdh*$^{Q7/Q7}$, ST*Hdh*$^{Q7/Q111}$, and ST*Hdh*$^{Q111/Q111}$cells, cells were transfected with pcDNA3+ or CBP-pcDNA3+ and serum-deprived for 24 h. To identify transfected cells, cells were transfected with GFP expressing vector (pEGFP-N1) or RFP expressing vector (mCherry-3L) and stained with EthD-1 or Fluoro-Jade C, respectively. The percentage of cells that were positive for EthD-1 and GFP per total number of GFP positive cells was increased in ST*Hdh*$^{Q7/Q7}$ cells transfected with CBP compared to ST*Hdh*$^{Q7/Q7}$cells transfected with empty vector, indicating that overexpressing CBP increased toxicity in ST*Hdh* cells expressing wild-type Htt (Fig. 3.9). The percentage of cells that were positive for EthD-1 and GFP per total number of GFP positive cells was decreased in ST*Hdh*$^{Q7/Q111}$ and ST*Hdh*$^{Q111/Q111}$cells transfected with CBP vector compared to ST*Hdh*$^{Q7/Q111}$ and ST*Hdh*$^{Q111/Q111}$cells, respectively, transfected with empty vector, indicating that overexpressing CBP was protective in ST*Hdh* cells expressing mHtt. The percentage of cells that were positive for EthD-1 and GFP per total number of GFP positive cells for ST*Hdh*$^{Q7/Q111}$ and ST*Hdh*$^{Q111/Q111}$cells transfected with CBP was not different than that of ST*Hdh*$^{Q7/Q7}$cells transfected with empty vector (Fig. 3.9). Similar effects of overexpressing full-length CBP were seen when using the Fluoro-Jade C staining technique (Fig. 3.10). Taken together, these data show that overexpressing full-length CBP increased toxicity in ST*Hdh* cells expressing wild-type Htt, but decreased toxicity in ST*Hdh* cells expressing 1 or 2 copies of mHtt to levels seen in untreated wild-type cells.

A)

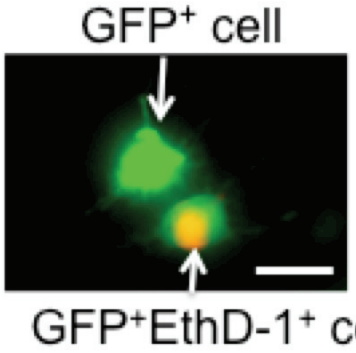

B)

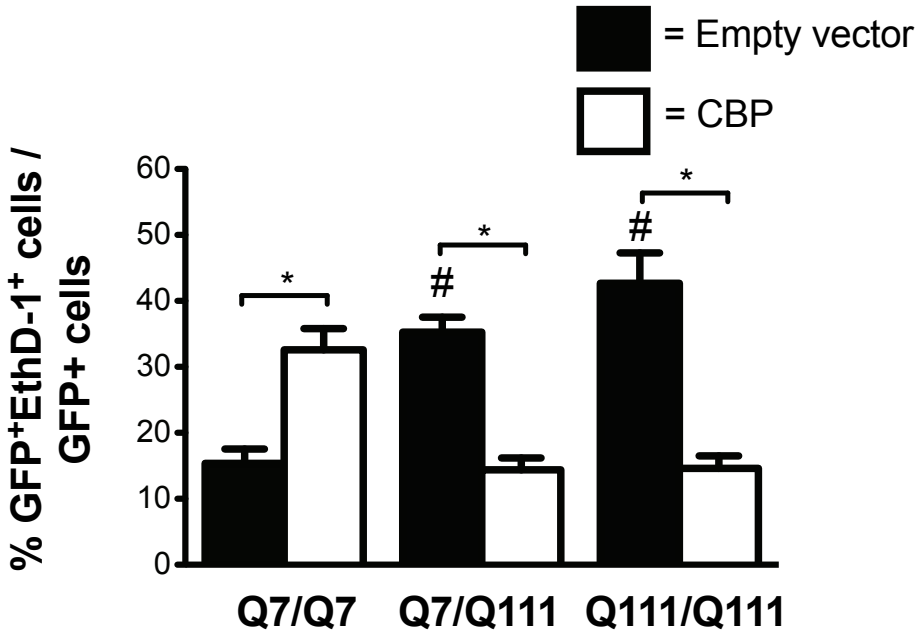

Figure 3.9. Overexpressing CBP increased EthD-1 staining in ST*Hdh*$^{Q7/Q7}$ cells, and decreased EthD-1 staining in ST*Hdh*$^{Q7/Q111}$ and ST*Hdh*$^{Q111/Q111}$ cells. Cells were grown to confluence in 96-well plates, serum-deprived, and transfected with 50 ng of GFP expressing vector along with 200 ng of empty vector (pcDNA3+), or CBP vector. Eighteen hours later, cells were incubated with 4 μM EthD-1, which stains nucleic acids in membrane permeable cells. **A**) Representative image showing a GFP positive cell (green; top) and a GFP positive cell stained with EthD-1 (red; bottom). **B)** Mean ± SEM (n = 9) percentage of GFP positive and EthD-1 positive cells per GFP positive cells. * $P <$ 0.05 and # $P <$ 0.05 compared to ST*Hdh*$^{Q7/Q7}$ cells transfected with empty vector, as determined by one-way ANOVA and Tukey *post-hoc* test. Scale bar equals 50 μm.

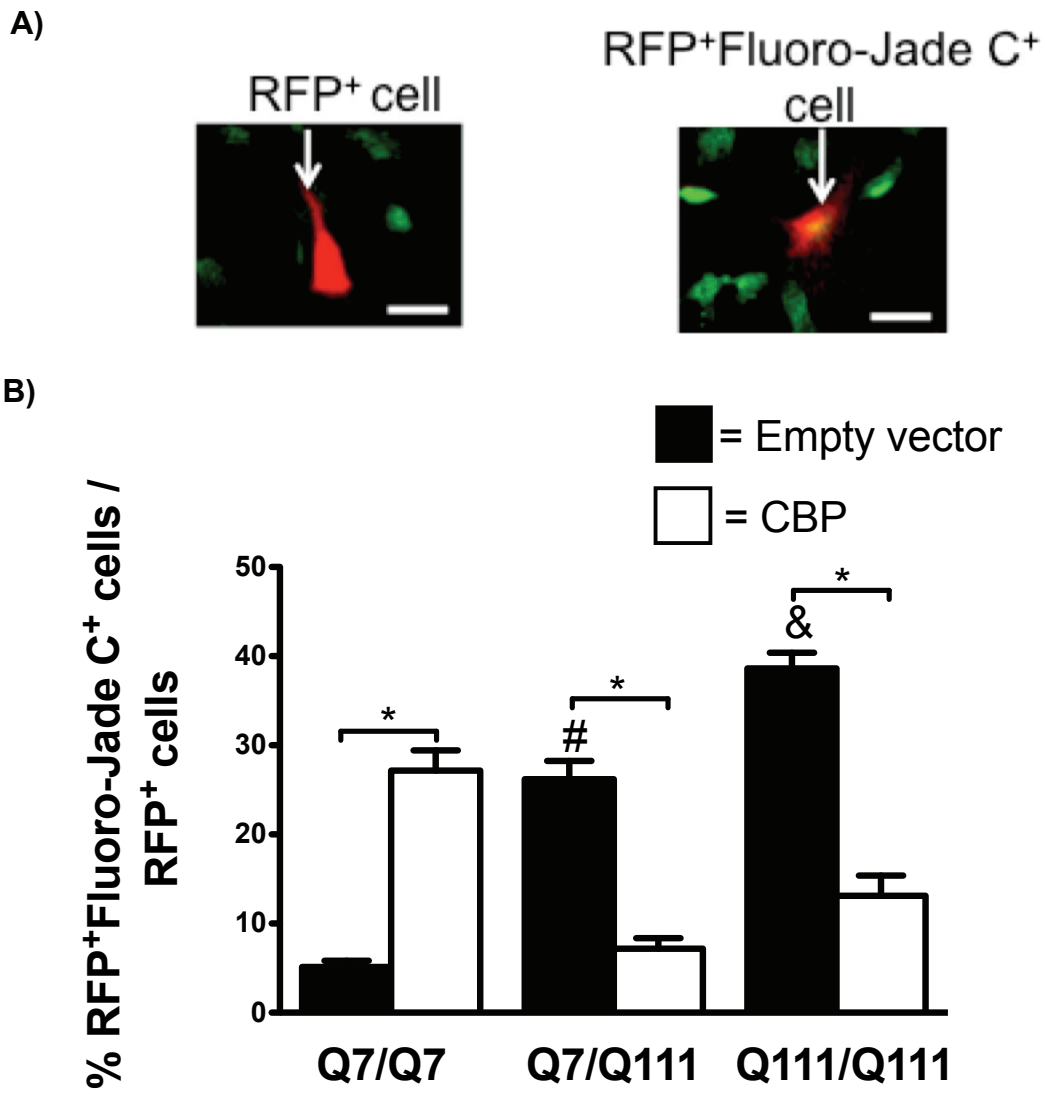

Figure 3.10. Overexpressing CBP increased Fluoro-Jade C staining in ST*Hdh*$^{Q7/Q7}$ cells, and decreased Fluro-Jade C staining in ST*Hdh*$^{Q7/Q111}$ and ST*Hdh*$^{Q111/Q111}$ cells. Cells were grown to confluence in 96-well plates, serum-deprived, and transfected with 50 ng of red fluorescent protein (RFP) expressing vector along with 200 ng of empty vector (pcDNA3+) or CBP vector. Eighteen hours later, cells were incubated with 0.0001% Fluoro-Jade C, which stains degenerating neurons. **A)** Representative images showing a RFP positive cell (red; left), a RFP and Fluoro-Jade C positive cell (yellow; right), and multiple Fluoro-Jade positive cells (green; left and right). **B)** Mean ± SEM (n = 9) percentage of RFP positive and Fluoro-Jade C positive cells. * $P < 0.05$, # $P < 0.05$ compared to ST*Hdh*$^{Q7/Q7}$ cells transfected with empty vector, and & $P < 0.05$ compared to ST*Hdh*$^{Q7/Q111}$ and ST*Hdh*$^{Q111/Q111}$ cells transfected with empty vector, as determined by one-way ANOVA and Tukey *post-hoc* test. Scale bars equal 50 μm.

CBP fragments corresponding to amino acids 1405-1846 (ATZnCBP) and 1709-1846 (ZnCBP) were cloned into pcDNA4HisC (Fig. 3.11). DNA sequencing was used to confirm that CBP fragments were cloned in-frame into pcDNA4HisC. To rule out the possibility that overexpressing ATZnCBP and ZnCBP may act as a dominant-negative to endogenous CBP function, we measured the effect of overexpressing ATZnCBP or ZnCBP on activity of an artificial promoter construct containing three tandem CREs driving expression of firefly *luciferase* (pCRE-Luc) in ST*Hdh*$^{Q7/Q7}$, ST*Hdh*$^{Q7/Q111}$, and ST*Hdh*$^{Q111/Q111}$ cells treated with forskolin. CRE-driven luciferase activity was not different between ST*Hdh*$^{Q7/Q7}$, ST*Hdh*$^{Q7/Q111}$, and ST*Hdh*$^{Q111/Q111}$ cells transfected with empty vector, indicating that mHtt did not decrease CRE-reporter activity (Fig. 3.12). CRE-driven luciferase activity was increased in ST*Hdh*$^{Q7/Q111}$ and ST*Hdh*$^{Q111/Q111}$ cells transfected with ATZnCBP or ZnCBP vectors compared to ST*Hdh*$^{Q7/Q111}$ and ST*Hdh*$^{Q111/Q111}$ cells, respectively, transfected with empty vector (Fig. 3.12), indicating that overexpressing ATZnCBP and ZnCBP did not act as a dominant-negative to endogenous CBP activity. CRE-driven luciferase activity was not different between ST*Hdh*$^{Q7/Q7}$ cells transfected with ATZnCBP or ZnCBP vectors and ST*Hdh*$^{Q7/Q7}$ cells transfected with empty vector (Fig. 3.12). Luciferase activity was negligible in ST*Hdh*$^{Q7/Q7}$, ST*Hdh*$^{Q7/Q111}$, and ST*Hdh*$^{Q111/Q111}$ cells transfected with control vector that lacked CREs and treated with forskolin (data not shown). Thus, overexpressing ATZnCBP and ZnCBP increased CRE promoter activity in ST*Hdh* cells expressing 1 and 2 copies of mHtt, but this effect was not related to the presence of mHtt, as CRE reporter activity was not different between ST*Hdh*$^{Q7/Q7}$, ST*Hdh*$^{Q7/Q111}$, and ST*Hdh*$^{Q111/Q111}$cells.

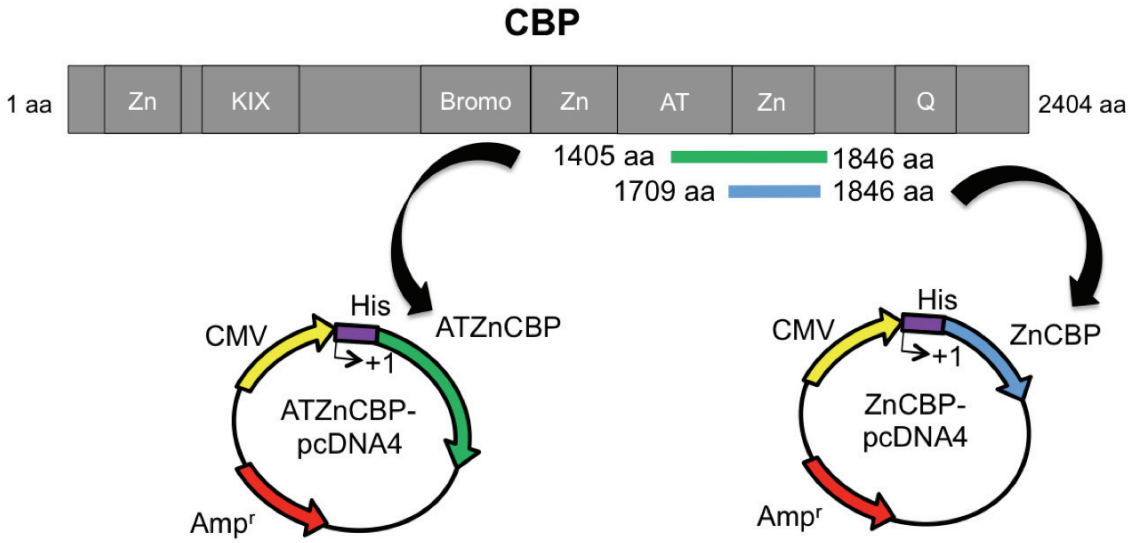

Figure 3.11. CBP fragments encompassing a portion of the acetyltransferase (AT) domain and the adjacent third zinc (Zn) finger region or the Zn finger region alone were cloned into the mammalian expression vector pcDNA4HisC. ATZnCBP and ZnCBP fragments are indicated relative to full-length CBP protein. Shown are the promoter and bacterial resistance elements of pcDNA4HisC. Amp^r, ampicillin resistance gene; Bromo, bromo domain; CMV, cytomegalovirus; His, 6 X N-terminal histidine tag; KIX, CREB-binding domain; Q, polyglutamine domain.

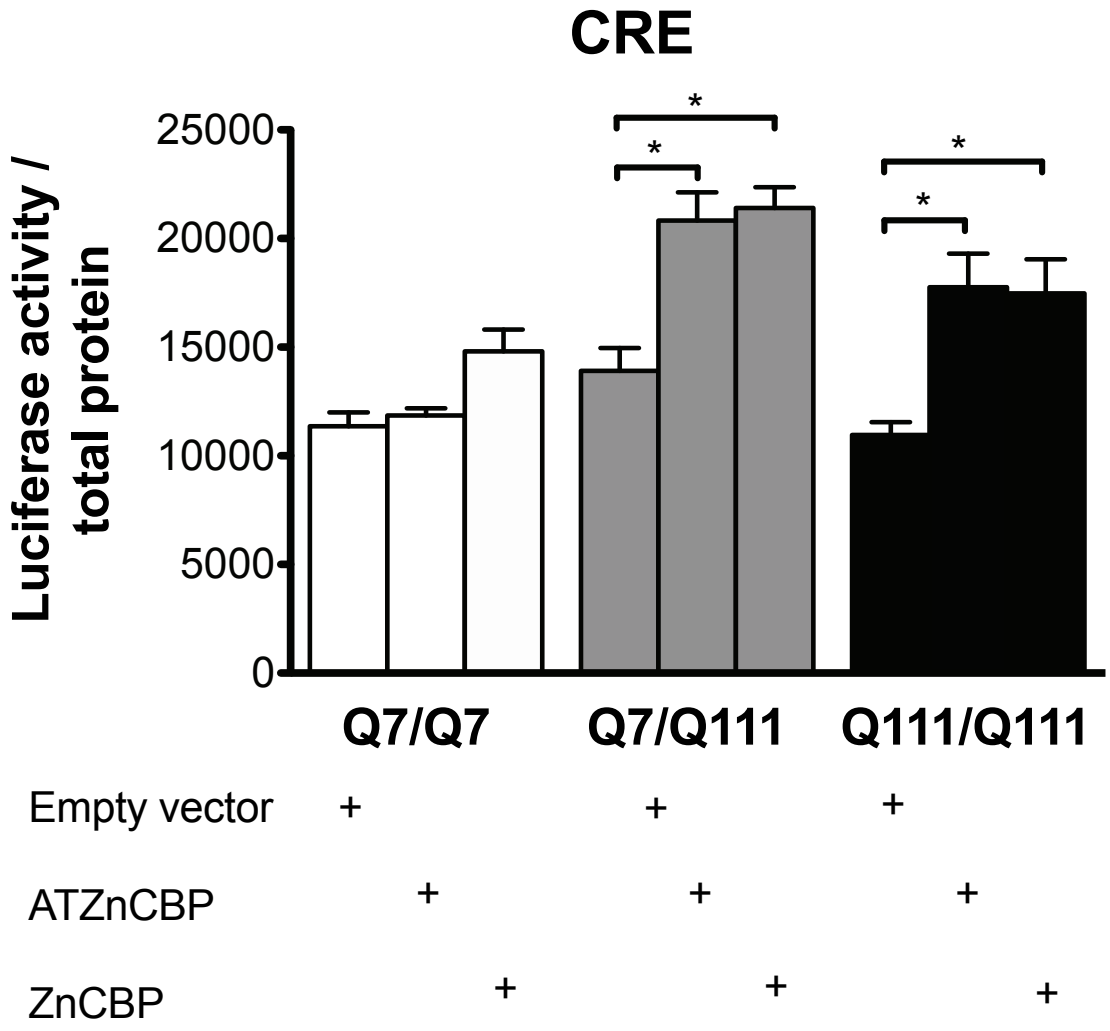

Figure 3.12. Overexpressing ATZnCBP and ZnCBP increased CRE promoter activity in ST*Hdh*$^{Q7/Q111}$and ST*Hdh*$^{Q111/Q111}$cells, but not in ST*Hdh*$^{Q7/Q7}$ cells. Cells were transfected with 200 ng of vector containing three CREs driving expression of firefly *luciferase* (pCRE-luc) along with 800 ng of empty vector (pcDNA4HisC), 800 ng of ATZnCBP-pcDNA4HisC, or 800 ng of ZnCBP-pCDNA4HisC. Eighteen hours later, cells were incubated with 10 μM forskolin for 2 h. Cells were lysed, luciferase activity was measured, and luciferase activity was normalized to total protein. Mean ± SEM (n = 6) is shown. * $P < 0.05$ as determined by one-way ANOVA and Tukey *post-hoc* test.

We hypothesized that overexpressing fragments of CBP lacking the KIX promoter association domain would block N-mHtt at the promoter and normalize N-mHtt-mediated transcriptional dysregulation. To determine whether overexpressing ATZnCBP and ZnCBP could increase PGC-1α and CMV promoter activity in cells expressing wild-type or mHtt, we measured luciferase activity in ST*Hdh*$^{Q7/Q7}$, ST*Hdh*$^{Q7/Q111}$, and ST*Hdh*$^{Q111/Q111}$ cells co-transfected with PGC-1α-pGL3 or CMV-pGL3 and either pcDNA4HisC, ATZnCBP vector, or ZnCBP vector. PGC-1α-driven luciferase activity was decreased in ST*Hdh*$^{Q111/Q111}$ cells compared to both ST*Hdh*$^{Q7/Q7}$and ST*Hdh*$^{Q7/Q111}$ cells transfected with empty vector (Fig. 3.13). PGC-1α-driven luciferase activity was increased in ST*Hdh*$^{Q7/Q7}$ and ST*Hdh*$^{Q7/Q111}$ cells, but not ST*Hdh*$^{Q111/Q111}$cells, transfected with ZnCBP vector compared to the same respective cell types transfected with empty vector (Fig. 3.13). PGC-1α-driven luciferase activity was not different between ST*Hdh*$^{Q7/Q7}$, ST*Hdh*$^{Q7/Q111}$, or ST*Hdh*$^{Q111/Q111}$ cells transfected with ATZnCBP vector and the same respective cell types transfected with empty vector (Fig. 3.13). Consequently, overexpressing ZnCBP, but not ATZnCBP, increased PGC-1α promoter activity in cells expressing 0 or 1 copies of mHtt. CMV-driven luciferase activity was decreased in ST*Hdh*$^{Q7/Q111}$ cells compared to ST*Hdh*$^{Q7/Q7}$ cells transfected with empty vector (Fig. 3.14). CMV-driven luciferase activity was decreased in ST*Hdh*$^{Q111/Q111}$ cells compared to both ST*Hdh*$^{Q7/Q7}$and ST*Hdh*$^{Q7/Q111}$ cells transfected with empty vector (Fig. 3.14). CMV-driven luciferase activity was increased in ST*Hdh*$^{Q7/Q7}$and ST*Hdh*$^{Q7/Q111}$cells transfected with ATZnCBP or ZnCBP vectors compared to ST*Hdh*$^{Q7/Q7}$and ST*Hdh*$^{Q7/Q111}$cells, respectively, transfected with empty vector (Fig. 3.14). CMV-driven luciferase was not different between ST*Hdh*$^{Q111/Q111}$cells transfected with ATZnCBP vector or ZnCBP

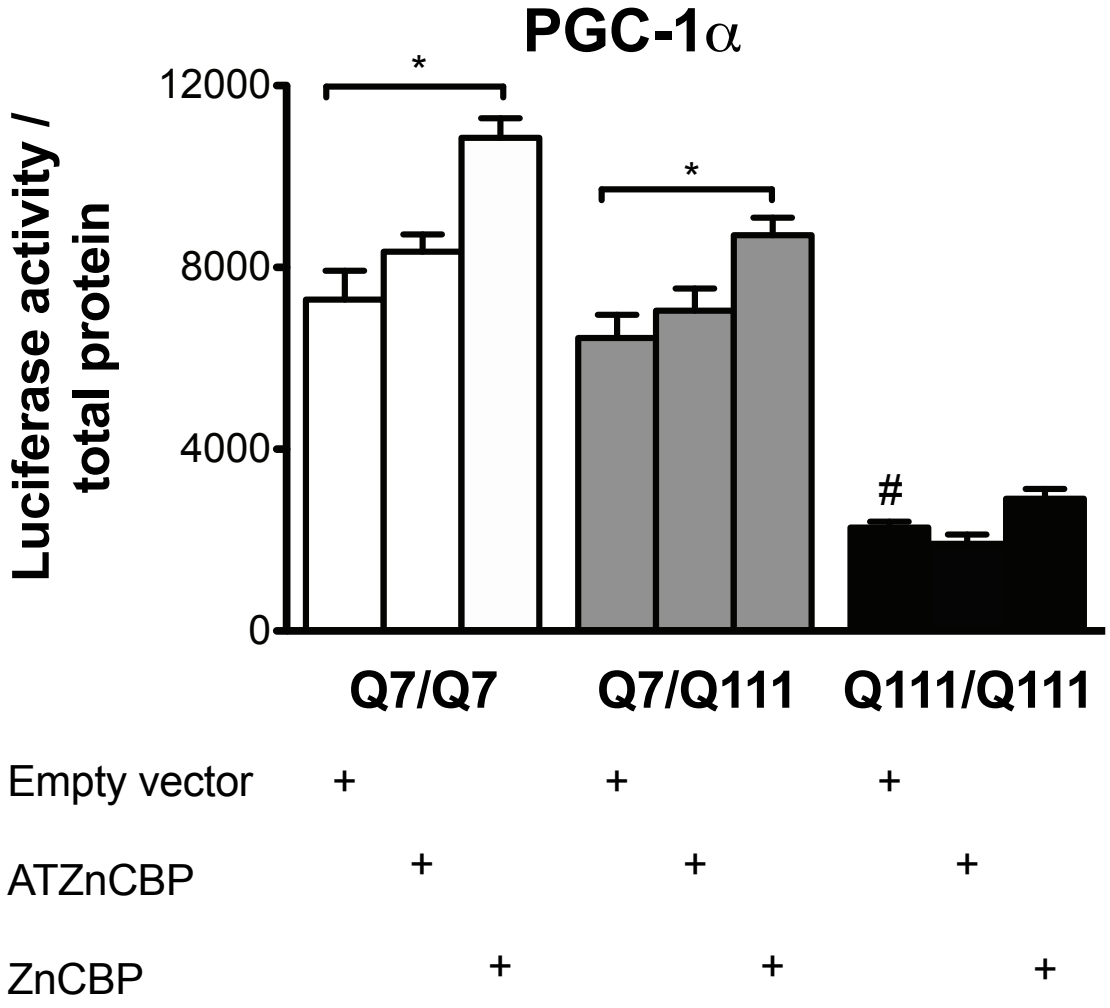

Figure 3.13. Overexpressing ZnCBP increased PGC-1α promoter activity in ST*Hdh*$^{Q7/Q7}$ and ST*Hdh*$^{Q7/Q111}$ cells but not in ST*Hdh*$^{Q111/Q111}$ cells, while overexpressing ATZnCBP had no effect on PGC-1α promoter activity. Cells were transfected with 200 ng of vector containing PGC-1α promoter driving expression of firefly *luciferase* (PGC-1α-pGL3) along with 800 ng of empty vector (pcDNA4HisC), 800 ng of ATZnCBP-pcDNA4HisC, or 800 ng of ZnCBP-pCDNA4HisC. Eighteen hours later, cells were incubated with 10 μM forskolin for 2 h. Cells were lysed and luciferase activity was measured. Luciferase activity was normalized to total protein. Mean ± SEM (n = 8) is shown. * $P < 0.05$, and # $P < 0.05$ compared to ST*Hdh*$^{Q7/Q7}$ cells transfected with empty vector, as determined by one-way ANOVA and Tukey *post-hoc* test.

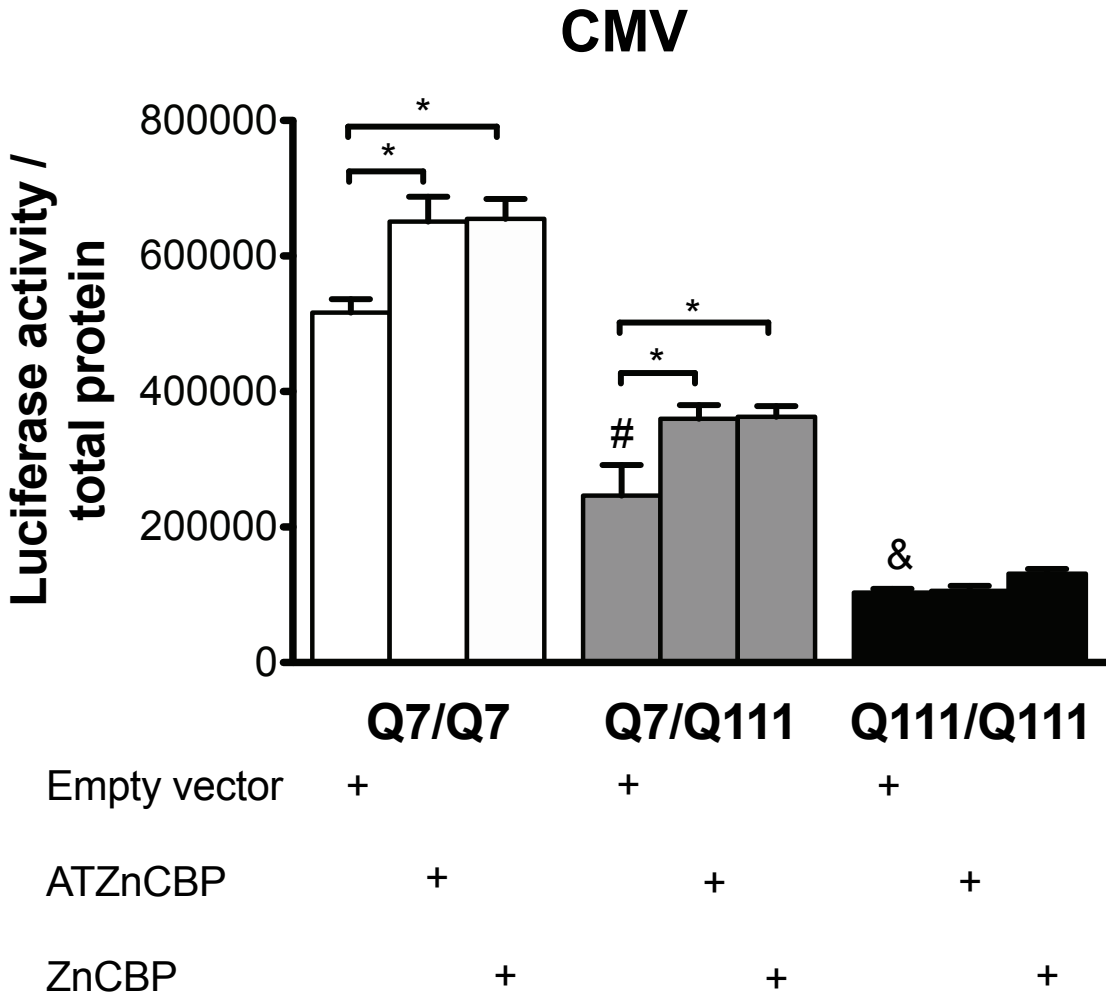

Figure 3.14. Overexpressing ATZnCBP and ZnCBP increased CMV promoter activity in ST*Hdh*$^{Q7/Q7}$and ST*Hdh*$^{Q7/Q111}$ cells, but not in ST*Hdh*$^{Q111/Q111}$ cells. Cells were transfected with 200 ng of vector containing CMV promoter driving expression of firefly *luciferase* (CMV-pGL3) along with 800 ng of empty vector (pcDNA4HisC), 800 ng of ATZnCBP-pcDNA4HisC, or 800 ng of ZnCBP-pCDNA4HisC. Eighteen hours later, cells were incubated with 10 μM forskolin for 2 h. Cells were lysed, luciferase activity was measured, and luciferase activity was normalized to total protein. Mean ± SEM (n = 6) is shown. * $P < 0.05$, # $P < 0.05$ compared to ST*Hdh*$^{Q7/Q7}$ cells transfected with empty vector, and & $P < 0.05$ compared to ST*Hdh*$^{Q7/Q7}$ and ST*Hdh*$^{Q7/Q111}$ cells transfected with empty vector, as determined by one-way ANOVA and Tukey *post-hoc* test.

vector and ST*Hdh*$^{Q111/Q111}$ cells transfected with empty vector (Fig. 3.14). Therefore, overexpressing ATZnCBP and ZnCBP increased CMV promoter activity in ST*Hdh* cells expressing 0, or 1 copies of mHtt, but failed to increase CMV promoter activity in ST*Hdh* cells expressing 2 copies of mHtt.

In addition to impairing transcription, mHtt causes a number of other cellular changes, which are believed to leave cells expressing mHtt more vulnerable to environmental stress (reveiwed in Zuccato *et al.*, 2010). Although, overexpressing fragments of CBP lacking the KIX promoter association domain did not reverse mHtt-mediated repression of the PGC-1α and CMV promoters, we hypothesized that overexpressing these fragments might be able to decrease mHtt-mediated toxicity through an alternative mechanism. To determine whether overexpressing ATZnCBP and ZnCBP could decrease toxicity in ST*Hdh*$^{Q7/Q7}$, ST*Hdh*$^{Q7/Q111}$, and ST*Hdh*$^{Q111/Q111}$cells, we transfected cells with pEGFP-N1 or mCherry-3L along with pcDNA4HisC, ATZnCBP vector, or ZnCBP vector, and stained cells with EthD-1 or Fluoro-Jade C. Transfected cells were identified by GFP or RFP expression for EthD-1 or Fluoro-Jade C experiments, respectively. The percentage of cells that were positive for EthD-1 and GFP per total number of GFP positive cells was increased in ST*Hdh*$^{Q7/Q7}$ cells transfected with ATZnCBP, but not ZnCBP, compared to ST*Hdh*$^{Q7/Q7}$cells transfected with empty vector (Fig. 3.15). The percentage of cells that were positive for EthD-1 and GFP per total number of GFP positive cells was decreased in ST*Hdh*$^{Q7/Q111}$ and ST*Hdh*$^{Q111/Q111}$cells transfected with ATZnCBP and ZnCBP vectors compared to ST*Hdh*$^{Q7/Q111}$ and ST*Hdh*$^{Q111/Q111}$cells transfected with empty vector (Fig. 3.15). The percentage of cells that were positive for EthD-1 and GFP per total number of GFP positive cells in

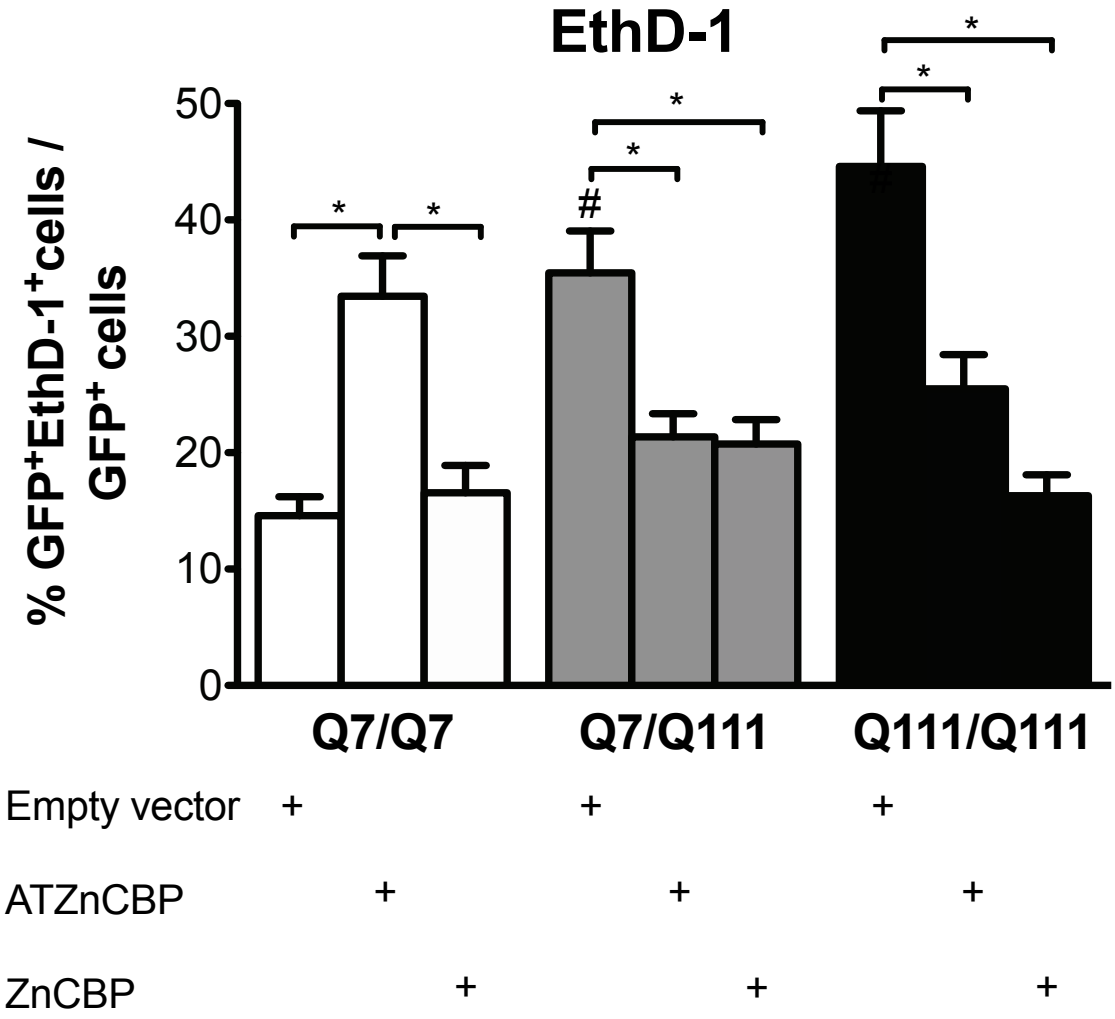

Figure 3.15. Overexpressing ATZnCBP, but not ZnCBP, increased EthD-1 staining in ST*Hdh*$^{Q7/Q7}$ cells. Overexpressing ATZnCBP and ZnCBP decreased EthD-1 staining in ST*Hdh*$^{Q7/Q111}$ and ST*Hdh*$^{Q111/Q111}$ cells. Cells were grown to confluence in 96-well plates, serum-deprived, and transfected with 50 ng of GFP expressing vector along with 200 ng of empty vector (pcDNA4HisC), ATZnCBP-pcDNA4HisC, or ZnCBP-pcDNA4HisC. Eighteen hours later, cells were incubated with 4 μM EthD-1, which stains nucleic acids in membrane permeable cells. Mean ± SEM (n = 9) percentage of GFP positive and EthD-1 positive cells per GFP positive cells is shown. * $P < 0.05$ and # $P < 0.05$ compared to ST*Hdh*$^{Q7/Q7}$ cells transfected with empty vector, as determined by one-way ANOVA and Tukey *post-hoc* test.

ST*Hdh*$^{Q7/Q111}$ and ST*Hdh*$^{Q111/Q111}$cells transfected with ATZnCBP or ZnCBP was not different than that of ST*Hdh*$^{Q7/Q7}$cells transfected with empty vector (Fig. 3.15). Similar effects of overexpressing ATZnCBP or ZnCBP were seen when using the Fluoro-Jade C staining technique (Fig. 3.16). Together, these data indicate that overexpressing ATZnCBP or ZnCBP decreased toxicity in cells expressing mHtt to levels seen in untreated wild-type cells. Removal of the AT domain ameliorated the toxic effect of overexpressing full-length CBP or ATZnCBP in wild-type cells.

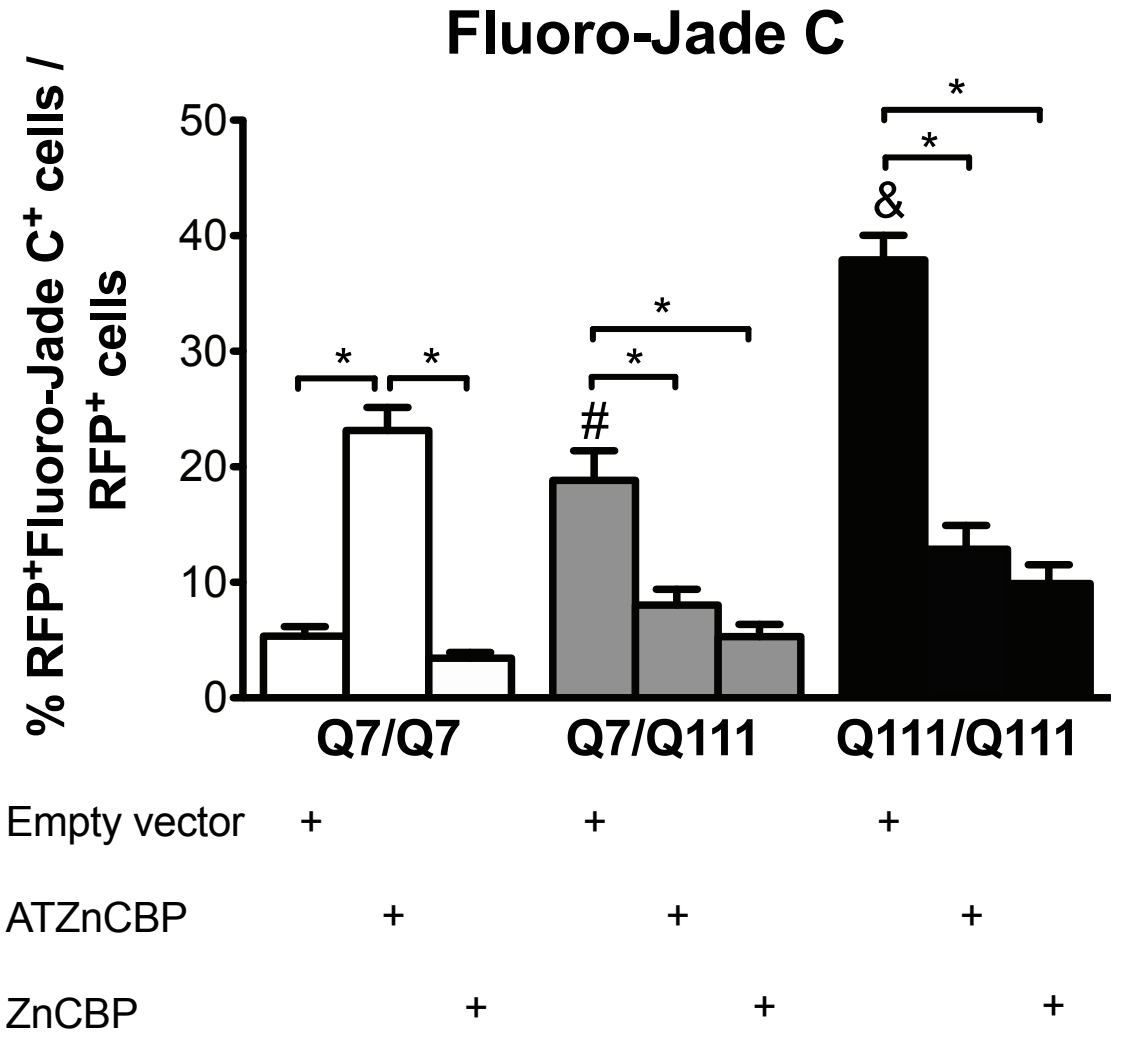

Figure 3.16. Overexpressing ATZnCBP, but not ZnCBP, increased Fluoro-Jade C staining in ST*Hdh*$^{Q7/Q7}$ cells. Overexpressing ATZnCBP and ZnCBP decreased Fluro-Jade C staining in ST*Hdh*$^{Q7/Q111}$ and ST*Hdh*$^{Q111/Q111}$ cells. Cells were grown to confluence in 96-well plates, serum-deprived, and transfected with 50 ng of RFP expressing vector along with 200 ng of empty vector (pcDNA4HisC), ATZnCBP-pcDNA4HisC, or ZnCBP-pcDNA4HisC. Eighteen hours later, cells were incubated with 0.0001% Fluoro-Jade C, which stains degenerating neurons. Mean ± SEM (n = 9) percentage of RFP positive and Fluoro-Jade C positive cells per RFP positive cells is shown. * $P < 0.05$, # $P < 0.05$ compared to ST*Hdh*$^{Q7/Q7}$ cells transfected with empty vector, and & $P < 0.05$ compared to ST*Hdh*$^{Q7/Q7}$ and ST*Hdh*$^{Q7/Q111}$ cells transfected with empty vector, as determined by one-way ANOVA and Tukey *post-hoc* test.

CHAPTER 4 DISCUSSION

Altered mRNA expression of a subset of genes occurs early during HD pathogenesis (Luthi-Carter *et al.*, 2000). Some genes are affected early in HD, while others are affected later in disease progression (Becanovic *et al.*, 2010). Levels of mRNA are affected because N-mHtt accumulates in the nucleus, binds abnormally to proteins involved in transcription, and impairs transcription of a subset of genes (Cui *et al.*, 2006; Hogel *et al.*, 2012). The working hypothesis for this effect is that aggregated, or soluble N-mHtt sequesters necessary proteins away from the promoter (Fig. 1.2A,B; Perutz *et al.*, 1994; Steffan *et al.*, 2000; Nucifora *et al.* 2001), or that N-mHtt incorporates into transcriptional complexes at the promoter (Fig. 1.2C; Kegel *et al.*, 2002; Cui *et al.*, 2006; Hogel *et al.*, 2012). Both the aggregated and soluble N-mHtt sequestration models predict that overexpressing N-mHtt-interacting proteins that are limiting for transcription would increase the pool of functional protein available for transcription, and normalize transcription of genes regulated by that protein. However, if N-mHtt impairs transcription by incorporating into transcriptional complexes at the promoter, overexpressing proteins that contain a promoter association domain would not be expected to relieve transcriptional dysregulation, as the overexpressed protein would recruit N-mHtt to the promoter, where N-mHtt would impair transcription (Fig. 1.3A). We hypothesized that overexpressing protein fragments that bind N-mHtt and lack a promoter association domain would block abnormal interactions of N-mHtt at the promoter, thereby preventing transcriptional dysregulation and delaying HD progression (Fig. 1.3B). Because it has previously been shown that N-mHtt binds to a fragment of CBP that lies outside of the KIX promoter association domain (Steffan *et al.*, 2001), we

wanted to test whether overexpressing full-length CBP or fragments of CBP lacking the KIX promoter association domain could recover transcriptional deficits and toxicity in the ST*Hdh* knock-in cell model of HD.

In this work, we demonstrate that PGC-1α and CMV promoter activity was differentially affected by the same concentration and state of mHtt as the two promoters had different activity in a defined cell line, the ST$Hdh^{Q7/Q111}$ cell line. We found that PGC-1α promoter activity was decreased in ST$Hdh^{Q111/Q111}$ cells compared to both ST$Hdh^{Q7/Q111}$ cells and ST$Hdh^{Q7/Q7}$ cells. Decreased PGC-1α promoter activity in ST$Hdh^{Q111/Q111}$ cells compared to ST$Hdh^{Q7/Q7}$ cells has been reported previously (Cui *et al.*, 2006). To the best of our knowledge, PGC-1α promoter activity or mRNA levels in ST$Hdh^{Q7/Q111}$ cells have not been reported. CMV promoter activity was decreased in ST$Hdh^{Q7/Q111}$ cells compared to ST$Hdh^{Q7/Q7}$ cells, and in ST$Hdh^{Q111/Q111}$ cells compared to both ST$Hdh^{Q7/Q7}$ cells and ST$Hdh^{Q7/Q111}$ cells. Assuming that both early and late changes in gene expression can be directly caused by mHtt, genes that are unaffected early in disease progression but exhibit decreased transcription at later stages may be more resistant to the concentration of N-mHtt than genes affected earlier in HD progression. Although CMV is an artificial model of N-mHtt-mediated transcriptional dysregulation, it may represent an artificial gene that is affected early in HD, while PGC-1α may represent an endogenous gene that is affected late in disease progression. Time-course studies for PGC-1α mRNA levels have not been reported in brain tissue, however, PGC-1α mRNA levels were decreased in adipocytes taken from 9 week-old symptomatic R6/2 mice, but not 3 week-old pre-symptomatic R6/2 mice (Phan *et al.*, 2009), supporting the idea that PGC-1α mRNA is decreased relatively late in HD progression.

If sequestration of N-mHtt-interacting proteins or incorporation of N-mHtt into promoter complexes via interactions with N-mHtt-interacting proteins contributes to N-mHtt transcriptional dysregulation, we would predict that sensitivity of a promoter to N-mHtt transcriptional dysregulation would depend on the number of N-mHtt-interacting proteins that regulate that promoter. Analysis of the sequence upstream of the CMV transcription start site showed 9 sites associated with N-mHtt-interacting transcription factors including, CREB, Sp1, retinoic acid receptor, and C/EBP, within the -757 to +1 region (Fig. 4.1). In contrast, we identified only 3 sites associated with N-mHtt-interacting proteins within the -2472 to +1 promoter region of PGC-1α (Fig. 4.1). The increased number of N-mHtt interacting proteins associated with the CMV promoter compared to the PGC-1α promoter could explain increased sensitivity of the CMV promoter to N-mHtt compared to the PGC-1α promoter. To test this hypothesis, we could use site directed mutagenesis to remove recognition sites associated with known N-mHtt-interacting proteins from the CMV promoter. If susceptibility of the CMV promoter to transcriptional dysregulation was dependent on the number of recognition sites for N-mHtt-interacting proteins, we would predict that removing recognition sites for N-mHtt-interacting proteins would decrease N-mHtt-transcriptional dysregulation at the CMV promoter.

Overexpressing full-length CBP failed to increase PGC-1α promoter activity in ST*Hdh*$^{Q111/Q111}$ cells. Similarly, we found that overexpressing CBP did not increase CMV promoter activity in ST*Hdh*$^{Q7/Q111}$ and ST*Hdh*$^{Q111/Q111}$ cells. These results suggest that overexpressing CBP did not overcome N-mHtt-mediated transcriptional dysregulation at either the CMV or PGC-1α promoters. Sequestration of CBP alone was therefore not

CMV promoter (5'→3')

AGATCTATACATTGAATCAATATTGGCCATTAGCCATATTATTCATTGGTTATATAGCATAAATCAATATTGGCTATTGG
CCATTGCATACGTTGTATCTATATCATAATATGTACATTTATATTGGCTCATGTCCAATATGACCGCCATGTTGACATTG
ATTATTGACTAGTTATTAATAGTAATCAATTACGGGGTCATTAGTTCATAGCCCATATATGGAGTTCCGCGTTACATAAC
TTACGGTAAATGGCCCGCCTGGCTGACCGCCCAACGACCCCCGCCCATTGACGTCAATAATGACGTATGTTCCCATAGTA
ACGCCAATAGGGACTTTCCATTGACGTCAATGGGTGGAGTATTTACGGTAAACTGCCCACTTGGCAGTACATCAAGTGTA
TCATATGCCAAGTCCGCCCCCTATTGACGTCAATGACGGTAAATGGCCCGCCTGGCATTATGCCCAGTACATGACCTTAC
GGGACTTTCCTACTTGGCAGTACATCTACGTATTAGTCATCGCTATTACCATGGTGATGCGGTTTTGGCAGTACACCAAT
GGGCGTGGATAGCGGTTTGACTCACGGGGATTTCCAAGTCTCCACCCCATTGACGTCAATGGGAGTTTGTTTTGGCACCA
AAATCAACGGGACTTTCCAAAATGTCGTAATAACCCCGCCCCGTTGACGCAAATGGGCGGTAGGCGTGTACGGTGGGAGG
TCTATATAAGCAGAGCTCGTTTAGTGAACCGTCAGAT→+1

PGC-1α promoter (5'→3')

CCTGTGCTCTCTCTAGCTTCACATACCCCTTTTTATGAAGGTAGAGGACAGAGTGGCTGTTTTAAGCAGATCATTAGCTT
CATGGATGTGCTGGGTTAGTTTCTTTTCTTTTCTTTTCTTTTCTTTTTTTAAAGTAGAATTAGGTGGCAAAAAAAGAAAG
AAAGAAAGAAAGAAAGAAAGAAATTATCTTTTCAAAGCAAAGAAAAAGAAAATCCTGCCACAATTCAGTGTGAGCAAGTT
AAGATATCAAAACAATAATGCAGAGTTATCTAGTGCAAGCAACCATCTGTAAGAAGAGGTGTGCATGAGGTTTGAAAAAG
TATGGTGGATGCCTAATGGATGACAAAGAGAAACCAAAGTATCAGTTACCATCAGGATGCCAGGATTGCTTGATAATGAT
GAATAAACATCGACTCTTTATAGCTAAGTGGCCAGCATTATTTCACAGTTGACTGTGTGGAAAGTAGAGCCCATGACCTT
TGTCCTGAATTTTAATAGTTTACTGAAGTTTTACATTAAGTAAAAATCTAATTGGCAAGAAAAATTAGTGTTTCTTTGTG
GGAGTACAGAGTAAGGCTACTAATTGCATGTAGAAAATGATCCCAGGGTTGTCTCTCTCTCTCTCTGAATTAGAAAATTA
AATGAATAATACCTTTCTGATGTTTGGAAGAGGACAGTTGTAGCAGTGAAGTATATTCACCTAATTTAGAATGTCAAAGC
TGTTGGCCATCTTGTTCTGTTCACTTATTGACAAACTGTCGATTTCATTACCATATTCCCTGTCTACTAGTTGTGGACAT
CCAAGCAAACAGACCCCTTATACGGGGTCTGAAGCAAACAGCAAGCTTGTGGGCTTTGTGTGTGTGTGTGTGTGTGTG
TGTGTGTGTGTGTGTGTGTGTGTGCACGCTCGCTGCATTTCTTTCTTTCACTTTACTGTATTAGTAACTGACTATATA
AAGTCAGACTGAGAGAAGTCACCAATGTTTTCCTTCTAAGGGGAGAGAAAATAAAGAGCACATTAAATTAACCTCAGTGG
AATAGGAGTTTAAATGAATGGTGCTTTATAAATTATATTTAGATGCATAGGGACTTTTTTCTTCTTCTAAATTACTGTCA
AGTAAAGGAAATGAGCTGGTTTTTGAGTCTGTGGGGTTTGAGGTATTGTGAAAATATGTTTTCAAAGGTCCCCTGTGCAT
TTCTCACTGGGCCTGGAAGGGTTAAGTCTGAGCACCCAAGTGTTATGGAAAGTGCTGAGAGTTGGTTATGTCCTCTGTCT
GTAATGTCACAGGAAAAACAGTGGCACCTGCATTACCCCTCATTGACTCAGGAACGACAAAAAAGTATTAGTAAGCAAAG
CTCAAGAAATGAGTATCTCTGCTGATACCATTTCAGTGTTTTTCCTTCATTCCCTGGACATTCTTGATTTCAAAAACAAA
CTGTACAGCCCAAGGCACTAGGGTTGGAGTCCAATGTTTATTCAAAAAGGCACCCTGAAGCCATGAGGAAGACTGTGCTA
CATATGAGAAAAGAAATAAGGGGTGGGGGCAGGTGAGTAGCTAAGCTGTTTCAGGGATGGCAGCAGCAATTGTATTTTCT
AGCATTTGTTTTCTGGGAGCCTATGAGATCCACGGAAAGAATCATGAGGGGGAACCCAAGAGTCTAGGGTGTTGTGGCTT
GCTTGCTTTACAAGGAGCAAGGCAAACTGCAGTAACAGTTTAGGAGACTGCATTCTCTACTGCCAAGGAGACAGCTGATT
TGGGGTAGAGAAATTTGTTTAGACCTAAACAAATGTGGCGGTTTTGTTGACTAAACATGGAAAGAAAGAAAGAAAGAAAG
AAAGAAAGAAAGAAAGAAAGAAAGAAAGAAAGAAAGAAACAAAGAAAGAAAGAAAGAAAGGAAGGAAGGAAGGAAGAAAG
GAAGAAAGGAAGGAAGGAAGGAAGGAAAGAAAGGAGAGAGAGAAAGAAAATCGGGGGTGTTGCCTTCAAACACTCCTCTA
ATAGGGAGGGAAAAAAAAGAATCTCATGAAAATGTATCACATGAGGAGCGCTTGCTTCAGTTCCAAGCTGAGTCTGGGGC
TACTTGGAAACCATTTCTTAAAGCACACACATTTTAGGCAAGGGTGTAGTTACTGTGTCAGTAACAGGGGATCTTTGCTA
TTTGCCTGTTTTGGATGGAAAATAAATTTAAAAAAAAAAGATTGCAGGAGATTTGAGTTATTATGTGAGCAGGGCTCCGG
TTTAGAGTTGGTGGCATTCAAAGCTGGCTTCAGTCACAGTGTGATGCTTGAAGCCTCCCAAAGGCCAAGTGTTTCCTTTT
CTTTCTTCTATTTTTTTTTTCCTCTCTCTCTAAGCGTTACTTCACTGAGGCAGAGGGCTGCCTTGGAGTGACGTCAGGAG
TTTGTGCAGCAAGCTTGCACAGGAGAAGGGAGGCTGGGTGAGTGACAGCCCAGCCTACTTTTTAATAGCTTT→+1

GC rich box:GGGCGG (Sp1)
CRE: TGACGTCA (CBP via CREB)
TATA box: TATAA found within 50 bp of the +1 transcription start site (TBP)
CCAAT box: CCAAT (C/EBP)

Figure 4.1. The CMV promoter contains more recognition sites associated with known N-mHtt-interacting proteins than the PGC-1α promoter. Shown in brackets beside each recognition site is the N-mHtt-interacting protein associated with it. The transcription start site is indicated by +1. bp, base pair; C/EBP, CCAAT-enhancer-binding protein; RARE, retinoic acid response element; Sp1, specificity protein 1; TBP, TATA-binding protein.

likely responsible for transcriptional repression at the PGC-1α and CMV promoters. In contrast, we found that overexpressing fragments of CBP lacking the KIX promoter association domain increased CMV promoter activity in ST*Hdh*$^{Q7/Q111}$ cells. As we would expect that CBP fragments lacking the KIX promoter association domain would associate at the promoter to a lesser extent than full-length CBP, this finding provides some support for the incorporation model of N-mHtt-mediated transcriptional dysregulation. p300 is structurally related to CBP, but does not bind N-mHtt (Cong *et al.*, 2005). To determine if increased transcription at N-mHtt-affected promoters was specific to overexpressing regions of CBP, we could test the effect of overexpressing regions of p300 that correspond to those regions of CBP tested in the current study.

We found that overexpressing full-length CBP and fragments of CBP lacking the KIX promoter association domain increased PGC-1α and CMV promoter activity in wild-type cells, but failed to normalize PGC-1α and CMV promoter activity in cells expressing 2 copies of mHtt, indicating that overexpressing these proteins increased transcription in a general manner, but did not overcome N-mHtt-mediated transcriptional dysregulation. Despite the finding that overexpressing CBP fragments increased CRE promoter activity only in ST*Hdh* cells expressing mHtt, this effect did not seem to be related to he presence of mHtt, as CRE promoter activity was not different between ST*Hdh*$^{Q7/Q7}$, ST*Hdh*$^{Q7/Q111}$, and ST*Hdh*$^{Q111/Q111}$ cells. Although we did not specifically examine how the presence of ATZnCBP or ZnCBP increased CMV and PGC-1α promoter activity, these fragments may have increased transcription through residual co-activator activity. The third Zn finger region of CBP mediates many of the known interactions of CBP, including p53 (Legge *et al.*, 2004), c-fos (Bannister and Kouzarides, 1995), c-myc (Vervoorts *et al.*,

2003), E2F-1 and TFIIB (O'Connor *et al.*, 1999). Theoretically, a CBP fragment containing only the third Zn finger region could bind two proteins at once and in this way act as a scaffold at the promoter. We observed that ZnCBP, but not ATZnCBP, increased PGC-1α promoter activity. It is possible that the presence of the AT domain limits ATZnCBP scaffolding function at some promoters due to steric hindrance by the AT domain with potential Zn domain-interacting proteins. Alternatively, ATZnCBP and ZnCBP may have acted as an indirect inducer and increased CMV and PGC-1α promoter activity by blocking association of a repressor at the promoter.

If a fraction of the population of N-mHtt molecules were able to associate at the promoter via interactions with CBP fragments lacking the KIX domain, it may explain why overexpressing these fragments failed to reverse N-mHtt-mediated transcriptional dysregulation completely. Transcriptional proteins, such as CBP, form protein complexes and are involved in multiple protein-protein interactions through different domains. Consequently, overexpressing one N-mHtt-interacting protein that lacks a promoter association domain may not effectively decrease the concentration of N-mHtt at the promoter because other interactions could bring N-mHtt to the promoter. A better approach may be to decrease the overall concentration of N-mHtt in the nucleus. This has been pursued through various techniques including, blocking cleavage of mHtt and thus nuclear accumulation of N-mHtt using caspase inhibitors (Leyva *et al.*, 2010), modulating phosphorylation of mHtt (Havel *et al.*, 2011), and decreasing overall levels of mHtt by RNA interference strategies (Rodriguez-Lebron *et al.*, 2005; Wang *et al.*, 2005; DiFiglia *et al.*, 2007; Vagner *et al.*, 2012). One additional way to do this might be to overexpress N-mHtt-interacting proteins that contain a nuclear export signal.

Assessment of cellular viability revealed decreased plasma membrane integrity and increased Fluoro-Jade C staining in ST*Hdh* cells expressing 1 or 2 copies of mHtt compared to cells expressing wild-type Htt following serum-deprivation. Although cells can recover from minor disruptions in the plasma membrane that are sustained for short periods of time, a break in the integrity of the plasma membrane compromises the membrane's essential role as a barrier and decreases cellular viability (McNeil and Steinhardt, 1997). Loss of plasma membrane integrity often accompanies programmed and non-programmed cell death (Fink and Cookson, 2005). Fluoro-Jade C staining correlates with TUNEL and is believed to specifically label degenerating neurons, although the mechanism of this is not known. We used loss of plasma membrane integrity and increased Fluoro-Jade C staining as markers of cellular toxicity. We showed that mHtt increased toxicity in a dose-dependent manner as EthD-1 and Fluoro-Jade C staining was significantly increased in cells expressing 2 copies of mHtt compared to cells expressing 1 copy of mHtt. Although toxicity was increased in ST*Hdh* cells expressing mHtt after 24 h serum-deprivation, we did not observe a change in mitochondrial membrane potential after 24 or 72 h serum-deprivation, indicating that toxicity was not a result of mitochondrial dysfunction. This is consistent with other studies, which showed that addition of the potent succinate dehydrogenase inhibitor, 3-nitropropionic acid, for 40 h was necessary to achieve a difference in mitochondrial membrane potential between ST$Hdh^{Q7/Q7}$ cells and ST$Hdh^{Q111/Q111}$ cells (Lim *et al.*, 2008).

Overexpressing full-length CBP increases toxicity in cerebellar granule neurons expressing wild-type Htt (Rouaux *et al.*, 2003), and decreases toxicity in N2a neuroblastoma cells expressing mHtt (Nucifora *et al.*, 2001). Consistent with this, we

found that overexpressing CBP increased toxicity in ST*Hdh* cells expressing wild-type Htt, but decreased toxicity in ST*Hdh* cells expressing 1 or 2 copies of mHtt. It was hypothesized that increased toxicity in wild-type cells occurred because of excess AT activity leading to increased histone acetylation and non-specific gene-expression (Rouaux *et al.*, 2003), while decreased toxicity in HD cells was believed to occur through compensation for loss of AT activity and normalization of histone acetylation levels (Nucifora *et al.*, 2001). Indeed, we found that overexpressing full-length CBP or ATZnCBP increased toxicity in wild-type ST*Hdh* cells, while overexpressing ZnCBP had no effect on toxicity, thus supporting the hypothesis that excess CBP AT activity contributes to toxicity in wild-type cells overexpressing CBP (Fig. 4.2). However, it does not appear that overexpressing full-length CBP or ATZnCBP compensated for loss of CBP AT activity, since decreased mHtt-mediated toxicity was observed with overexpression of ZnCBP, which did not contain the AT domain. Instead, it is more likely that overexpressing full-length CBP, ATZnCBP, or ZnCBP competitively inhibited interactions of N-mHtt with endogenous ATs, thereby normalizing histone acetylation levels (Fig. 4.3). Through this same effect, the presence of mHtt would be expected to block any toxic effect due to excess CBP AT activity, which would explain why we did not see a toxic effect with overexpression of the CBP AT domain in ST*Hdh* cells expressing mHtt.

In addition to normalizing histone acetylation levels, it is possible that overexpressing full-length CBP or CBP fragments decreased mHtt-mediated toxicity by modulating processes unrelated to chromatin remodeling. Neurons have a high cholesterol demand for the maintenance of plasma membrane fluidity, as well as the

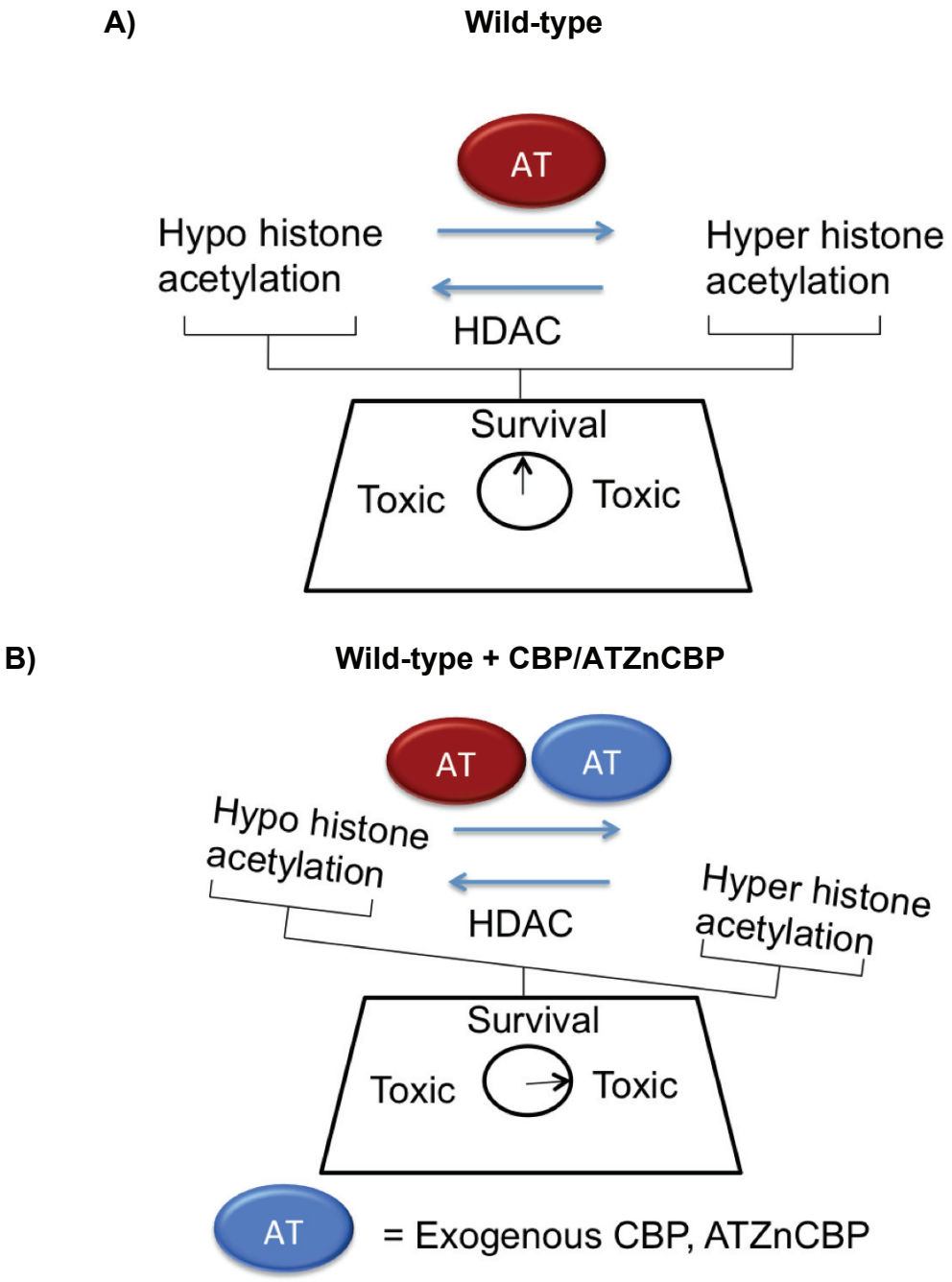

Figure 4.2. Model showing how excess CBP AT activity may contribute to toxicity in wild-type cells. **A)** In wild-type cells, histone acetylation levels are balanced by opposing actions of ATs, such as CBP, and histone deacetylases (HDACs). **B)** Overexpressing full-length CBP or a fragment of CBP containing the AT domain in wild-type cells leads to hyper histone acetylation and increased toxicity due to non-specific gene expression.

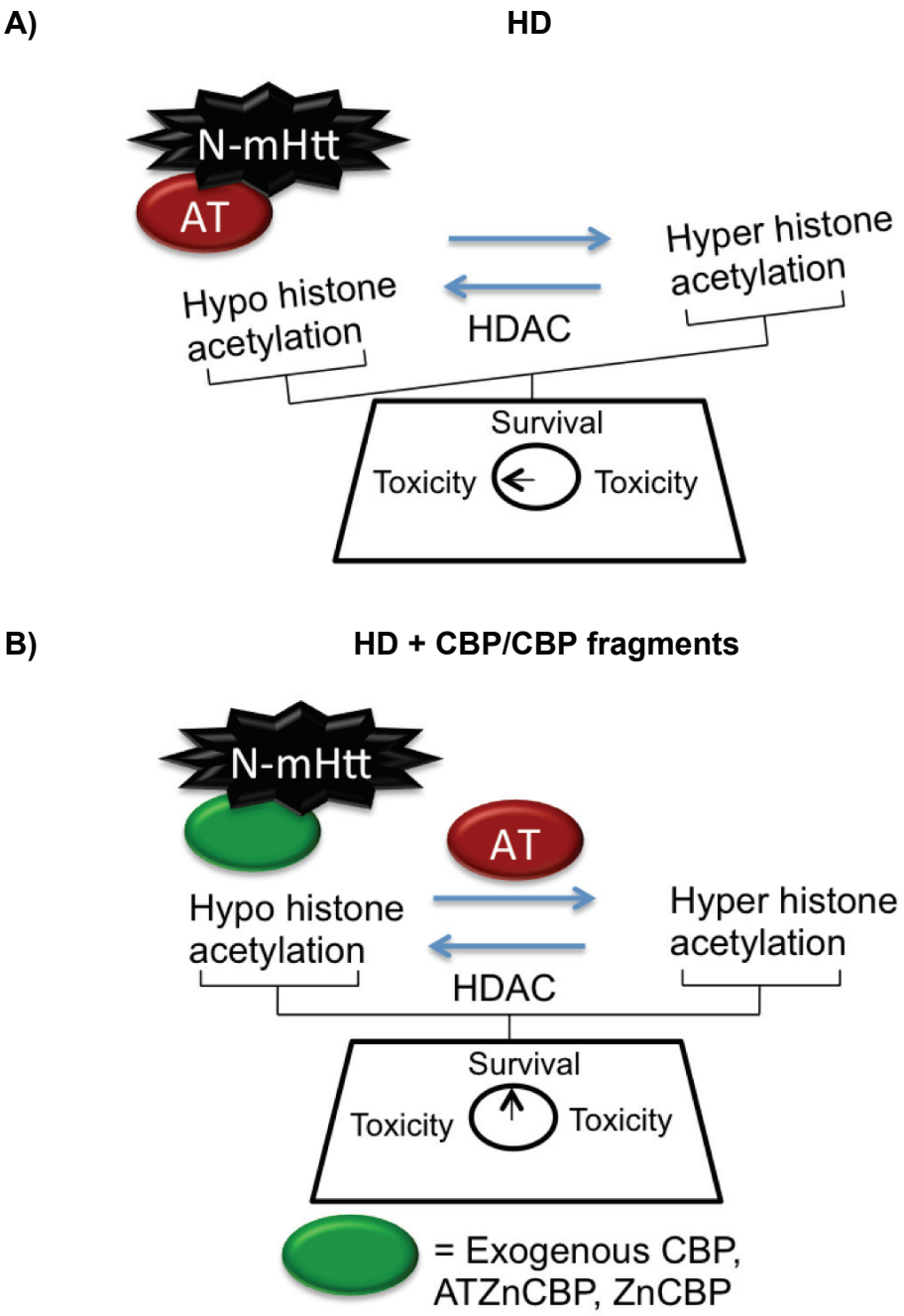

Figure 4.3. Model showing how overexpressing CBP or CBP fragments may limit mHtt-mediated toxicity by normalizing histone acetylation levels. **A)** In cells expressing mHtt, N-mHtt inhibits AT activity, which leads to histone hypoacetylation, decreased expression of pro-survival genes, and increased toxicity. **B)** Overexpressing full-length CBP, ATZnCBP, or ZnCBP blocks abnormal interactions of N-mHtt with endogenous ATs, thereby normalizing histone acetylation levels and limiting mHtt-mediated toxicity.

formation and maintenance of axons, dendrites and synaptic connections (Goritz *et al.*, 2005). Neurons are mostly dependent on cholesterol supplied by astrocytes (Mauch *et al.*, 2001; Fünfschilling *et al.*, 2007) and in culture, it is believed that neurons take up cholesterol from serum-containing media. Under conditions of low cholesterol uptake, such as during serum-deprivation, sterol regulatory element binding protein (SREBP) isoforms translocate to the nucleus and stimulate transcription of genes in the cholesterol biosynthesis pathway, including the rate-limiting enzyme HMG-CoA reductase (Horton *et al.*, 2002). mHtt binds SREBP-1 and SREBP-2 (Kaltenbach *et al.*, 2007) and overall levels of cholesterol are decreased in cell and animal models of HD (Valenza *et al.*, 2005). The presence of mHtt decreased nuclear entry of SREBP-1 by approximately 50% and decreased expression of SRE-reporters and genes in the cholesterol pathway, including HMG-CoA reductase (Valenza *et al.*, 2005). Addition of exogenous cholesterol decreased toxicity in primary striatal rat neurons transiently transfected with N-mHtt following incubation in media lacking lipoproteins in a dose-dependent manner (Valenza *et al.*, 2005), indicating that lack of cholesterol biosynthesis contributes to mHtt-mediated toxicity following serum-deprivation. CREs are often found in the DNA sequence adjacent to SREs. Full-length CBP binds to SREBP-1 and SREBP-2 isoforms and acts as a co-activator for SREBP-1 and SREBP-2 (Oliner *et al.*, 1996). CBP fragments containing only the third Zn finger region of CBP have been shown to interact with both SREBP-1 and SREBP-2 isoforms, albeit to a less extent than amino-terminal fragments of CBP (Oliner *et al.*, 1996). If impaired cholesterol biosynthesis contributed to mHtt-toxicity following serum-deprivation, overexpressing full-length CBP or CBP fragments may have decreased mHtt-mediated toxicity by stimulating transcription of SREBP-

regulated genes. We have performed preliminary immunocytochemistry experiments showing that ATZnCBP and ZnCBP were present in the cytoplasm and the nucleus of ST*Hdh* cells (data not shown). It is possible that ATZnCBP and ZnCBP decreased mHtt-mediated toxicity by blocking mHtt-mediated impairment of SREBP translocation to the nucleus (Fig. 4.4).

Evidence also implicates p53-mediated apoptosis in HD pathogensis and overexpressing CBP or CBP fragments may have produced beneficial effects in ST*Hdh* cells expressing mHtt by modulating this aberrant pathway. p53 protein levels are increased in HD patients as well as cell and animal models of HD compared to unaffected individuals and wild-type controls, respectively (Bae *et al.*, 2005). p53 protein levels are increased more than 6-fold in ST$Hdh^{Q111/Q111}$ cells compared to ST$Hdh^{Q7/Q7}$ cells (Trettel *et al.*, 2000). Genetic or pharmacological knock-down of p53 ameliorated toxicity in PC12 cells expressing N-mHtt (Bae *et al.*, 2005). CBP can interact with p53 through the third Zn finger region and binding of CBP to p53 at the promoter activates p53-mediated transcription (Avantaggiati *et al.*, 1997; Scolnick *et al.*, 1997). Overexpressing CBP fragments containing the third Zn finger region decreased promoter activity of p53-regulated genes (Scolnick *et al.*, 1997). Overexpressing fragments of p300 containing the third Zn finger region decreased expression of p53-regulated pro-apoptotic genes and decreased overall levels of apoptosis in cells overexpressing p53 (Avantaggiati *et al.*, 1997). Authors hypothesized that overexpressing fragments containing the third Zn finger region of CBP or p300 blocked p53-mediated transcription by binding to p53 and failing to associate at the promoter (Avantaggiati *et al.*, 1997; Scolnick *et al.*, 1997). If p53-mediated apoptosis contributes to mHtt-mediated toxicity following serum-

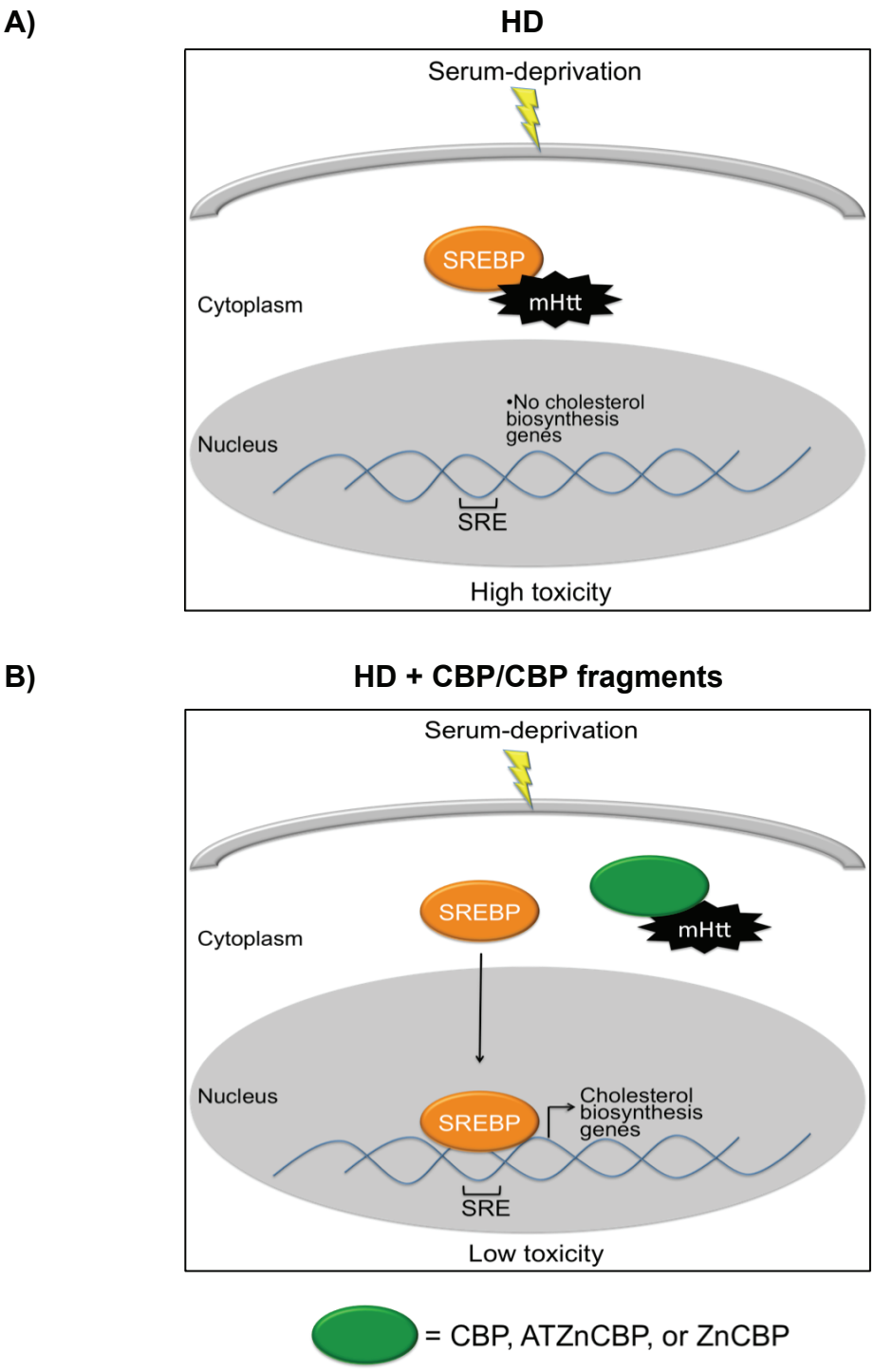

Figure 4.4. Working model for how overexpressing CBP or CBP fragments may decrease mHtt-mediated toxicity by modulating cholesterol biosynthesis. **A)** mHtt blocks nuclear translocation of sterol regulatory element binding protein (SREBP), leading to decreased expression of cholesterol biosynthesis genes and increased toxicity. **B)** Overexpressing CBP or CBP fragments enhances SREBP-mediated expression of cholesterol biosynthesis genes by blocking mHtt-mediated impairment of SREBP nuclear translocation. This limits toxicity in cells expressing mHtt.

deprivation, overexpressing CBP fragments containing the third Zn finger region may have ameliorated mHtt-mediated toxicity by blocking association of p53 at the promoter, and thereby blocking p53-mediated transcription of pro-apoptotic genes (Fig. 4.5). This hypothesis does not invoke a reversal of N-mHtt-mediated transcriptional dysregulation, and so, fits with our findings that overexpressing full-length CBP or CBP fragments did not significantly block N-mHtt-mediated transcriptional dysregulation.

4.1 CONCLUSION

Overall, this work provides insight into the mechanism of N-mHtt-mediated transcriptional dysregulation and identifies a region of CBP that may block some detrimental effects of mHtt, the third Zn finger region. Future experiments should aim to identify the mechanisms by which overexpressing CBP fragments containing the third Zn finger region decreased mHtt-mediated toxicity. To determine whether the presence of N-mHtt blocks toxicity caused by excess CBP AT activity, we could co-express CBP and N-mHtt in ST*Hdh*$^{Q7/Q7}$ cells and stain cells with EthD-1 or Fluoro-Jade C to evaluate toxicity. If the presence of N-mHtt blocks toxicity due to excess CBP AT activity, we would predict that co-expression of CBP and N-mHtt would have no effect on toxicity in ST*Hdh*$^{Q7/Q7}$ cells. Overexpressing CBP fragments containing the third Zn finger region may have ameliorated mHtt-mediated toxicity by increasing SREBP-mediated expression of cholesterol biosynthesis genes and by decreasing p53-mediated transcription of pro-apoptotic genes. By testing the effect of overexpressing CBP fragments on expression of SREBP-regulated genes, such as HMG-CoA reductase, or p53-regulated pro-apoptotic genes, such as *Bax*, it may answer whether decreased mHtt-mediated toxicity occurred

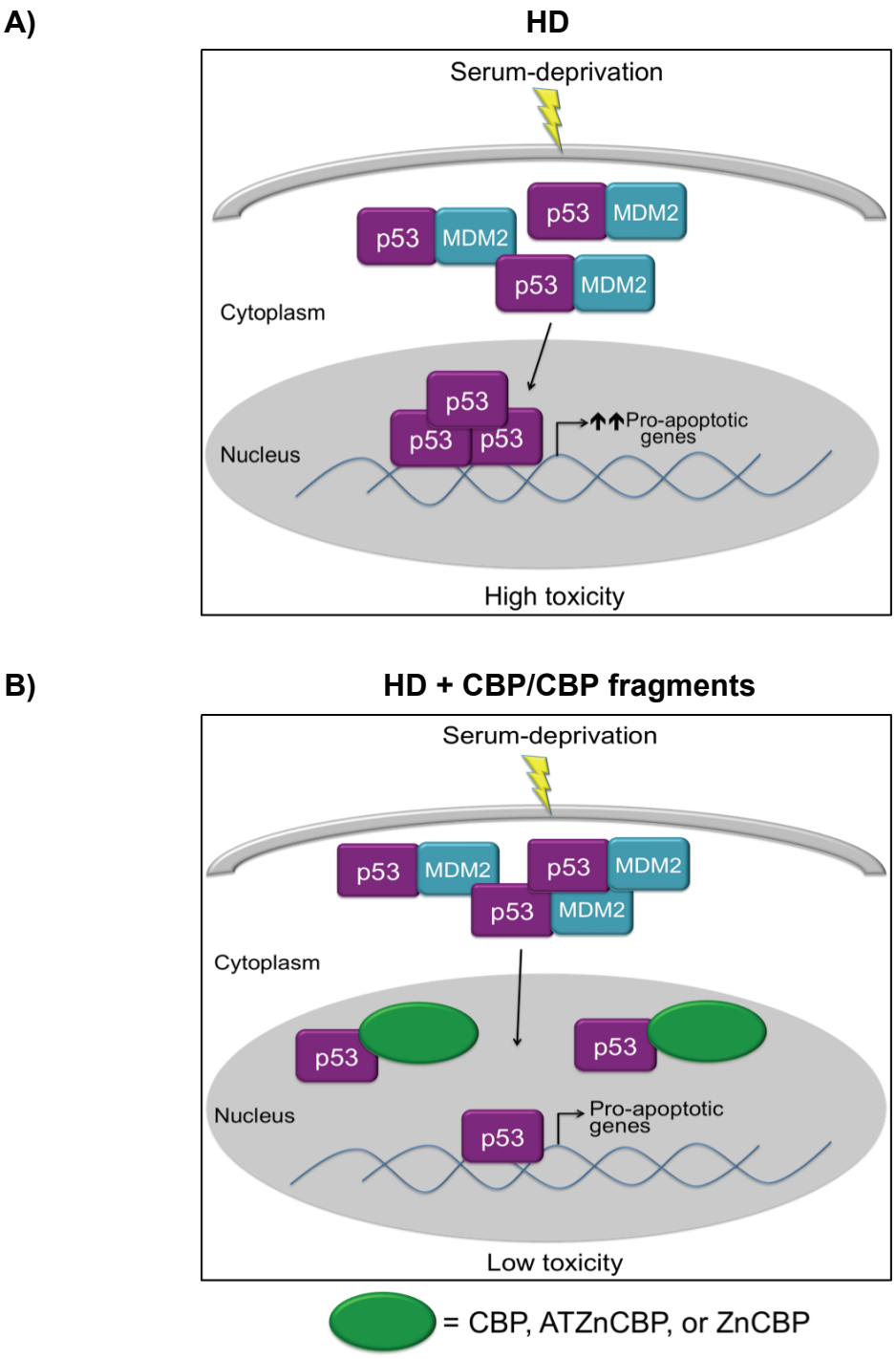

Figure 4.5. Working model for how overexpressing CBP or CBP fragments may limit mHtt-mediated toxicity by decreasing excess p53-mediated apoptosis. **A)** Following serum-deprivation, p53 separates from MDM2, translocates to the nucleus, and activates expression of pro-apoptotic genes. In cells expressing mHtt, there are high levels of p53, leading to excess expression of pro-apoptotic genes and increased toxicity. **B)** Overexpressing CBP or CBP fragments blocks p53-mediated expression of pro-apoptotic genes in HD cells by binding excess p53 and failing to associate at the promoter. MDM2; murine double minute 2 (named murine because it was originally identified in mice).

through modulation of these aberrant pathways. Identification of CBP fragments that can reduce mHtt-mediated cellular toxicity may prove useful for designing small molecule inhibitors of mHtt to improve symptoms of HD.

REFERENCES

Adams P, Falek A, Arnold J (1988) Huntington disease in Georgia: age at onset. American journal of human genetics 43:695–704.

Anderson KE, Gehl CR, Marder KS, Beglinger LJ, Paulsen JS (2010) Comorbidities of obsessive and compulsive symptoms in Huntington's disease. The journal of nervous and mental disease 198:334–338.

Andrade L, Caraveo-Anduaga JJ, Berglund P, Bijl RV, De Graaf R, Vollebergh W, Dragomirecka E, Kohn R, Keller M, Kessler RC, Kawakami N, Kiliç C, Offord D, Ustun TB, Wittchen H-U (2003) The epidemiology of major depressive episodes: results from the International Consortium of Psychiatric Epidemiology (ICPE) Surveys. International journal of methods in psychiatric research 12:3–21.

Arrasate M, Mitra S, Schweitzer ES, Segal MR, Finkbeiner S (2004) Inclusion body formation reduces levels of mutant huntingtin and the risk of neuronal death. Nature 431:805–810.

Atwal RS, Xia J, Pinchev D, Taylor J, Epand RM, Truant R (2007) Huntingtin has a membrane association signal that can modulate huntingtin aggregation, nuclear entry and toxicity. Human molecular genetics 16:2600–2615.

Augood SJ, Faull RL, Emson PC (1997) Dopamine D1 and D2 receptor gene expression in the striatum in Huntington's disease. Annals of neurology 42:215–221.

Augood SJ, Faull RL, Love DR, Emson PC (1996) Reduction in enkephalin and substance P messenger RNA in the striatum of early grade Huntington's disease: a detailed cellular *in situ* hybridization study. Neuroscience 72:1023–1036.

Avantaggiati ML, Ogryzko V, Gardner K, Giordano A, Levine AS, Kelly K (1997) Recruitment of p300/CBP in p53-dependent signal pathways. Cell 89:1175–1184.

Aylward EH, Liu D, Nopoulos PC, Ross CA, Pierson RK, Mills JA, Long JD, Paulsen JS (2011) Striatal volume contributes to the prediction of onset of Huntington disease in incident cases. Biological psychiatry 71:822-828

Bae BI, Hara MR, Cascio MB, Wellington CL, Hayden MR, Ross C a, Ha HC, Li X-J, Snyder SH, Sawa A (2006) Mutant huntingtin: nuclear translocation and cytotoxicity mediated by GAPDH. Proceedings of the National Academy of Sciences of the United States of America 103:3405–3409.

Bae BI, Xu H, Igarashi S, Fujimuro M, Agrawal N, Taya Y, Hayward SD, Moran TH, Montell C, Ross CA, Snyder SH, Sawa A (2005) p53 mediates cellular dysfunction and behavioral abnormalities in Huntington's disease. Neuron 47:29–41.

Bannister AJ, Kouzarides T (1995) CBP-induced stimulation of c-Fos activity is abrogated by E1A. The EMBO journal 14:4758–4762.

Bannister AJ, Oehler T, Wilhelm D, Angel P, Kouzarides T (1995) Stimulation of c-Jun activity by CBP: c-Jun residues Ser63/73 are required for CBP induced stimulation in vivo and CBP binding in vitro. Oncogene 11:2509–2514.

Bañez-Coronel M, Porta S, Kagerbauer B, Mateu-Huertas E, Pantano L, Ferrer I, Guzmán M, Estivill X, Martí E (2012) A pathogenic mechanism in Huntington's disease involves small CAG-repeated RNAs with neurotoxic activity. PLoS genetics 8:e1002481.

Becanovic K, Pouladi MA, Lim RS, Kuhn A, Pavlidis P, Luthi-Carter R, Hayden MR, Leavitt BR (2010) Transcriptional changes in Huntington disease identified using genome-wide expression profiling and cross-platform analysis. Human molecular genetics 19:1438–1452.

Benn CL, Sun T, Sadri-Vakili G, McFarland KN, DiRocco DP, Yohrling GJ, Clark TW, Bouzou B, Cha J-HJ (2008) Huntingtin modulates transcription, occupies gene promoters *in vivo*, and binds directly to DNA in a polyglutamine-dependent manner. The journal of neuroscience 28:10720–10733.

Bibb JA, Yan Z, Svenningsson P, Snyder GL, Pieribone VA, Horiuchi A, Nairn AC, Messer A, Greengard P (2000) Severe deficiencies in dopamine signaling in presymptomatic Huntington's disease mice. Proceedings of the National Academy of Sciences of the United States of America 97:6809–6814.

Blázquez C, Chiarlone A, Sagredo O, Aguado T, Pazos MR, Resel E, Palazuelos J, Julien B, Salazar M, Börner C, Benito C, Carrasco C, Diez-Zaera M, Paoletti P, Díaz-Hernández M, Ruiz C, Sendtner M, Lucas JJ, de Yébenes JG, Marsicano G, Monory K, Lutz B, Romero J, Alberch J, Ginés S, Kraus J, Fernández-Ruiz J, Galve-Roperh I, Guzmán M (2011) Loss of striatal type 1 cannabinoid receptors is a key pathogenic factor in Huntington's disease. Brain 134:119–136.

Bonelli RM, Wenning GK (2006) Pharmacological management of Huntington's disease: an evidence-based review. Current pharmaceutical design 12:2701–2720.

Boutell JM, Thomas P, Neal JW, Weston VJ, Duce J, Harper PS, Jones AL (1999) Aberrant interactions of transcriptional repressor proteins with the Huntington's disease gene product, huntingtin. Human molecular genetics 8:1647–1655.

Carroll JB, Southwell AL, Graham RK, Lerch JP, Ehrnhoefer DE, Cao L-P, Zhang W-N, Deng Y, Bissada N, Henkelman RM, Hayden MR (2011) Mice lacking caspase-2 are protected from behavioral changes, but not pathology, in the YAC128 model of Huntington Disease. Molecular neurodegeneration 6:59.

Cattaneo E, Sipione S (2001) Modeling Huntington's disease in cells, flies, and mice. Molecular neurobiology 23:21–52.

Clarke G, Collins RA, Leavitt BR, Andrews DF, Hayden MR, Lumsden CJ, McInnes RR (2000) A one-hit model of cell death in inherited neuronal degenerations. Nature 406:195–199.

Cong S-Y, Pepers B a, Evert BO, Rubinsztein DC, Roos R a C, van Ommen G-JB, Dorsman JC (2005) Mutant huntingtin represses CBP, but not p300, by binding and protein degradation. Molecular and cellular neurosciences 30:12–23.

Cornett J, Cao F, Wang C-E, Ross C a, Bates GP, Li S-H, Li X-J (2005) Polyglutamine expansion of huntingtin impairs its nuclear export. Nature genetics 37:198–204.

Cui L, Jeong H, Borovecki F, Parkhurst CN, Tanese N, Krainc D (2006) Transcriptional repression of PGC-1alpha by mutant huntingtin leads to mitochondrial dysfunction and neurodegeneration. Cell 127:59–69.

Dai P, Akimaru H, Tanaka Y, Hou DX, Yasukawa T, Kanei-Ishii C, Takahashi T, Ishii S (1996) CBP as a transcriptional coactivator of c-Myb. Genes & development 10:528–540.

Dallas PB, Yaciuk P, Moran E (1997) Characterization of monoclonal antibodies raised against p300: both p300 and CBP are present in intracellular TBP complexes. Journal of virology 71:1726–1731.

Davies SW, Turmaine M, Cozens BA, DiFiglia M, Sharp AH, Ross CA, Scherzinger E, Wanker EE, Mangiarini L, Bates GP (1997) Formation of neuronal intranuclear inclusions underlies the neurological dysfunction in mice transgenic for the HD mutation. Cell 90:537–548.

DeBose-Boyd RA (2008) Feedback regulation of cholesterol synthesis: sterol-accelerated ubiquitination and degradation of HMG CoA reductase. Cell research 18:609–621.

De Marchi N, Daniele F, Ragone MA (2001) Fluoxetine in the treatment of Huntington's disease. Psychopharmacology 153:264–266.

De Mezer M, Wojciechowska M, Napierala M, Sobczak K, Krzyzosiak WJ (2011) Mutant CAG repeats of Huntingtin transcript fold into hairpins, form nuclear foci and are targets for RNA interference. Nucleic acids research 39:3852–3863.

DiFiglia M, Sapp E, Chase KO, Davies SW, Bates GP, Vonsattel JP, Aronin N (1997) Aggregation of huntingtin in neuronal intranuclear inclusions and dystrophic neurites in brain. Science (New York, NY) 277:1990–1993.

DiFiglia M, Sena-Esteves M, Chase K, Sapp E, Pfister E, Sass M, Yoder J, Reeves P, Pandey RK, Rajeev KG, Manoharan M, Sah DWY, Zamore PD, Aronin N (2007) Therapeutic silencing of mutant huntingtin with siRNA attenuates striatal and cortical neuropathology and behavioral deficits. Proceedings of the National Academy of Sciences of the United States of America 104:17204–17209.

van Dijk JG, van der Velde EA, Roos RA, Bruyn GW (1986) Juvenile Huntington's disease. Human genetics 73:235–239.

Duyao M, Ambrose C, Myers R, Novelletto A, Persichetti F, Frontali M, Folstein S, Ross C, Franz M, Abbott M (1993) Trinucleotide repeat length instability and age of onset in Huntington's disease. Nature genetics 4:387–392.

Duyao MP, Auerbach AB, Ryan A, Persichetti F, Barnes GT, McNeil SM, Ge P, Vonsattel JP, Gusella JF, Joyner AL (1995) Inactivation of the mouse Huntington's disease gene homolog *Hdh*. Science (New York, NY) 269:407–410.

Fennema-Notestine C, Archibald SL, Jacobson MW, Corey-Bloom J, Paulsen JS, Peavy GM, Gamst AC, Hamilton JM, Salmon DP, Jernigan TL (2004) *In vivo* evidence of cerebellar atrophy and cerebral white matter loss in Huntington disease. Neurology 63:989–995.

Fink SL, Cookson BT (2005) Apoptosis, pyroptosis, and necrosis: mechanistic description of dead and dying eukaryotic cells. Infection and immunity 73:1907–1916.

Fish DR, Sawyers D, Allen PJ, Blackie JD, Lees AJ, Marsden CD (1991) The effect of sleep on the dyskinetic movements of Parkinson's disease, Gilles de la Tourette syndrome, Huntington's disease, and torsion dystonia. Archives of neurology 48:210–214.

Folstein S, Abbott MH, Chase GA, Jensen BA, Folstein MF (1983) The association of affective disorder with Huntington's disease in a case series and in families. Psychological medicine 13:537–542.

Fünfschilling U, Saher G, Xiao L, Möbius W, Nave K-A (2007) Survival of adult neurons lacking cholesterol synthesis *in vivo*. BMC neuroscience 8:1.

Gafni J, Ellerby LM (2002) Calpain activation in Huntington's disease. The journal of neuroscience 22:4842–4849.

Gafni J, Hermel E, Young JE, Wellington CL, Hayden MR, Ellerby LM (2004) Inhibition of calpain cleavage of huntingtin reduces toxicity: accumulation of calpain/caspase fragments in the nucleus. The journal of biological chemistry 279:20211–20220.

Goehler H, Lalowski M, Stelzl U, Waelter S, Stroedicke M, Worm U, Droege A, Lindenberg KS, Knoblich M, Haenig C, Herbst M, Suopanki J, Scherzinger E, Abraham C, Bauer B, Hasenbank R, Fritzsche A, Ludewig AH, Büssow K, Coleman SH, Gutekunst CA, Landwehrmeyer BG, Lehrach H, Wanker EE (2004) A protein interaction network links GIT1, an enhancer of huntingtin aggregation, to Huntington's disease. Molecular cell 15:853–865.

Goldberg YP, Nicholson DW, Rasper DM, Kalchman MA, Koide HB, Graham RK, Bromm M, Kazemi-Esfarjani P, Thornberry NA, Vaillancourt JP, Hayden MR (1996) Cleavage of huntingtin by apopain, a proapoptotic cysteine protease, is modulated by the polyglutamine tract. Nature genetics 13:442–449.

Goodman RH, Smolik S (2000) CBP/p300 in cell growth, transformation, and development. Genes & development 14:1553–1577.

Goritz C, Mauch DH, Pfrieger FW (2005) Multiple mechanisms mediate cholesterol-induced synaptogenesis in a CNS neuron. Molecular and cellular neurosciences 29:190–201.

Graham RK, Deng Y, Slow EJ, Haigh B, Bissada N, Lu G, Pearson J, Shehadeh J, Bertram L, Murphy Z, Warby SC, Doty CN, Roy S, Wellington CL, Leavitt BR, Raymond LA, Nicholson DW, Hayden MR (2006) Cleavage at the caspase-6 site is required for neuronal dysfunction and degeneration due to mutant huntingtin. Cell:1179–1191.

Gray M, Shirasaki DI, Cepeda C, André VM, Wilburn B, Lu X-H, Tao J, Yamazaki I, Li S-H, Sun YE, Li X-J, Levine MS, Yang XW (2008) Full-length human mutant huntingtin with a stable polyglutamine repeat can elicit progressive and selective neuropathogenesis in BACHD mice. The journal of neuroscience 28:6182–6195.

Gusella JF, MacDonald ME (2009) Huntington's disease: the case for genetic modifiers. Genome medicine 1:80.

Gusella JF, Wexler NS, Conneally PM, Naylor SL, Anderson MA, Tanzi RE, Watkins PC, Ottina K, Wallace MR, Sakaguchi AY (1983) A polymorphic DNA marker genetically linked to Huntington's disease. Nature 306:234–238.

Hackam a S, Singaraja R, Wellington CL, Metzler M, McCutcheon K, Zhang T, Kalchman M, Hayden MR (1998) The influence of huntingtin protein size on nuclear localization and cellular toxicity. The journal of cell biology 141:1097–1105.

Harjes P, Wanker EE (2003) The hunt for huntingtin function: interaction partners tell many different stories. Trends in biochemical sciences 28:425–433.

Havel LS, Li S, Li X-J (2009) Nuclear accumulation of polyglutamine disease proteins and neuropathology. Molecular brain 2:21.

Havel LS, Wang C-E, Wade B, Huang B, Li S, Li X-J (2011) Preferential accumulation of N-terminal mutant huntingtin in the nuclei of striatal neurons is regulated by phosphorylation. Human molecular genetics 20:1424–1437.

Hebb ALO, Robertson HA, Denovan-Wright EM (2004) Striatal phosphodiesterase mRNA and protein levels are reduced in Huntington's disease transgenic mice prior to the onset of motor symptoms. Neuroscience 123:967–981.

Heinsen H, Rüb U, Bauer M, Ulmar G, Bethke B, Schüler M, Böcker F, Eisenmenger W, Götz M, Korr H, Schmitz C (1999) Nerve cell loss in the thalamic mediodorsal nucleus in Huntington's disease. Acta neuropathologica 97:613–622.

Hermel E, Gafni J, Propp SS, Leavitt BR, Wellington CL, Young JE, Hackam AS, Logvinova AV, Peel AL, Chen SF, Hook V, Singaraja R, Krajewski S, Goldsmith PC, Ellerby HM, Hayden MR, Bredesen DE, Ellerby LM (2004) Specific caspase interactions and amplification are involved in selective neuronal vulnerability in Huntington's disease. Cell death and differentiation 11:424–438.

Hodges A, Strand AD, Aragaki AK, Kuhn A, Sengstag T, Hughes G, Elliston LA, Hartog C, Goldstein DR, Thu D, Hollingsworth ZR, Collin F, Synek B, Holmans PA, Young AB, Wexler NS, Delorenzi M, Kooperberg C, Augood SJ, Faull RL, Olson JM, Jones L, Luthi-Carter R (2006) Regional and cellular gene expression changes in human Huntington's disease brain. Human molecular genetics 15:965–977.

Hodges A, Hughes G, Brooks S, Elliston L, Holmans P, Dunnett SB, Jones L (2008) Brain gene expression correlates with changes in behavior in the R6/1 mouse model of Huntington's disease. Genes, brain, and behavior 7:288–299.

Hogel M, Laprairie RB, Denovan-Wright EM (2012) Promoters are differentially sensitive to N-terminal mutant huntingtin-mediated transcriptional repression. PLoS one 7:e41152.

Holbert S, Denghien I, Kiechle T, Rosenblatt A, Wellington C, Hayden MR, Margolis RL, Ross CA, Dausset J, Ferrante RJ, Néri C (2001) The Gln-Ala repeat transcriptional activator CA150 interacts with huntingtin: neuropathologic and genetic evidence for a role in Huntington's disease pathogenesis. Proceedings of the National Academy of Sciences of the United States of America 98:1811–1816.

Holl AK, Wilkinson L, Painold A, Holl EM, Bonelli RM (2010) Combating depression in Huntington's disease: effective antidepressive treatment with venlafaxine XR. International clinical psychopharmacology 25:46–50.

Hoogeveen AT, Willemsen R, Meyer N, de Rooij KE, Roos RA, van Ommen GJ, Galjaard H (1993) Characterization and localization of the Huntington disease gene product. Human molecular genetics 2:2069–2073.

Horton JD, Goldstein JL, Brown MS (2002) SREBPs: activators of the complete program of cholesterol and fatty acid synthesis in the liver. The journal of clinical investigation 109:1125–1131.

Huntington's Disease Collaborative Research Group (1993) A Novel gene containing a trinucleotide that is expanded and unstable on Huntington's disease chromosomes. Cell 72:971–983.

Janknecht R (2002) The versatile functions of the transcriptional coactivators p300 and CBP and their roles in disease. Histology and histopathology 17:657–668.

Jiang H, Poirier M a, Liang Y, Pei Z, Weiskittel CE, Smith WW, DeFranco DB, Ross C a (2006) Depletion of CBP is directly linked with cellular toxicity caused by mutant huntingtin. Neurobiology of disease 23:543–551.

Julien CL, Thompson JC, Wild S, Yardumian P, Snowden JS, Turner G, Craufurd D (2007) Psychiatric disorders in preclinical Huntington's disease. Journal of neurology, neurosurgery, and psychiatry 78:939–943.

Kalkhoven E (2004) CBP and p300: HATs for different occasions. Biochemical pharmacology 68:1145–1155.

Kalkhoven E, Roelfsema JH, Teunissen H, den Boer A, Ariyurek Y, Zantema A, Breuning MH, Hennekam RCM, Peters DJM (2003) Loss of CBP acetyltransferase activity by PHD finger mutations in Rubinstein-Taybi syndrome. Human molecular genetics 12:441–450.

Kaltenbach LS, Romero E, Becklin RR, Chettier R, Bell R, Phansalkar A, Strand A, Torcassi C, Savage J, Hurlburt A, Cha G-H, Ukani L, Chepanoske CL, Zhen Y, Sahasrabudhe S, Olson J, Kurschner C, Ellerby LM, Peltier JM, Botas J, Hughes RE (2007) Huntingtin interacting proteins are genetic modifiers of neurodegeneration. PLoS genetics 3:e82.

Kegel KB, Meloni AR, Yi Y, Kim YJ, Doyle E, Cuiffo BG, Sapp E, Wang Y, Qin Z-H, Chen JD, Nevins JR, Aronin N, DiFiglia M (2002) Huntingtin is present in the nucleus, interacts with the transcriptional corepressor C-terminal binding protein, and represses transcription. The journal of biological chemistry 277:7466–7476.

Kirkwood SC, Su JL, Conneally P, Foroud T (2001) Progression of symptoms in the early and middle stages of Huntington disease. Archives of neurology 58:273–278.

Klevytska AM, Tebbenkamp ATN, Savonenko AV, Borchelt DR (2010) Partial depletion of CREB-binding protein reduces life expectancy in a mouse model of Huntington disease. Journal of neuropathology and experimental neurology 69:396–404.

Koller WC, Trimble J (1985) The gait abnormality of Huntington's disease. Neurology 35:1450–1454.

Kremer B, Goldberg P, Andrew SE, Theilmann J, Telenius H, Zeisler J, Squitieri F, Lin B, Bassett A, Almqvist E (1994) A worldwide study of the Huntington's disease mutation. The sensitivity and specificity of measuring CAG repeats. The New England journal of medicine 330:1401–1406.

Kremer HP, Roos RA, Dingjan G, Marani E, Bots GT (1990) Atrophy of the hypothalamic lateral tuberal nucleus in Huntington's disease. Journal of neuropathology and experimental neurology 49:371–382.

Kwok RP, Lundblad JR, Chrivia JC, Richards JP, Bächinger HP, Brennan RG, Roberts SG, Green MR, Goodman RH (1994) Nuclear protein CBP is a coactivator for the transcription factor CREB. Nature 370:223–226.

Lanska DJ, Lanska MJ, Lavine L, Schoenberg BS (1988) Conditions associated with Huntington's disease at death. A case-control study. Archives of neurology 45:878–880.

Legge GB, Martinez-Yamout MA, Hambly DM, Trinh T, Lee BM, Dyson HJ, Wright PE (2004) ZZ domain of CBP: an unusual zinc finger fold in a protein interaction module. Journal of molecular biology 343:1081–1093.

Lemiere J, Decruyenaere M, Evers-Kiebooms G, Vandenbussche E, Dom R (2004) Cognitive changes in patients with Huntington's disease (HD) and asymptomatic carriers of the HD mutation--a longitudinal follow-up study. Journal of neurology 251:935–942.

Leonard DP, Kidson MA, Brown JG, Shannon PJ, Taryan S (1975) A double blind trial of lithium carbonate and haloperidol in Huntington's chorea. The Australian and New Zealand journal of psychiatry 9:115–118.

Leyva MJ, Degiacomo F, Kaltenbach LS, Holcomb J, Zhang N, Gafni J, Park H, Lo DC, Salvesen GS, Ellerby LM, Ellman J a (2010) Identification and evaluation of small molecule pan-caspase inhibitors in Huntington's disease models. Chemistry & biology 17:1189–1200.

Li S-H, Cheng AL, Zhou H, Lam S, Rao M, Li H, Li X-J (2002) Interaction of Huntington disease protein with transcriptional activator Sp1. Molecular and cellular biology 22:1277–1287.

Li S-H, Li X-J (2004) Huntingtin-protein interactions and the pathogenesis of Huntington's disease. Trends in genetics 20:146–154.

Li SH, Schilling G, Young WS, Li XJ, Margolis RL, Stine OC, Wagster MV, Abbott MH, Franz ML, Ranen NG (1993) Huntington's disease gene (IT15) is widely expressed in human and rat tissues. Neuron 11:985–993.

Lill NL, Grossman SR, Ginsberg D, DeCaprio J, Livingston DM (1997) Binding and modulation of p53 by p300/CBP coactivators. Nature 387:823–827.

Lim D, Fedrizzi L, Tartari M, Zuccato C, Cattaneo E, Brini M, Carafoli E (2008) Calcium homeostasis and mitochondrial dysfunction in striatal neurons of Huntington disease. The journal of biological chemistry 283:5780–5789.

Lin J, Handschin C, Spiegelman BM (2005) Metabolic control through the PGC-1 family of transcription coactivators. Cell metabolism 1:361–370.

Lin WC, Chou Y-H (2008) Aripiprazole effects on psychosis and chorea in a patient with Huntington's disease. The American journal of psychiatry 165:1207–1208.

Luthi-Carter R (2000) Decreased expression of striatal signaling genes in a mouse model of Huntington's disease. Human molecular genetics 9:1259–1271.

Luthi-Carter R, Hanson SA, Strand AD, Bergstrom DA, Chun W, Peters NL, Woods AM, Chan EY, Kooperberg C, Krainc D, Young AB, Tapscott SJ, Olson JM (2002) Dysregulation of gene expression in the R6/2 model of polyglutamine disease: parallel changes in muscle and brain. Human molecular genetics 11:1911–1926

Macdonald V, Halliday GM, Trent RJ, McCusker EA (1997) Significant loss of pyramidal neurons in the angular gyrus of patients with Huntington's disease. Neuropathology and applied neurobiology 23:492–495.

Mangiarini L, Sathasivam K, Seller M, Cozens B, Harper A, Hetherington C, Lawton M, Trottier Y, Lehrach H, Davies SW, Bates GP (1996) Exon 1 of the HD gene with an expanded CAG repeat is sufficient to cause a progressive neurological phenotype in transgenic mice. Cell 87:493–506.

Mann DM, Oliver R, Snowden JS (1993) The topographic distribution of brain atrophy in Huntington's disease and progressive supranuclear palsy. Acta neuropathologica 85:553–559.

Mauch DH, Nägler K, Schumacher S, Göritz C, Müller EC, Otto A, Pfrieger FW (2001) CNS synaptogenesis promoted by glia-derived cholesterol. Science (New York, NY) 294:1354–1357.

McCaw EA, Hu H, Gomez GT, Hebb ALO, Kelly MEM, Denovan-Wright EM (2004) Structure, expression and regulation of the cannabinoid receptor gene (CB1) in Huntington's disease transgenic mice. European journal of biochemistry / FEBS 271:4909–4920.

McNeil PL, Steinhardt RA (1997) Loss, restoration, and maintenance of plasma membrane integrity. The journal of cell biology 137:1–4.

Menalled L, El-Khodor BF, Patry M, Suárez-Fariñas M, Orenstein SJ, Zahasky B, Leahy C, Wheeler V, Yang XW, MacDonald M, Morton AJ, Bates G, Leeds J, Park L, Howland D, Signer E, Tobin A, Brunner D (2009) Systematic behavioral evaluation of Huntington's disease transgenic and knock-in mouse models. Neurobiology of disease 35:319–336.

Merz K, Herold S, Lie DC (2011) CREB in adult neurogenesis: master and partner in the development of adult-born neurons? The European journal of neuroscience 33:1078–1086.

Miller JP, Hughes RE (2011) Chapter 3: Protein interactions and target discovery in Huntington's disease. *In*: Neurobiology of Huntington's disease: Applications to drug discovery. *Editors:* Lo DC, Hughes RE. Boca Raton (FL): CRC Press.

Mitchell IJ, Cooper AJ, Griffiths MR (1999) The selective vulnerability of striatopallidal neurons. Progress in neurobiology 59:691–719.

Morton a J, Wood NI, Hastings MH, Hurelbrink C, Barker R a, Maywood ES (2005) Disintegration of the sleep-wake cycle and circadian timing in Huntington's disease. The journal of neuroscience 25:157–163.

Nakajima T, Uchida C, Anderson SF, Lee CG, Hurwitz J, Parvin JD, Montminy M (1997) RNA helicase A mediates association of CBP with RNA polymerase II. Cell 90:1107–1112.

Newcombe RG, Walker DA, Harper PS (1981) Factors influencing age at onset and duration of survival in Huntington's chorea. Annals of human genetics 45:387–396.

Nucifora FC, Sasaki M, Peters MF, Huang H, Cooper JK, Yamada M, Takahashi H, Tsuji S, Troncoso J, Dawson VL, Dawson TM, Ross C a (2001) Interference by huntingtin and atrophin-1 with cbp-mediated transcription leading to cellular toxicity. Science (New York, NY) 291:2423–2428.

Oliner JD, Andresen JM, Hansen SK, Zhou S, Tjian R (1996) SREBP transcriptional activity is mediated through an interaction with the CREB-binding protein. Genes & development 10:2903–2911.

Oliveira JMA (2010) Nature and cause of mitochondrial dysfunction in Huntington's disease: focusing on huntingtin and the striatum. Journal of neurochemistry 114:1–12.

Ondo WG, Tintner R, Thomas M, Jankovic J (2002) Tetrabenazine treatment for Huntington's disease-associated chorea. Clinical neuropharmacology 25:300–302.

Orr HT, Zoghbi HY (2007) Trinucleotide repeat disorders. Annual review of neuroscience 30:575–621.

Oyanagi K, Takeda S, Takahashi H, Ohama E, Ikuta F (1989) A quantitative investigation of the substantia nigra in Huntington's disease. Annals of neurology 26:13–19.

O'Connor MJ, Zimmermann H, Nielsen S, Bernard HU, Kouzarides T (1999) Characterization of an E1A-CBP interaction defines a novel transcriptional adapter motif (TRAM) in CBP/p300. Journal of virology 73:3574–3581.

Paleacu D (2007) Tetrabenazine in the treatment of Huntington's disease. Neuropsychiatric disease and treatment 3:545–551.

Patzold T, Brüne M (2002) Obsessive compulsive disorder in huntington disease: a case of isolated obsessions successfully treated with sertraline. Neuropsychiatry, neuropsychology, and behavioral neurology 15:216–219.

Paulsen JS, Langbehn DR, Stout JC, Aylward E, Ross CA, Nance M, Guttman M, Johnson S, MacDonald M, Beglinger LJ, Duff K, Kayson E, Biglan K, Shoulson I, Oakes D, Hayden M (2008) Detection of Huntington's disease decades before diagnosis: the Predict-HD study. Journal of neurology, neurosurgery, and psychiatry 79:874–880.

Paulsen JS, Ready RE, Hamilton JM, Mega MS, Cummings JL (2001) Neuropsychiatric aspects of Huntington's disease. Journal of neurology, neurosurgery, and psychiatry 71:310–314.

Pendergrass W, Wolf N, Poot M (2004) Efficacy of MitoTracker Green and CMXrosamine to measure changes in mitochondrial membrane potentials in living cells and tissues. Cytometry Part A 61:162–169.

Perutz MF, Johnson T, Suzuki M, Finch JT (1994) Glutamine repeats as polar zippers: their possible role in inherited neurodegenerative diseases. Proceedings of the National Academy of Sciences of the United States of America 91:5355–5358.

Peters MF, Nucifora FC, Kushi J, Seaman HC, Cooper JK, Herring WJ, Dawson VL, Dawson TM, Ross CA (1999) Nuclear targeting of mutant Huntingtin increases toxicity. Molecular and cellular neurosciences 14:121–128.

Pettibone DJ, Totaro JA, Pflueger AB (1984) Tetrabenazine-induced depletion of brain monoamines: characterization and interaction with selected antidepressants. European journal of pharmacology 102:425–430.

Phan J, Hickey MA, Zhang P, Chesselet M-F, Reue K (2009) Adipose tissue dysfunction tracks disease progression in two Huntington's disease mouse models. Human molecular genetics 18:1006–1016.

Puddifoot C, Martel M-A, Soriano FX, Camacho A, Vidal-Puig A, Wyllie DJA, Hardingham GE (2012) PGC-1 negatively regulates extrasynaptic NMDAR activity and excitotoxicity. The journal of neuroscience 32:6995–7000.

Quarrell OW, Rigby AS, Barron L, Crow Y, Dalton A, Dennis N, Fryer AE, Heydon F, Kinning E, Lashwood A, Losekoot M, Margerison L, McDonnell S, Morrison PJ, Norman A, Peterson M, Raymond FL, Simpson S, Thompson E, Warner J (2007) Reduced penetrance alleles for Huntington's disease: a multi-centre direct observational study. Journal of medical genetics 44:e68.

van Raamsdonk JM, Pearson J, Slow EJ, Hossain SM, Leavitt BR, Hayden MR (2005) Cognitive dysfunction precedes neuropathology and motor abnormalities in the YAC128 mouse model of Huntington's disease. The journal of neuroscience 25:4169–4180.

Reches A, Burke RE, Kuhn CM, Hassan MN, Jackson VR, Fahn S (1983) Tetrabenazine, an amine-depleting drug, also blocks dopamine receptors in rat brain. The journal of pharmacology and experimental therapeutics 225:515–521.

Robbins AO, Ho AK, Barker RA (2006) Weight changes in Huntington's disease. European journal of neurology 13:e7.

Rodriguez-Lebron E, Denovan-Wright EM, Nash K, Lewin AS, Mandel RJ (2005) Intrastriatal rAAV-mediated delivery of anti-huntingtin shRNAs induces partial reversal of disease progression in R6/1 Huntington's disease transgenic mice. Molecular therapy 12:618–633.

van Roon-Mom WMC, Reid SJ, Jones AL, MacDonald ME, Faull RLM, Snell RG (2002) Insoluble TATA-binding protein accumulation in Huntington's disease cortex. Brain research Molecular brain research 109:1–10.

Rosas HD, Koroshetz WJ, Chen YI, Skeuse C, Vangel M, Cudkowicz ME, Caplan K, Marek K, Seidman LJ, Makris N, Jenkins BG, Goldstein JM (2003) Evidence for more widespread cerebral pathology in early HD: an MRI-based morphometric analysis. Neurology 60:1615–1620.

Rosenblatt A, Kumar BV, Mo A, Welsh CS, Margolis RL, Ross CA (2012) Age, CAG repeat length, and clinical progression in Huntington's disease. Movement disorders 27:272-276.

Ross CA, Tabrizi SJ (2011) Huntington's disease: from molecular pathogenesis to clinical treatment. The Lancet neurology 10:83–98.

Rouaux C, Jokic N, Mbebi C, Boutillier S, Loeffler JP, Boutillier AL (2003) Critical loss of CBP/p300 histone acetylase activity by caspase-6 during neurodegeneration. The EMBO journal 22:6537–6549.

Rouaux C, Loeffler J-P, Boutillier A-L (2004) Targeting CREB-binding protein (CBP) loss of function as a therapeutic strategy in neurological disorders. Biochemical pharmacology 68:1157–1164.

Runne H, Régulier E, Kuhn A, Zala D, Gokce O, Perrin V, Sick B, Aebischer P, Déglon N, Luthi-Carter R (2008) Dysregulation of gene expression in primary neuron models of Huntington's disease shows that polyglutamine-related effects on the striatal transcriptome may not be dependent on brain circuitry. The journal of neuroscience 28:9723–9731.

Sadri-Vakili G, Bouzou B, Benn CL, Kim M-O, Chawla P, Overland RP, Glajch KE, Xia E, Qiu Z, Hersch SM, Clark TW, Yohrling GJ, Cha J-HJ (2007) Histones associated with downregulated genes are hypo-acetylated in Huntington's disease models. Human molecular genetics 16:1293–1306.

Saudou F, Finkbeiner S, Devys D, Greenberg ME (1998) Huntingtin acts in the nucleus to induce apoptosis but death does not correlate with the formation of intranuclear inclusions. Cell 95:55–66.

Schilling G, Becher MW, Sharp AH, Jinnah HA, Duan K, Kotzuk JA, Slunt HH, Ratovitski T, Cooper JK, Jenkins NA, Copeland NG, Price DL, Ross CA, Borchelt DR (1999) Intranuclear inclusions and neuritic aggregates in transgenic mice expressing a mutant N-terminal fragment of huntingtin. Human molecular genetics 8:397–407.

Schmued LC, Stowers CC, Scallet AC, Xu L (2005) Fluoro-Jade C results in ultra high resolution and contrast labeling of degenerating neurons. Brain research 1035:24–31.

Scolnick DM, Chehab NH, Stavridi ES, Lien MC, Caruso L, Moran E, Berger SL, Halazonetis TD (1997) CREB-binding Protein and p300 / CBP-associated Factor Are Transcriptional Coactivators of the p53 Tumor Suppressor Protein Coactivators of the p53 Tumor Suppressor Protein. Cancer research 57:3693–3696.

Seitz DP, Millson RC (2004) Quetiapine in the management of psychosis secondary to Huntington's disease: a case report. Canadian journal of psychiatry 49:413.

Sieradzan KA, Mechan AO, Jones L, Wanker EE, Nukina N, Mann DM (1999) Huntington's disease intranuclear inclusions contain truncated, ubiquitinated huntingtin protein. Experimental neurology 156:92–99.

Sipione S, Rigamonti D, Valenza M, Zuccato C, Conti L, Pritchard J, Kooperberg C, Olson JM, Cattaneo E (2002) Early transcriptional profiles in huntingtin-inducible striatal cells by microarray analyses. Human molecular genetics 11:1953–1965.

Slow EJ, van Raamsdonk J, Rogers D, Coleman SH, Graham RK, Deng Y, Oh R, Bissada N, Hossain SM, Yang Y-Z, Li X-J, Simpson EM, Gutekunst CA, Leavitt BR, Hayden MR (2003) Selective striatal neuronal loss in a YAC128 mouse model of Huntington disease. Human molecular genetics 12:1555–1567.

Spargo E, Everall IP, Lantos PL (1993) Neuronal loss in the hippocampus in Huntington's disease: a comparison with HIV infection. Journal of neurology, neurosurgery, and psychiatry 56:487–491.

Squitieri F, Frati L, Ciarmiello A, Lastoria S, Quarrell O (2006) Juvenile Huntington's disease: does a dosage-effect pathogenic mechanism differ from the classical adult disease? Mechanisms of ageing and development 127:208–212.

Stack EC, Kubilus JK, Smith K, Cormier K, Del Signore SJ, Guelin E, Ryu H, Hersch SM, Ferrante RJ (2005) Chronology of behavioral symptoms and neuropathological sequela in R6/2 Huntington's disease transgenic mice. The journal of comparative neurology 490:354–370.

Steffan JS, Bodai L, Pallos J, Poelman M, Mccampbell A, Apostol BL, Kazantsev A, Schmidt E, Zhu Y-zhen, Greenwald M, Kurokawak R, Housman DE, Jackson GR, Marsh JL, Thompson LM (2001) Histone deacetylase inhibitors arrest neurodegeneration in *Drosophila*. Nature:739–743.

Steffan JS, Kazantsev a, Spasic-Boskovic O, Greenwald M, Zhu YZ, Gohler H, Wanker EE, Bates GP, Housman DE, Thompson LM (2000) The Huntington's disease protein interacts with p53 and CREB-binding protein and represses transcription. Proceedings of the National Academy of Sciences of the United States of America 97:6763–6768.

Swope DL, Mueller CL, Chrivia JC (1996) CREB-binding protein activates transcription through multiple domains. The journal of biological chemistry 271:28138–28145.

Taylor JP, Taye AA, Campbell C, Kazemi-Esfarjani P, Fischbeck KH, Min K-T (2003) Aberrant histone acetylation, altered transcription, and retinal degeneration in a *Drosophila* model of polyglutamine disease are rescued by CREB-binding protein. Genes & development 17:1463–1468.

Thompson PD, Berardelli A, Rothwell JC, Day BL, Dick JP, Benecke R, Marsden CD (1988) The coexistence of bradykinesia and chorea in Huntington's disease and its implications for theories of basal ganglia control of movement. Brain 111 (Pt 2):223–244.

Trejo A, Tarrats RM, Alonso ME, Boll M-C, Ochoa A, Velásquez L (2004) Assessment of the nutrition status of patients with Huntington's disease. Nutrition 20:192–196.

Trettel F, Rigamonti D, Hilditch-Maguire P, Wheeler VC, Sharp AH, Persichetti F, Cattaneo E, MacDonald ME (2000) Dominant phenotypes produced by the HD mutation in ST*Hdh*^{Q111} striatal cells. Human molecular genetics 9:2799–2809.

Vagner T, Young D, Mouravlev A (2012) Nucleic Acid-Based Therapy Approaches for Huntington's Disease. Neurology research international 2012:358370.

Valenza M, Cattaneo E (2011) Emerging roles for cholesterol in Huntington's disease. Trends in neurosciences 34:474–486.

Valenza M, Leoni V, Tarditi A, Mariotti C, Björkhem I, Di Donato S, Cattaneo E (2007) Progressive dysfunction of the cholesterol biosynthesis pathway in the R6/2 mouse model of Huntington's disease. Neurobiology of disease 28:133–142.

Valenza M, Rigamonti D, Goffredo D, Zuccato C, Fenu S, Jamot L, Strand A, Tarditi A, Woodman B, Racchi M, Mariotti C, Di Donato S, Corsini A, Bates G, Pruss R, Olson JM, Sipione S, Tartari M, Cattaneo E (2005) Dysfunction of the cholesterol biosynthetic pathway in Huntington's disease. The journal of neuroscience 25:9932–9939.

Vervoorts J, Lüscher-Firzlaff JM, Rottmann S, Lilischkis R, Walsemann G, Dohmann K, Austen M, Lüscher B (2003) Stimulation of c-MYC transcriptional activity and acetylation by recruitment of the cofactor CBP. EMBO reports 4:484–490.

Vonsattel JP, Myers RH, Stevens TJ, Ferrante RJ, Bird ED, Richardson EP (1985) Neuropathological classification of Huntington's disease. Journal of neuropathology and experimental neurology 44:559–577.

Vousden KH, Lane DP (2007) p53 in health and disease. Nature reviews 8:275–283.

Walker FO (2007) Huntington's disease. Lancet 369:218–228.

Wang R, Ma W-G, Gao G-D, Mao Q-X, Zheng J, Sun L-Z, Liu Y-L (2011) Fluoro jade-C staining in the assessment of brain injury after deep hypothermia circulatory arrest. Brain research 1372:127–132.

Wang Y-L, Liu W, Wada E, Murata M, Wada K, Kanazawa I (2005) Clinico-pathological rescue of a model mouse of Huntington's disease by siRNA. Neuroscience research 53:241–249.

Wellington CL, Ellerby LM, Hackam AS, Margolis RL, Trifiro MA, Singaraja R, McCutcheon K, Salvesen GS, Propp SS, Bromm M, Rowland KJ, Zhang T, Rasper D, Roy S, Thornberry N, Pinsky L, Kakizuka A, Ross CA, Nicholson DW, Bredesen DE, Hayden MR (1998) Caspase cleavage of gene products associated with triplet expansion disorders generates truncated fragments containing the polyglutamine tract. The journal of biological chemistry 273:9158–9167.

Wellington CL, Ellerby LM, Gutekunst CA, Rogers D, Warby S, Graham RK, Loubser O, van Raamsdonk J, Singaraja R, Yang YZ, Gafni J, Bredesen D, Hersch SM, Leavitt BR, Roy S, Nicholson DW, Hayden MR (2002) Caspase cleavage of mutant huntingtin precedes neurodegeneration in Huntington's disease. The journal of neuroscience 22:7862–7872.

Wheeler VC, White JK, Gutekunst CA, Vrbanac V, Weaver M, Li XJ, Li SH, Yi H, Vonsattel JP, Gusella JF, Hersch S, Auerbach W, Joyner AL, MacDonald ME (2000) Long glutamine tracts cause nuclear localization of a novel form of huntingtin in medium spiny striatal neurons in Hdh^{Q92} and Hdh^{Q111} knock-in mice. Human molecular genetics 9:503–513.

Wiegand M, Möller AA, Lauer CJ, Stolz S, Schreiber W, Dose M, Krieg JC (1991) Nocturnal sleep in Huntington's disease. Journal of neurology 238:203–208.

Zhai W, Jeong H, Cui L, Krainc D, Tjian R (2005) *In vitro* analysis of huntingtin-mediated transcriptional repression reveals multiple transcription factor targets. Cell 123:1241–1253.

Zuccato C, Ciammola A, Rigamonti D, Leavitt BR, Goffredo D, Conti L, MacDonald ME, Friedlander RM, Silani V, Hayden MR, Timmusk T, Sipione S, Cattaneo E (2001) Loss of huntingtin-mediated BDNF gene transcription in Huntington's disease. Science (New York, NY) 293:493–498.

Zuccato C, Tartari M, Crotti A, Goffredo D, Valenza M, Conti L, Cataudella T, Leavitt BR, Hayden MR, Timmusk T, Rigamonti D, Cattaneo E (2003) Huntingtin interacts with REST/NRSF to modulate the transcription of NRSE-controlled neuronal genes. Nature genetics 35:76–83.

Zuccato C, Valenza M, Cattaneo E (2010) Molecular mechanisms and potential therapeutical targets in Huntington's disease. Physiological reviews 90:905–981.